An investigation into the proportional discharge of air from side outlets on a small-scale terminal ventilation duct

J. O. Weatherall

U N I V E R S I T Y O F D U R H A M

AN INVESTIGATION INTO THE PROPORTIONAL DISCHARGE OF AIR FROM SIDE OUTLETS ON A SMALL-SCALE TERMINAL VENTILATING DUCT.

Thesis submitted for the Degree of
Master of Science in the Faculty
of Engineering Science

by

J. O. WEATHERALL. B.Sc.

December, 1970.

ABSTRACT.

This investigation relates to a small-scale air duct of rectangular cross-section with variably sized rectangular apertures pitched evenly along one face of the duct.

Measurements of air velocities were made mainly with a hot-wire anemometer and to a lesser extent with a pitot-static tube. Details are given of the calibration and use of these instruments together with an outline of the precautions which must be taken to ensure reliability of results.

Aperture air flow patterns determined by the use of the hot-wire anemometer were found to be complex and dependent primarily on the interrelated factors of duct gauge static pressure, aperture size, and that fraction of the approaching air which escaped through an aperture.

It was established that aperture air volume flow could be determined accurately from a single, half-height, horizontal traverse of an aperture with the hot-wire probe and consequently the expenditure of time and effort required for a multi-row traverse was eliminated.

Some evidence was found to support the supposition that variation in the magnitude of the total duct air flow does not affect the proportions into which it is divided by fixed aperture settings.

Relationships between non-dimensional parameters were determined from which a method was devised by which the requisite aperture areas associated with specified aperture proportional air flows were predicted.

ACKNOWLEDGEMENTS.

This work was carried out in the Department of Engineering Science of the University of Durham by the kind permission of Professor R.Hoyle, B.A., Ph.D., whom the author wishes to thank for supervising the work and giving valuable advice.

Sincere thanks are also due to Mr.M.J.Holgate of the University for his continual encouragement and time freely spent on discussion of the project.

Additionally, the assistance rendered by Mr.Campbell, Senior Technician, and his Staff is cordially acknowledged.

CONTENTS

NOTATION

a	Area of aperture.	ft^2
A	Area of duct.	ft^2
b	Breadth of aperture.	in
B	Breadth of duct.	in
D_e	Equivalent diameter of duct.	ft
f	Friction factor.	
h	Static gauge pressure in general.	in w.g. / ft air
h_a	Static gauge pressure at any point in plane of aperture.	in w.g. / ft air
h_d	Duct static gauge pressure recorded at tapping point downstream of aperture.	in w.g. / ft air
h_L	Friction head loss in duct.	in w.g. / ft air
h_u	Duct static gauge pressure recorded at tapping point upstream of aperture.	in w.g. / ft air
h_v	Velocity head.	in w.g. / ft air
k	Energy loss factor.	
K_e	Correction factor for kinetic energy term.	
L	Length along duct.	ft
q	Air volume flow through aperture.	ft^3/sec
Q	Air volume flow in duct.	ft^3/sec
R_e	Reynolds number.	
U	Velocity in general.	ft/sec
U_d	Velocity at any given point in duct.	ft/sec
$\bar{U}_{dd}$	Average velocity in duct downstream of aperture.	ft/sec
$\bar{U}_{du}$	Average velocity in duct upstream of aperture.	ft/sec
U_m	Velocity at any given point in aperture (maximum).	ft/sec
U_n	Component of U_m normal to aperture. ($U_n = U_m.\sin\theta$)	ft/sec
$\bar{U}_n$	Average normal velocity through aperture.	ft/sec

V	Voltage in general.	volts
V_m	Voltage corresponding to U_m.	volts
V_θ	Voltage corresponding to oblique impingement of air.	volts
β	Angle U_d makes with longitudinal axis of duct.	
η	Aperture air discharge expressed as a proportion of the duct air volume flow upstream of the aperture.	
θ	Angle U_m makes with longitudinal axis of duct.	
ν	Kinematic viscosity of air.	ft^2/sec
ρ	Specific weight of air.	lbf/ft^3

SECTION 1.

1.1 Introduction.

Good ventilation consists very largely of ensuring that at all times requisite quantities of fresh air are made available at specified locations to displace stale or contaminated air. With the increasing size and complexity of modern structures using mechanical ventilation the attainment of good ventilation results in the designer being confronted with increasingly formidable distribution problems.

For example, in a vehicular road tunnel it is vital to arrange for the noxious fumes emitted by passing vehicles to be extracted and replaced by clean air all along the tunnel and considerable difficulty may be experienced in achieving this. In an early paper on this subject Singstad (1) surveyed the known physiological effects of the fumes emitted by motor vehicles and emphasised the importance of good ventilation in ensuring the dilution of any injurious gases present to harmless levels. In addition, he outlined the results of work carried out to determine the laws governing the flow of air in concrete ducts of constant cross-section, associated air friction factors and power losses in bends, inlet and outlet ports.

Road tunnels in general, except comparatively short ones, require mechanical ventilation of one sort or another and the various systems ordinarily employed, together with the principles on which they are based, have been described by Atkinson, Pursall and Statham (2). Such tunnels commonly employ slot ventilation, which is essentially a method of ventilation where air enters at one end of a blind duct and is progressively bled from the duct through slots, ideally, at a uniform rate. Of course, in order to ensure that the air leaks away at a uniform rate it is necessary to suitably adjust the size of the slots from the fan end of the duct, where the duct air flow is greatest, to the

sealed-off end, where there is zero flow.

Because the slots are closely pitched along the entire length of the tunnel the controlled leakage of air may be regarded as a continuous process thus making it amenable to analysis by the calculus. Using this approach Pursall (3) devised a method of predicting the slot areas necessary to give uniform air scavenging of the tunnel thereby eliminating tedious and time consuming trial-and error methods.

A somewhat different problem is encountered in many large buildings where the air is initially supplied through main ducts which are successively sub-divided, the resulting branches being led, as required, to the various spaces needing ventilation. Dampers are usually fitted at the junctions of such branches so that by suitable adjustment of them the design volume flow of air in a branch can be attained.

However, as Ramsay (4) has pointed out, every alteration of a damper alters the flow rate in every part of the system. Since the measurement of air flow rates is inevitably a lengthy process, trial-and-error methods of setting dampers, even by highly skilled and experienced operators, can be extremely long and laborious.

Considerable amelioration of this situation is claimed for a method devised by Harrison and Gibbard (5) which is called proportional balancing. This provides a systemmatic procedure for setting dampers at branch junctions so that the correct proportion of the total air flow exists in each branch. The paper purports to show that once the dampers have been correctly set to give the correct proportions of air flow in the various distributive ducts, then these proportions will be unaffected by any changes in the magnitude of the total flow in the main supply duct. By reducing to a minimum the expenditure of time and effort spent on balancing air flows the above method represents a considerable improvement on previous trial-and-error procedures.

Ultimately, of course, the air will be fed into a branch, commonly terminating in a bulkhead, with various openings along its length and a remaining problem is to decide what size these openings should be in order to discharge specified quantities of air. Surprisingly, perhaps, very little seems to have been published on this aspect of ventilation.

Of the few publications, one, by Nelson and Smedberg (6), refers to work which is not too dissimilar to the work on which this thesis is based. It relates to a series of tests on ducts of various rectangular cross-sections having two openings along one vertical side of the duct and a third opening at the end of the duct itself, instead of a bulkhead as in this investigation. However, as the sole purpose of this series of tests was to discover the type of outlets from the duct which produced the best air flow characteristics for ventilating purposes, no attempt was made to relate the size of an outlet with the volume flow of air it discharged.

Another work by Horlock (7) mathematically analyses the flow of a fluid from a slot cut along the length of a manifold. Although this is of considerable background interest it is not directly related to the main objective of this thesis which is concerned primarily with determining what proportions of the total air flow entering a terminal duct will be discharged through the various openings or apertures situated along the duct.

Considering the above mentioned objective, it is obvious that a completely comprehensive investigation is out of the question because the number of possible variants is so large. For example, duct size and shape; size, shape, number and spacing of apertures; whether the apertures should be located on one or more sides of the duct; the method by which aperture area is to be regulated; the range of air flows entering the duct; etc.

Indeed, to obtain any worthwhile correlation of the experimental results it is obligatory to limit drastically the number of variants, the final choice of which is indicated elsewhere in this thesis. Necessarily, this means that only limited conclusions can be reached but it is hoped, nevertheless, that the information given in this thesis will help, in however small a way, to a better understanding of air distribution problems.

SECTION 2. APPARATUS AND INSTRUMENTATION.

2.1. General arrangement of small-scale air duct.

A general arrangement of the small-scale air duct and its ancillary equipment is given by Plates 1 to 3, and fig.1. Apart from a number of instrument calibration tests which were conducted using a standard laboratory low-speed wind tunnel, the entire experimental work was carried out on the 10 ft. long air duct of 8" by 4" nominal cross-section.

2.2. Air duct and fan.

Air to the duct was supplied by a radial fan having a circular inlet diameter of 7.25" and powered by a single-phase repulsion-type electric motor. Two layers of fine gauze were fitted across the fan inlet flange to filter out any relatively large dirt or soot particles which otherwise would have adversely affected the air measuring instrument readings. A hinged metal plate was provided at the fan inlet to act as an adjustable fan suction damper, so that the fan inlet opening could be varied at will and any desired air speed obtained within the available operational range.

Between the fan and the duct entrance there was a smoothing section approximately 4 ft. long consisting of three interconnected parts: a divergent section; a straight section; and a convergent section. Gauze diaphragms were fitted at each of the joints. As subsequent tests showed, this smoothing section very largely fulfilled its purpose of ensuring that the air entering the duct was reasonably uniform in velocity across the duct section.

The air duct itself was 10 ft. long, of 8" by 4" nominal cross-section, and had 12 apertures equally spaced at 9" intervals along the front face of the duct. The ceiling, floor and rear of the duct were made of $\frac{1}{2}$" thick plywood with the front face made of $\frac{1}{4}$" thick perspex.

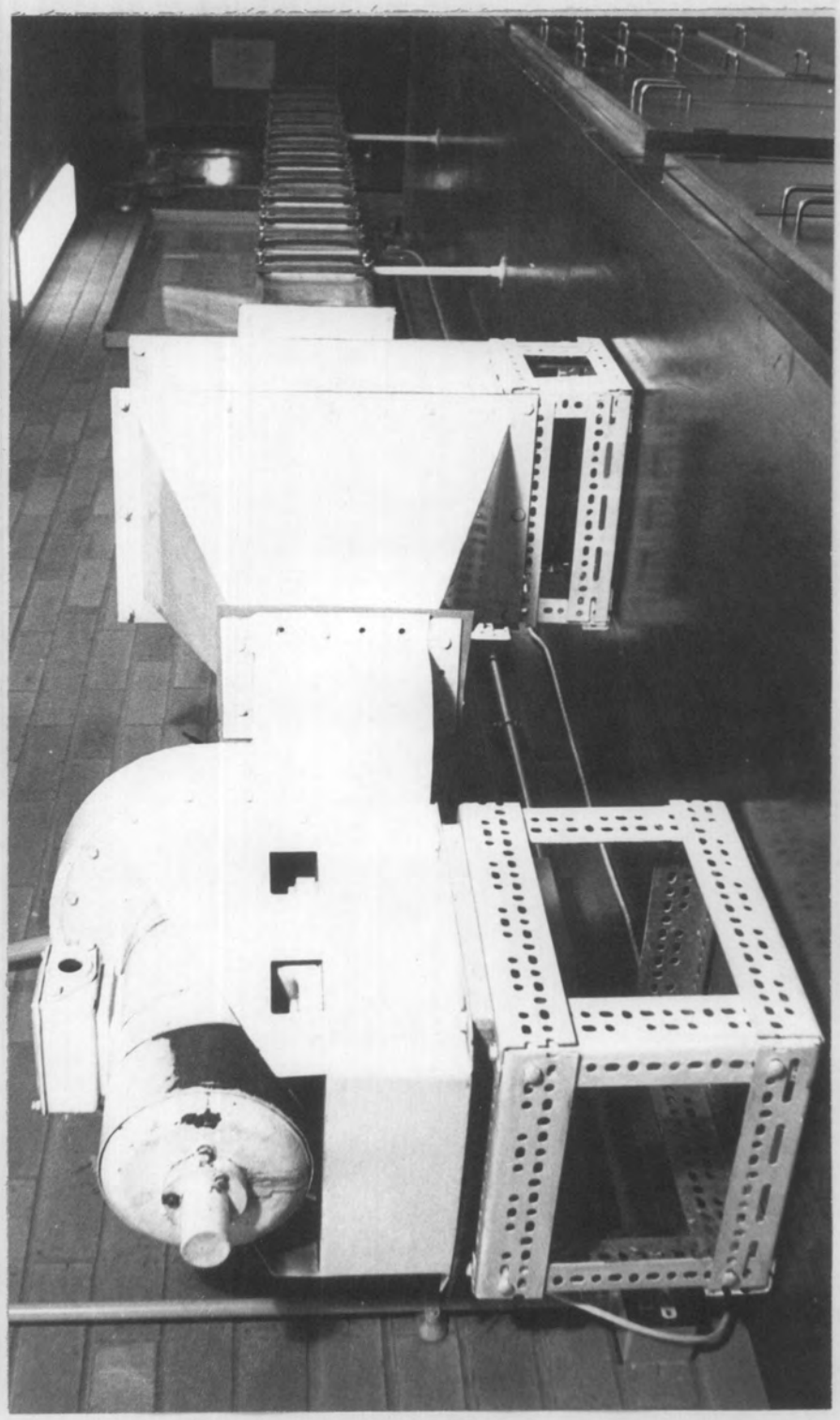

PLATE 1. MOTOR, FAN, SMOOTHING SECTION & SMALL-SCALE AIR DUCT.

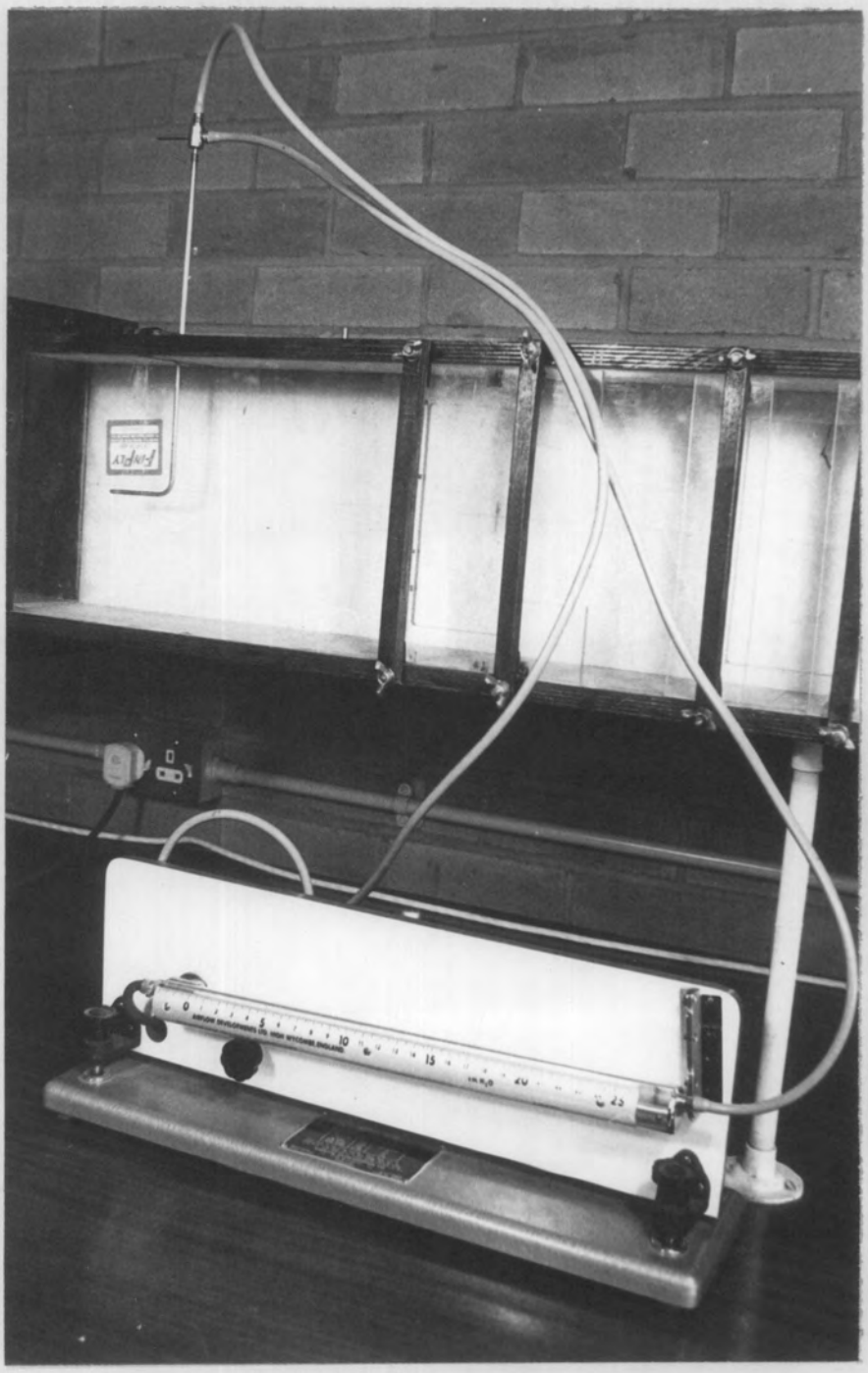

PLATE 2. PITOT-STATIC TUBE & 'AIRFLOW' MANOMETER.

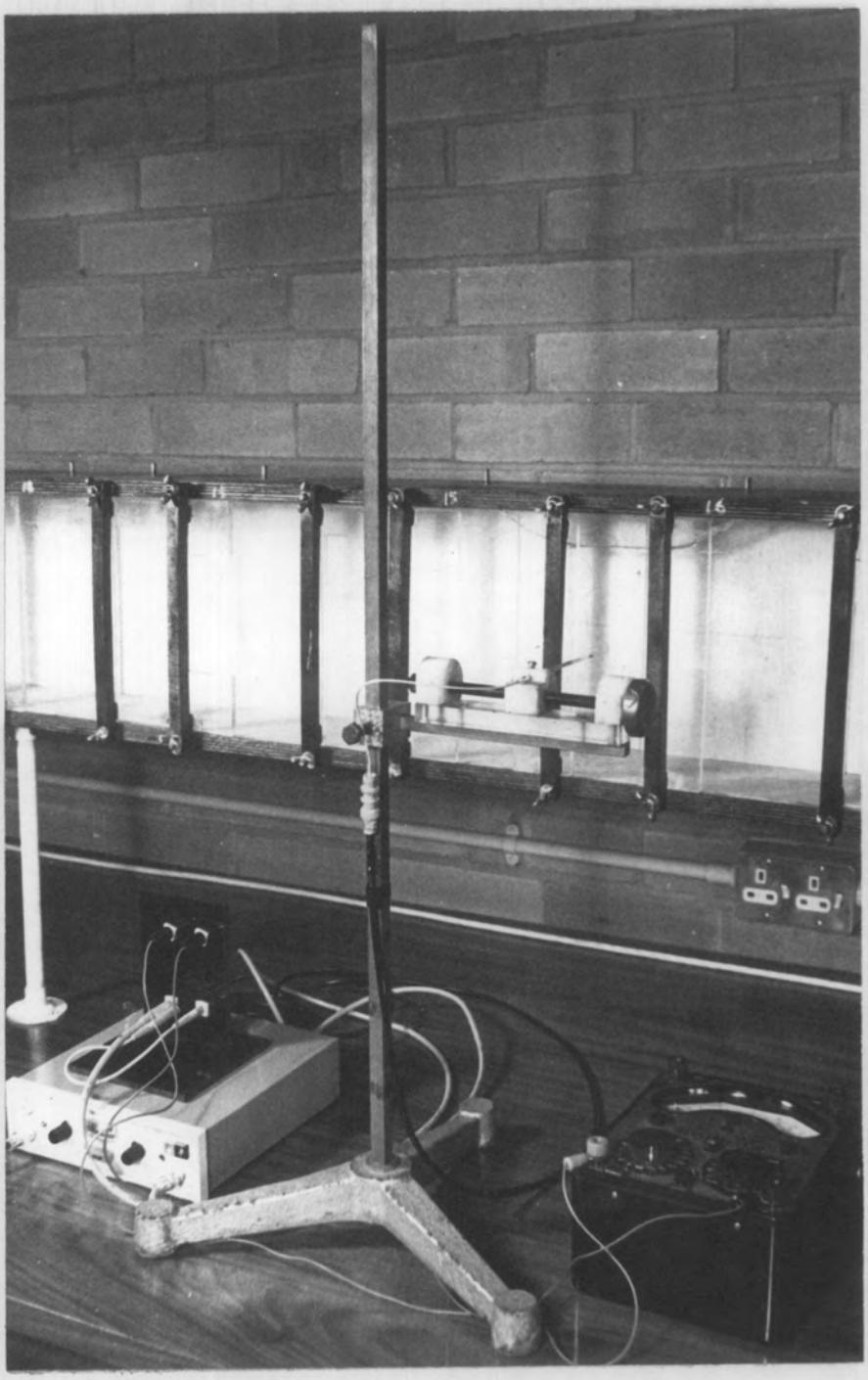

PLATE 3. HOT-WIRE ANEMOMETER & ANCILLARY EQUIPMENT.

T indicates pitot-static tube traversing plane
Static pressure tapping points on duct ceiling numbered 10 to 24

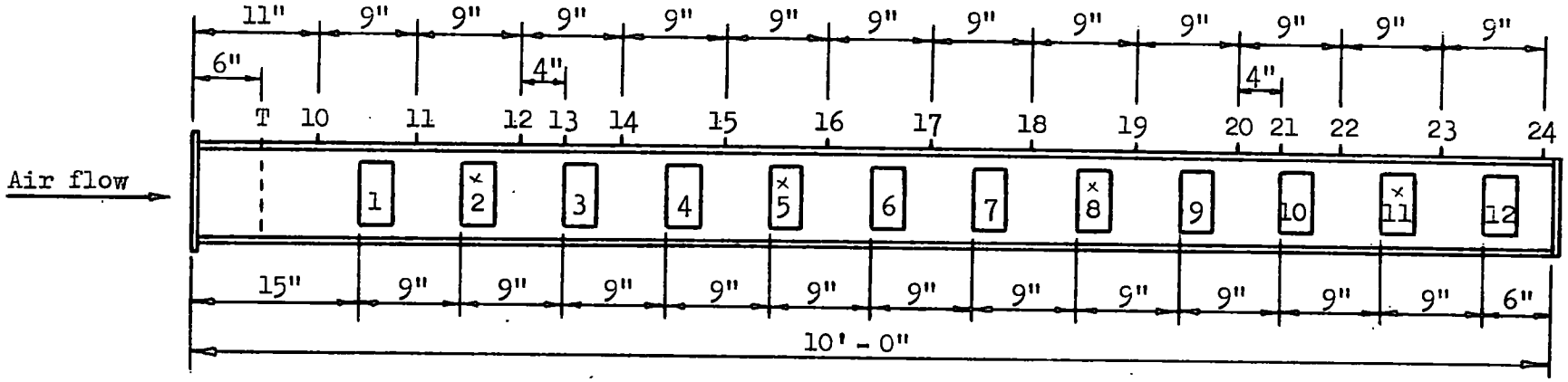

Openings 1 to 12 on front face of duct 6" by 3"

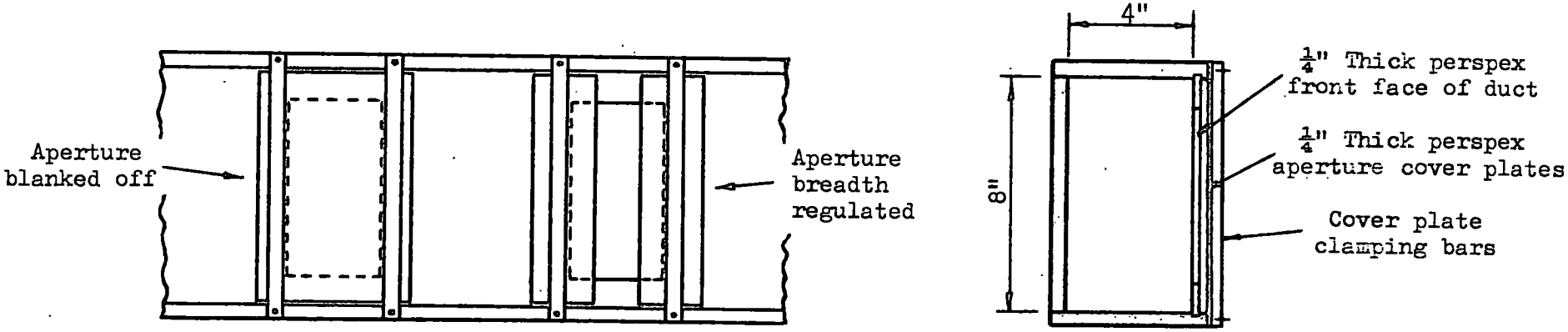

Detail showing method of blanking-off and regulating aperture area.

FIG.1 ARRANGEMENT OF THE SMALL-SCALE AIR DUCT.

It can be seen from fig.1 that the maximum aperture area available was 6" by 3" but that this could be reduced by adjustment of the $\frac{1}{4}$" thick perspex cover plates which could be clamped in any desired position. For the sake of accuracy and convenience a number of slip gauges were made ranging in width from 0.500" to 2.500" in 0.500" steps, so that aperture openings within this range could be obtained to within a tolerance of a few thousandths of an inch. Other widths for special tests were obtained using an inside micrometer. The longer edges of the perspex cover plates forming the vertical sides of an aperture were also ground flat to remove any slight irregularities which might have been present. Prior to the start of experimental work a soap solution was used to locate any slight air leaks from joints in the air duct so that they could be eliminated.

2.3. Pitot-static tube.

This instrument, which was used in conjunction with the manometer described below, was constructed throughout from stainless steel with welded joints. Its main shaft was 12" long of outside diameter 0.15" and the pitot head, which was at right angles to the shaft, was 2.5" long. Stagnation pressure was transmitted to the manometer through a single facing hole in the ellipsoidal nose at the tip of the pitot head. Static pressure was transmitted to the manometer through 4 side holes equally spaced around the periphery of the head in a plane $1\frac{1}{8}$" from the tip of the pitot head.

2.4. 'Portable Airflow Testing Set Mark 5'.

Plate 2 shows the testing set which had one adjustable limb manometer of length 12.6" which covered the following ranges according to the inclination of the manometer: 0 to 0.5" w.g.; 0 to 1" w.g.; 0 to 2" w.g.; and 0 to 10" w.g. In general, the air velocities to be measured were less than 45 ft/sec. and consequently for velocity head

measurements the 0 to 0.5" scale was the most suitable. Occasionally, for the measurement of total and static pressure heads separately, the other scales were used.

The manometer panel was connected to the base by means of a centrally placed flexible mounting at the rear and two widely spaced levelling screws at the front. Two sensitive spirit levels were set substantially parallel to lines between the flexible mounting and the two levelling screws. Thus each spirit level was affected by only one of the two levelling screws and complete levelling in all directions was carried out quickly and accurately by operating the two knobs on the front of the panel.

The manometer liquid was a pink dyed blend of paraffin having a specific gravity of 0.787 at 60°F, and zero adjustment of the manometer was effected by rotating the levelling knob on the front panel, which displaced the liquid up or down in the reservoir tank as required. For the measurement of velocity the instrument was used as a differential type manometer and for the measurement of static pressure along the air duct a connection was made from the required static pressure tapping on the duct to the reservoir tank on the manometer, the upper end of the manometer limb being open to the atmosphere. In conducting tests, frequent checks were made to ascertain that the manometer 'zeroed' properly when the pitot-static tube was inoperative, and also that bench vibration had not altered the original settings of the two spirit levels, corrective action being taken as necessary.

2.5. Battery-operated constant temperature anemometer.

Plate 3 shows the DISA type 55D05 battery-operated constant temperature anemometer used for measuring air velocity through an aperture. This entirely transistorised instrument, using a hot-wire probe as a transducer, was used to measure the instantaneous velocity of the air

at any chosen point in an aperture. Basically, the principle of measurement depends on the convective heat loss from the electrically heated hot-wire to the flow of air over the wire, and essentially, what is measured is the power required to keep the temperature of the hot-wire constant at any given operating condition.

The theory governing two-dimensional heat transfer from a cylinder shows that the square of the output voltage from the anemometer will be proportional to the square root of the velocity of the air flowing over the hot-wire probe. Although in theory it is possible to deduce the relationship between voltage and velocity, in practice it is necessary to calibrate the probe using known velocities. The probes originally used for measuring air velocity at apertures were therefore calibrated in a low-speed wind tunnel using a Prandtl-tube and Betz manometer to establish air velocities in the tunnel. It was subsequently discovered however that it was sufficiently accurate, and much more convenient, to calibrate probes against the pitot-static tube in the small-scale air duct itself and hence this is how they were usually calibrated.

Briefly, the anemometer operated as follows. The hot-wire formed one arm of a bridge circuit, the bridge being powered by an amplifier whose output voltage was controlled by the bridge unbalance. The amplifier was arranged so that if the temperature (and hence the resistance) of the hot-wire probe fell below the preselected value it caused additional current to flow through the probe, with consequent heating of the hot-wire, until the preselected temperature was reached. Conversely, if the probe temperature became too high it reduced the current until the correct temperature was attained.

Originally, a digital voltmeter was used with the anemometer but even with a degree of damping incorporated in the voltage reading

circuit it was found to be too sensitive to the voltage fluctuations corresponding to the turbulent velocity fluctuations and it was eventually discarded. In place of it a Universal Avometer was used which, with its inherently lower frequency response, proved a much more satisfactory instrument for obtaining the necessary mean velocity readings.

SECTION 3. PITOT-STATIC TUBE EXPERIMENTAL TECHNIQUE.

3.1. Calibration of the pitot-static tube and 'Airflow' manometer.

Before giving detailed consideration to any particular method of measuring air flow it was decided to check the accuracy of the pitot-static tube and its associated 'Airflow' single-limb inclined manometer by calibration against a relatively large Prandtl tube in a standard laboratory low-speed wind tunnel. Since the suppliers of the Prandtl tube and the Betz manometer to which it was attached guaranteed these instruments to a high order of accuracy it was felt that readings recorded from them could be regarded as 'true' and could be used as a standard with which the pitot-static tube readings could be compared. Fig.2 shows the arrangement for the calibration test, for which the following procedure was adopted.

With the Prandtl tube positioned as shown in fig.2(a) and connected to the Betz manometer, which read in kgf/m^2, the fan suction damper was adjusted to give a suitable air speed and the manometer reading in kgf/m^2 on the manometer was recorded. As shown in fig.2(b) the Prandtl tube was then retracted and the pitot-static tube lowered vertically through its split collets until its stagnation hole was in the same position as that occupied by the tip of the Prandtl tube a moment before. After allowing adequate time for the reading on the 'Airflow' manometer to steady, its value was recorded. The pitot-static tube was then raised to its uppermost position, the Prandtl tube repositioned, and it was verified that the reading on the Betz manometer had not changed by any significant amount. By suitable adjustment of the fan suction damper various air speeds were selected and the corresponding readings on the Betz and 'Airflow' manometers were obtained. Fig.3 shows that the deviation of the pitot-static tube readings from the true values was extremely small, well within 2%, over the range of values to be

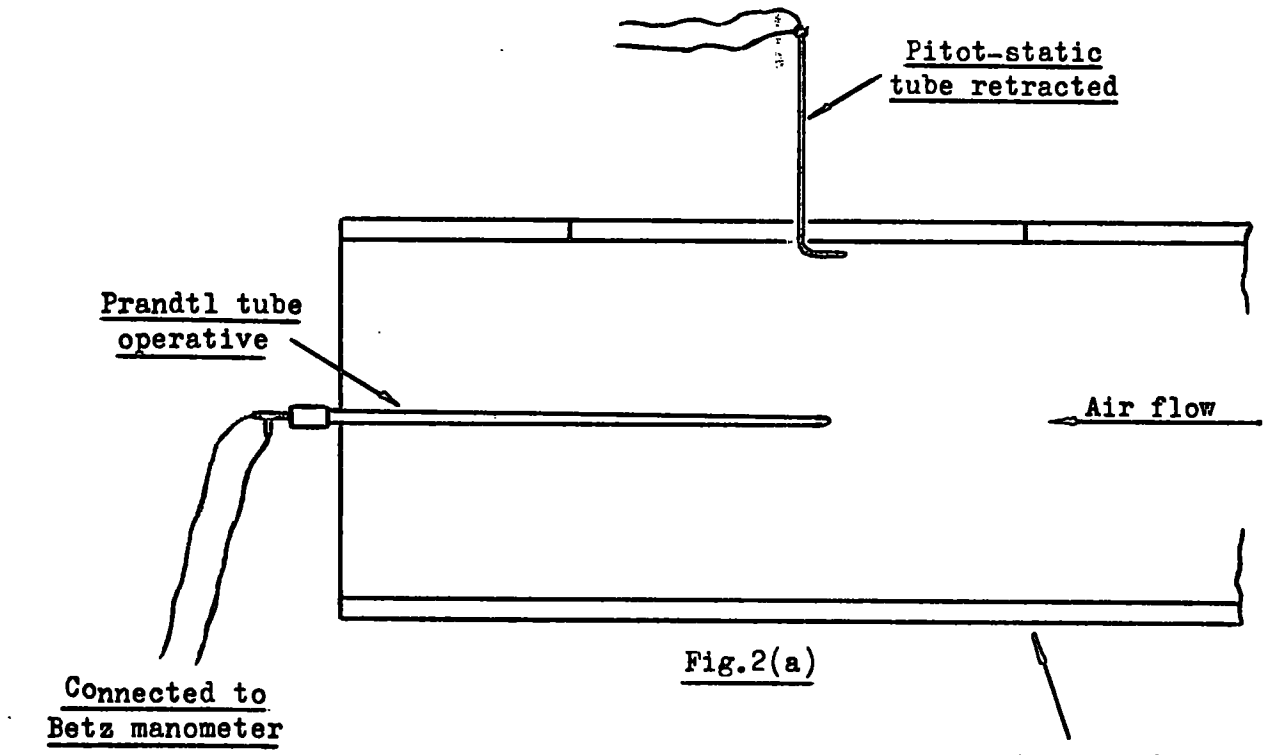

Fig.2(a)

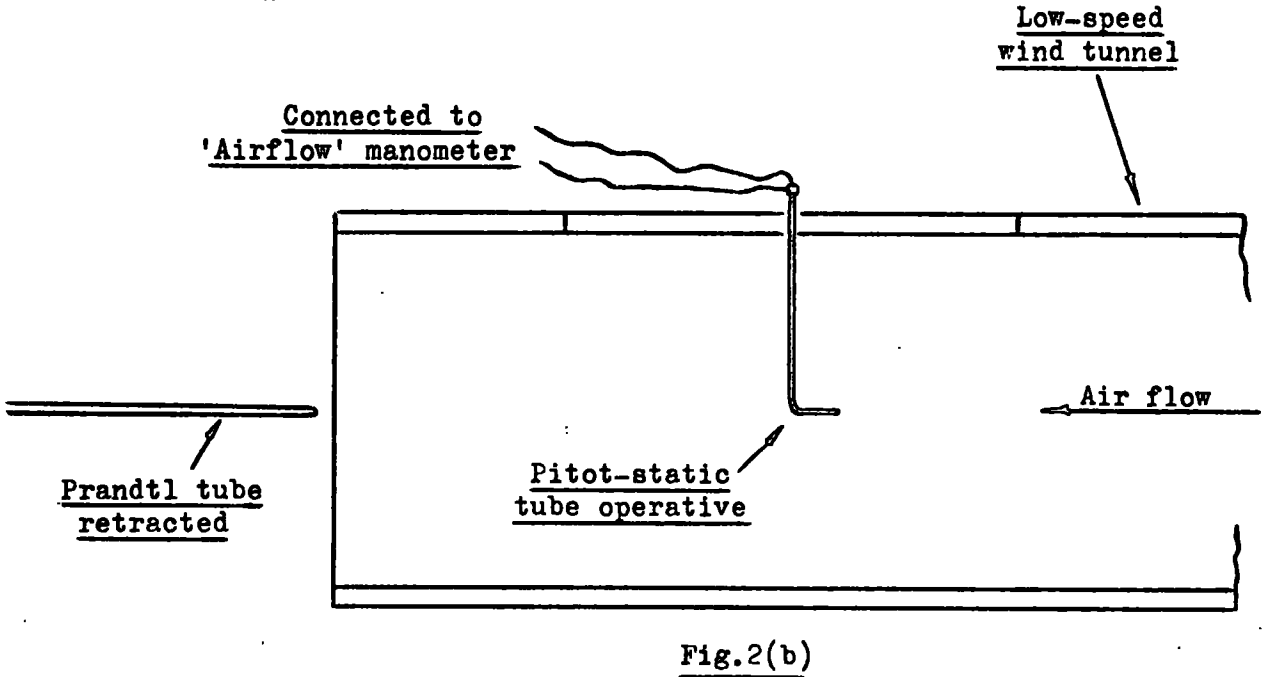

Fig.2(b)

FIG.2 CALIBRATION OF THE PITOT-STATIC TUBE & 'AIRFLOW' MANOMETER AGAINST A PRANDTL TUBE & BETZ MANOMETER.

Column 'A' Pitot-static tube & 'Airflow' manometer readings.

Column 'B' Conversion of column 'A' readings to kgf/m^2.

Column 'C' Prandtl tube & Betz manometer readings.

1 in.w.g. = 25.4 kgf/m^2.

'A' ins.w.g.	'B' kgf/m^2.	'C' kgf/m^2.
0.0320	0.813	0.82
0.0620	1.575	1.56
0.1130	2.87	2.83
0.2045	5.20	5.13
0.2965	7.53	7.42
0.4445	11.30	11.10

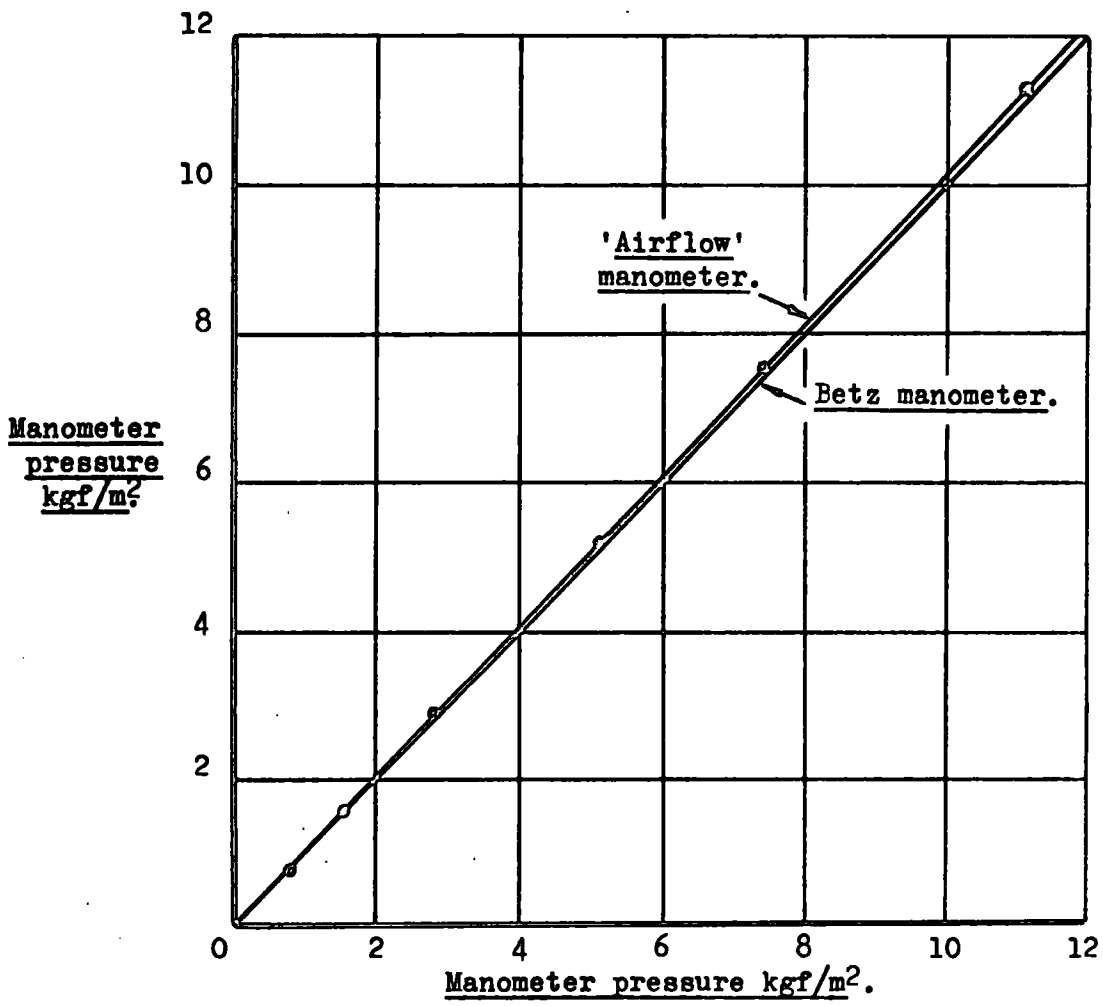

FIG. 3 CALIBRATION OF PITOT-STATIC TUBE & 'AIRFLOW' MANOMETER AGAINST PRANDTL TUBE & BETZ MANOMETER.

encountered using the small-scale air duct.

3.2. Measurement of the volume flow of air entering the duct.

An essential purpose of this investigation was to determine in detail how a given volume flow of air entering the duct would be discharged through the various apertures situated along the duct. Consequently, it was necessary to decide how both the duct inlet and aperture air flows could be measured with acceptable accuracy. Considering first the incoming air, it would naturally have been desirable to measure the volume flow by two independent methods and a calibrated orifice as one method, and a pitot-static tube traverse as the other, were two that obviously suggested themselves.

The use of an orifice plate however was not physically possible because the limited space in the vicinity of the test rig would not permit the installation of the two comparatively long sections of circular duct necessary on either side of the orifice plate. This, of course, left the pitot-static tube traverse as the sole practicable method of measuring the incoming air flow.

Although, as mentioned above, it would have been preferable to have had a second corroborative method of measuring the incoming air flow, it was felt that, provided certain precautions were taken, the pitot-static tube traverse would be in itself satisfactory. One self-evident precaution was to locate the traversing plane sufficiently far upstream of the first aperture to ensure that under all test conditions the flow there would be parallel with the duct.

A convenient location was 9" upstream of N°1 aperture's leading edge and tests here with simple flow indicators showed that the air flow was virtually parallel with the length of the duct even when N°2 aperture was fully open. With N°1 aperture open however the air flow deviated from parallel to an extent, which although slight,

suggested that it would not be desirable to conduct tests with this aperture open. It was decided therefore that N°1 aperture would be permanently covered and on this understanding a $\frac{1}{2}$" wide transverse slot was cut in the ceiling of the duct at the above stated location and labelled the T (traversing) plane. Wooden split collets were made which fitted tightly into the slot and through which the pitot-static tube could be inserted and gripped in any selected position.

A Ministry of Technology report, NEL Report N°251, (8) indicated that for rectangular ducts a 26-point traverse was in most cases more accurate than the 48-point method given in the 1943 British Standard for flow measurement so it was decided to consider the application of the former, shorter, method. Fig.4 shows the required positions of the 26 measuring points in the nominally 8" by 4" air duct. Since it was considered feasible to introduce the pitot-static tube only through the ceiling of the duct at the T plane, it was evident that the use of the 26-point method would require 9 vertical traverses. As this would take an appreciable amount of time it was felt that an acceptable compromise might be the 25-point traverse shown in fig.5 which would reduce the number of vertical traverses from 9 to 5, provided this did not lead to any significant error in the measurement of the air flow. Several tests under varying conditions were therefore carried out with the volume flow being measured by both the 26-point and the 25-point traversing methods the results of which showed that, for this small-scale duct at least, there was no important difference between the two differently computed air flows.

Figs.6 to 9 show typical velocity head readings and velocity contours obtained from initial tests with various aperture openings from which it was apparent that the air flow was reasonably constant across the duct section for any given aperture setting.

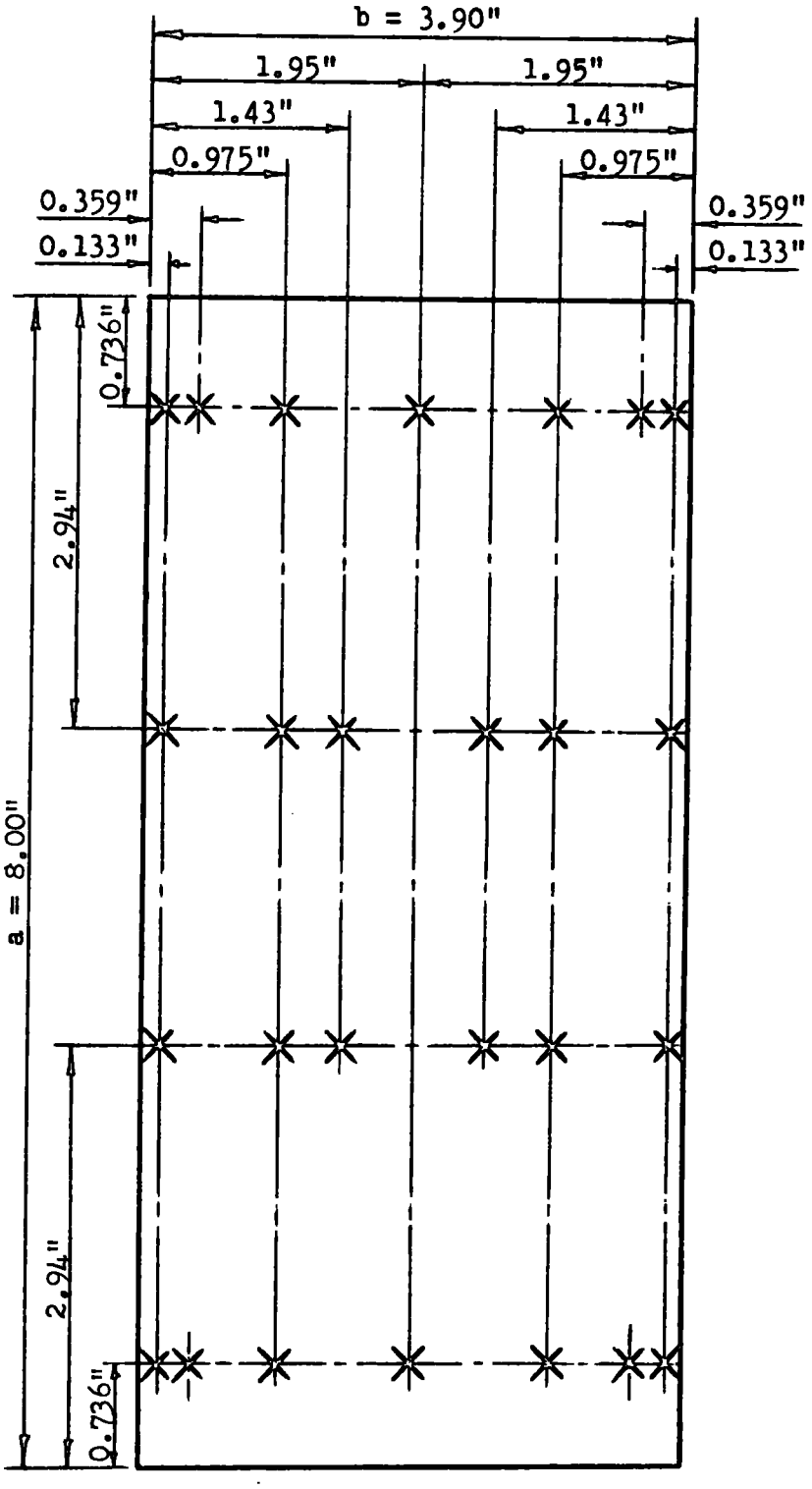

Nominal cross-section of duct : 8" by 4"

Measured cross-section of duct : 8.00" by 3.90"

FIG.4 TRAVERSING POSITIONS OF 26-POINT LOG-LINEAR METHOD OF MEASURING AIR FLOW. (N.E.L. REPORT N° 251)

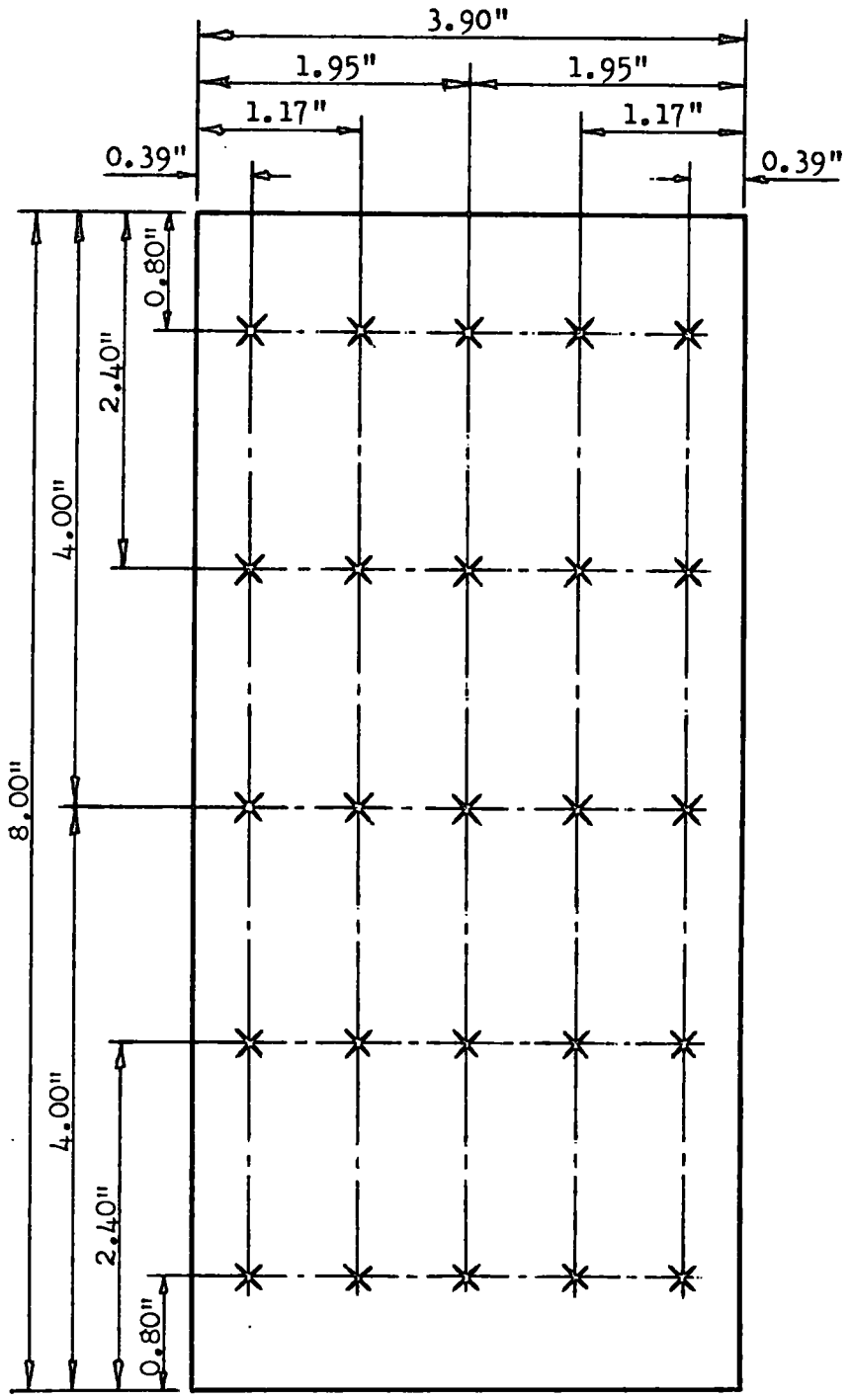

Bottom of duct

Nominal cross-section of duct : 8" by 4"

Measured cross-section of duct : 8.00" by 3.90"

FIG.5 TRAVERSING POSITIONS OF 25-POINT METHOD OF MEASURING AIR FLOW.

COMPARISON BETWEEN THE AVERAGE VELOCITY COMPUTED FROM THE 26-POINT LOG-LINEAR METHOD AND THE 25-POINT METHOD OF TRAVERSING THE DUCT.

Barometer : 29.68 "Hg

Air temp. : 76°F

$U = 66.7\sqrt{\frac{30.0}{29.68} \times \frac{536}{528} \times h_v}$ ft/sec. $= 67.5\sqrt{h_v}$ ft/sec.

h_v = Velocity head ins.w.g.

Points 1 to 26, and 1 to 25, numbered from left to right, starting from top of duct, looking upstream.

Point	h_v ins. w.g.	$\sqrt{h_v}$	U ft/sec
1	0.285	0.534	36.0
2	0.293	0.541	36.5
3	0.280	0.529	35.7
4	0.279	0.528	35.7
5	0.281	0.530	35.8
6	0.283	0.532	35.9
7	0.277	0.526	35.5
8	0.256	0.506	34.2
9	0.248	0.498	34.6
10	0.241	0.491	33.2
11	0.241	0.491	33.2
12	0.248	0.498	33.6
13	0.251	0.501	33.8
14	0.229	0.479	32.3
15	0.228	0.478	32.3
16	0.224	0.473	32.0
17	0.225	0.473	32.0
18	0.227	0.476	32.1
19	0.232	0.482	32.5
20	0.219	0.468	31.6
21	0.222	0.471	31.8
22	0.218	0.467	31.5
23	0.226	0.475	32.1
24	0.222	0.471	31.8
25	0.219	0.468	31.6
26	0.219	0.468	31.6

Average velocity = 33.4 ft/sec.

Point	h_v ins. w.g.	$\sqrt{h_v}$	U ft/sec
1	0.287	0.536	36.2
2	0.280	0.529	35.7
3	0.277	0.526	35.5
4	0.283	0.532	35.9
5	0.280	0.529	35.7
6	0.269	0.519	35.0
7	0.250	0.500	33.8
8	0.250	0.500	33.8
9	0.263	0.513	34.7
10	0.259	0.509	34.4
11	0.246	0.496	33.5
12	0.237	0.487	32.9
13	0.231	0.481	32.5
14	0.230	0.480	32.4
15	0.239	0.489	33.0
16	0.225	0.473	31.9
17	0.223	0.472	31.9
18	0.223	0.472	31.9
19	0.227	0.476	32.2
20	0.226	0.475	32.1
21	0.219	0.468	31.6
22	0.220	0.469	31.7
23	0.226	0.475	32.1
24	0.222	0.471	31.8
25	0.220	0.471	31.8

Average velocity = 33.4 ft/sec.

A further noticeable feature was that the velocity calculated from the centre point reading alone was only slightly lower than the average velocity in the duct deduced from the 25-point traverse. Many subsequent tests showed that the ratio of the air velocity calculated from the centre point reading only was consistently 2 to 2½% lower than the true average velocity. Hence, in carrying out tests it was not strictly necessary to measure the velocity head at 25 points. Instead, the velocity calculated from the centre point could be simply multiplied by 1.02 to give a sufficiently accurate velocity. Usually, however, the 25-point traverse was made as a safeguard against any possible changes in the simple correlation given above. In cases where the air velocity distribution in the duct was of no special interest time was saved by finding the square root of the arithmetric average velocity head rather than finding the square roots of the 25 individual velocity heads and then taking the average. Because the variation in the velocity heads across the duct was so small it was of course quite accurate to adopt this simplifying procedure.

3.3. Measurement of the volume flow of air discharged from the apertures.

Having established that the above mentioned 25-point pitot-static tube traverse, or even a single centre-point reading, was a sufficiently accurate way of measuring the air flow entering the duct, the next matter for consideration was the method of measuring the air issuing from the apertures. It seemed reasonable to assume initially that the vertical variation of air velocity in an aperture would be very small, in which case a transverse measurement of air velocity at half aperture height would be representative of the average aperture air velocity.

An immediate problem concerning the direct measurement of air flow through an aperture was the fact, established by the use of flow indicators, that in the horizontal plane the direction of the issuing air varied

Barometer : 29.71 "Hg

Air temp. : 80°F

$U = 66.7\sqrt{\frac{30.0}{29.71} \times \frac{540}{528} \times h_v}$ ft/sec. $= 67.7\sqrt{h_v}$ ft/sec.

h_v = Velocity head ins.w.g.

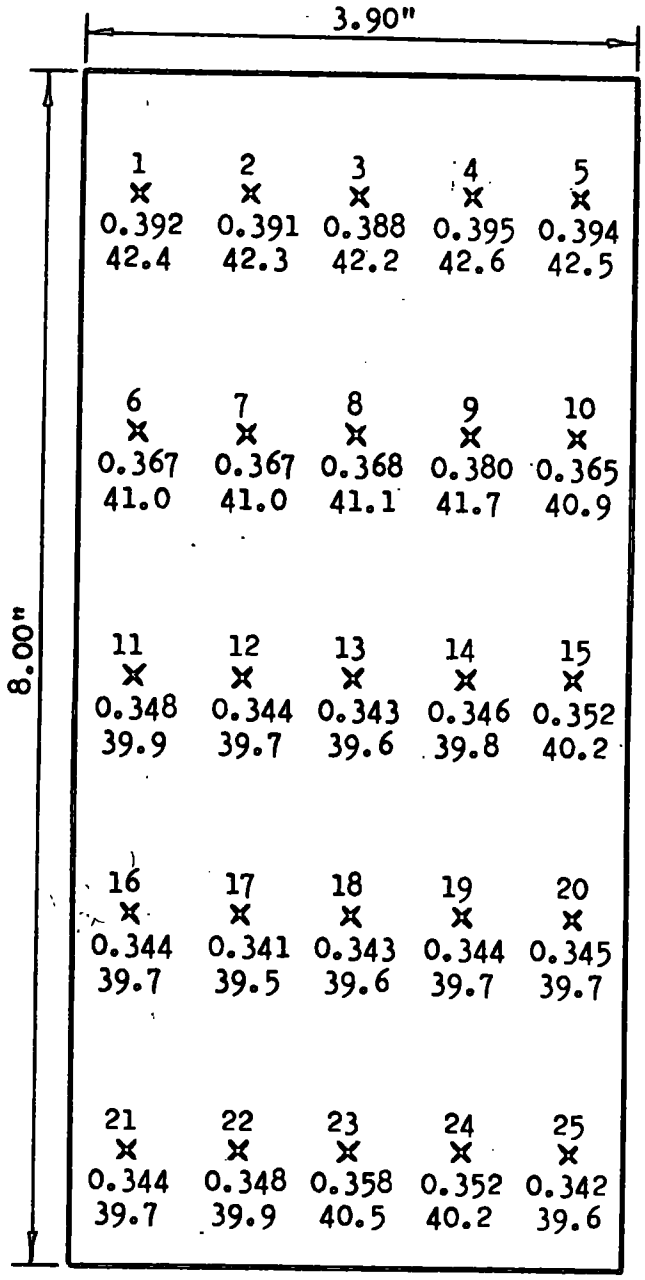

Bottom of duct

(Looking upstream)

Upper numbers : Location of 25 measuring points.

Middle numbers: Velocity heads ins.w.g.

Lower numbers : Air velocities ft/sec.

FIG.6 VELOCITY HEAD MEASUREMENTS USING 25-POINT TRAVERSING METHOD. APERTURES 2,5,8 & 11, 6" by 2". AIR FLOW 8.80 ft^3/sec.

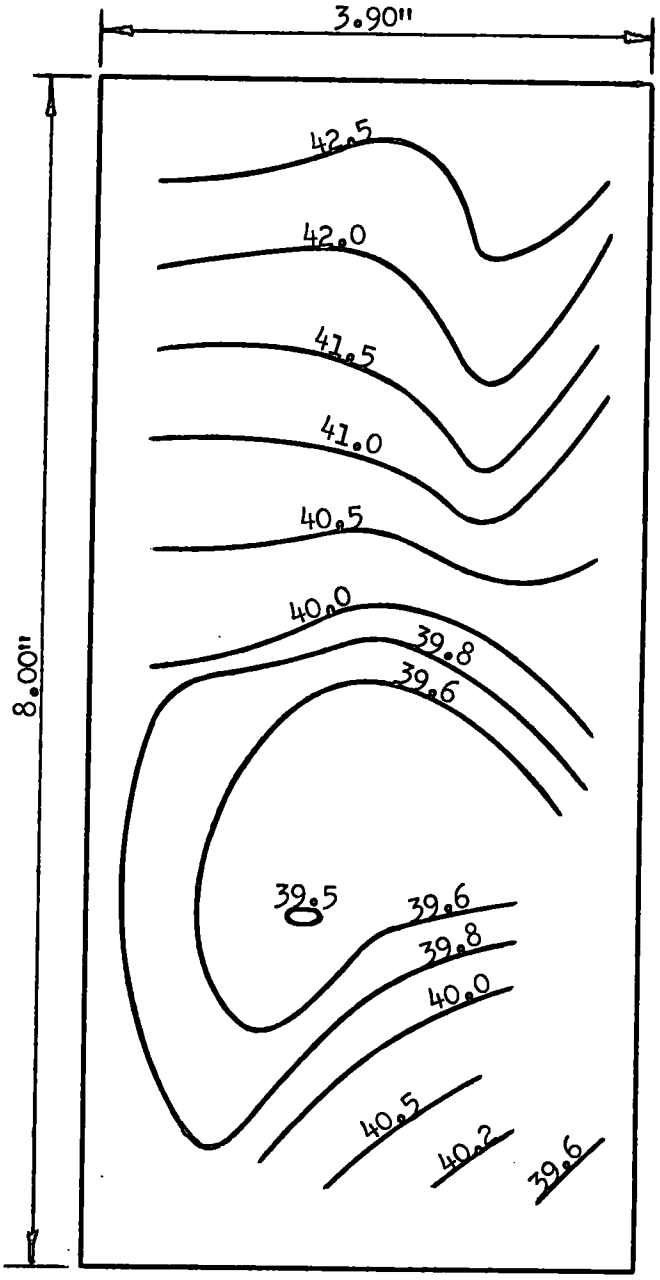

Lines of const. vel. numbered in ft/sec.

Bottom of duct.

(Looking upstream)

FIG.7 VELOCITY CONTOURS OF AIR FLOW AT T PLANE.

APERTURES 2,5,8 & 11, 6" by 2".

AIR FLOW 8.80 ft^3/sec.

Barometer : 29.90 "Hg

Air temp. : 81°F

$U = 66.7\sqrt{\frac{30.0}{29.90} \times \frac{541}{528} \times h_v}$ ft/sec. $= 67.7\sqrt{h_v}$ ft/sec.

h_v = Velocity head ins.w.g.

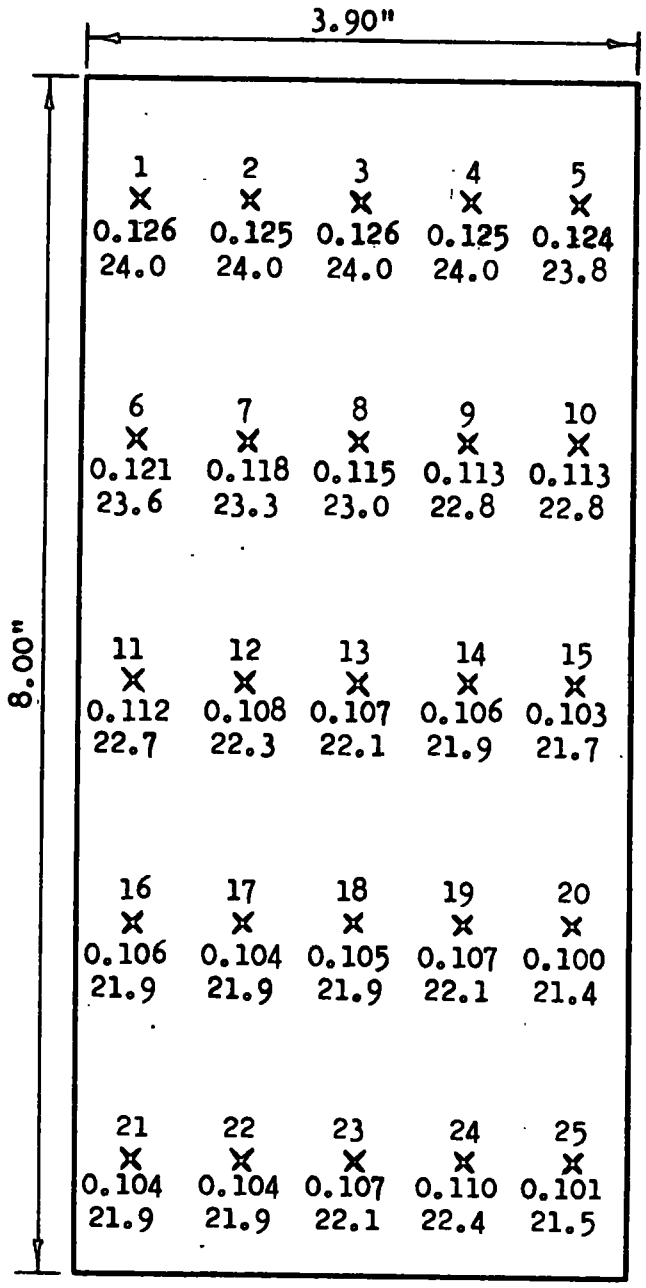

Bottom of duct

(Looking upstream)

Upper numbers : Location of 25 measuring points.

Middle numbers: Velocity heads ins.w.g.

Lower numbers : Air velocities ft/sec.

FIG.8 VELOCITY HEAD MEASUREMENTS USING 25-POINT TRAVERSING METHOD.
APERTURES 2,5,8 & 11, 6" by 2". AIR FLOW 4.90 ft^3/sec.

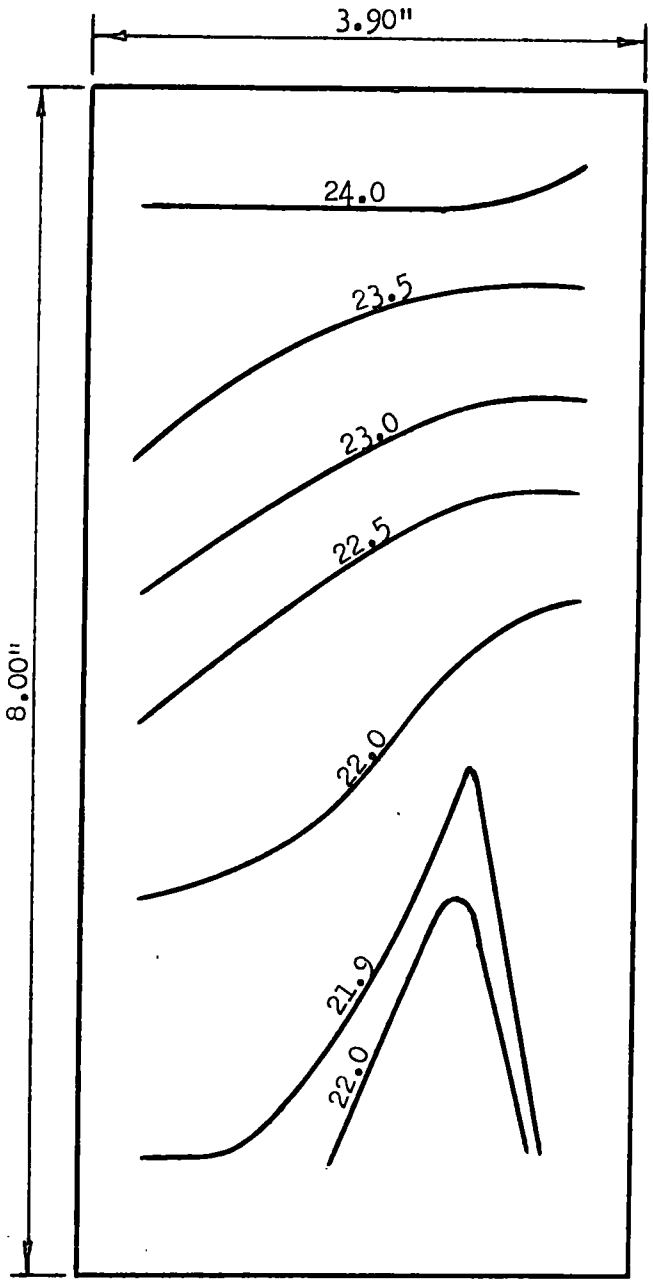

Lines of const. vel. numbered in ft/sec.

Bottom of duct.
(Looking upstream)

FIG.9 VELOCITY CONTOURS OF AIR FLOW AT T PLANE.
APERTURES 2,5,8 & 11, 6" by 2"
AIR FLOW 4.90 ft^3/sec.

considerably across an aperture and also there was a variation in the velocity pattern from aperture to aperture. This meant that before taking any readings in the plane of the aperture the pitot-static tube had to be aligned as exactly as possible with the issuing air. It was soon evident from a number of tests that this method of measuring the air flow was highly unsatisfactory because the total flow from the apertures was measured as considerably greater than that entering the duct, which of course was impossible.

As fig.10 indicates, the tip of the pitot-static tube had been deliberately kept $\frac{1}{8}$" in from the outside face of the aperture cover plates during a half-height horizontal traverse in order to measure the total pressure of the outflowing air in the correct measuring plane. It was obvious however that with this arrangement the static pressure was being recorded $1\frac{1}{8}$" from the measuring plane. A test was therefore conducted to determine the variation in static pressure as the pitot-static tube was withdrawn from the measuring plane, a typical result of which is also shown by fig.10. Because the variation in static pressure was so sensitive to the distance of the static tappings from the measuring plane, and also because it was not satisfactory to attempt to measure total and static pressures separately at the same point, it was concluded that direct measurement of the air issuing from an aperture with the pitot-static tube was quite impracticable.

A possible alternative to direct measurement of aperture air flow appeared to be the measurement of the air flowing along the duct at sections upstream and downstream of an aperture, the difference between the two quantities evidently being the amount of air that had been discharged through the aperture. This had a number of disadvantages, the chief being that for some distance both upstream and downstream of an aperture the air flowing in the duct was disturbed and had

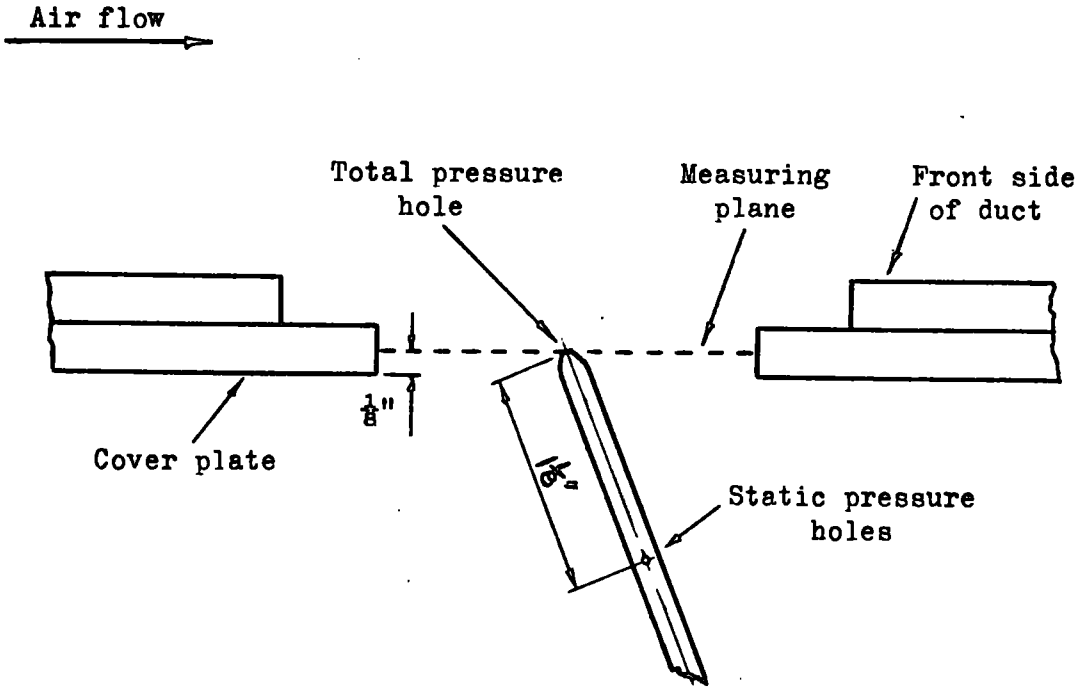

Plan on duct.

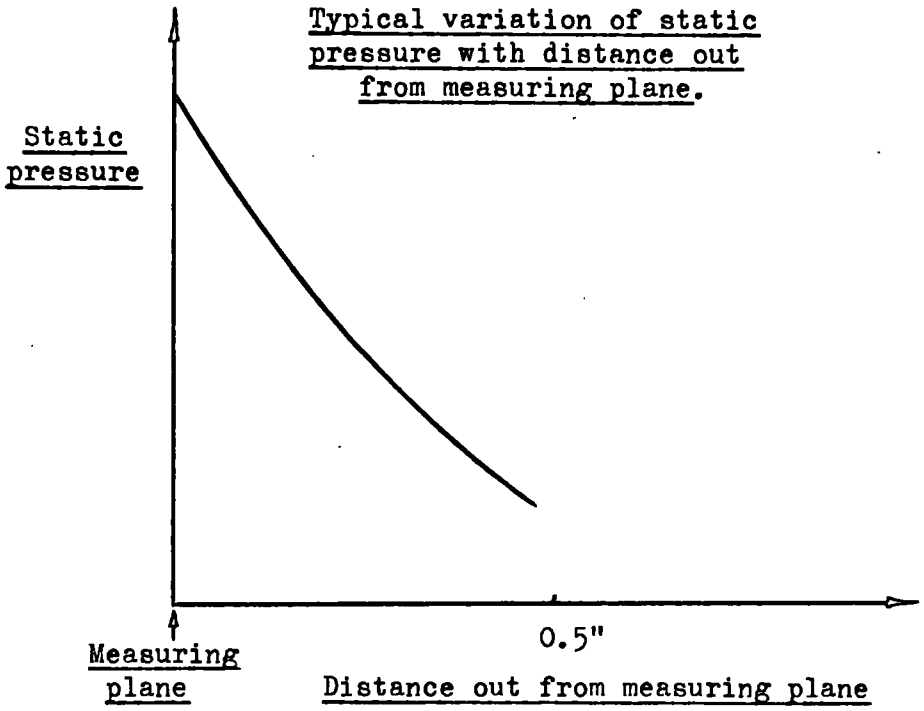

FIG.10 PITOT-STATIC TUBE MEASUREMENTS AT AN APERTURE.

appreciable transverse components which made correct alignment of the pitot-static tube very difficult. Again, there was the aforementioned difficulty that the total and static pressures were being measured at unrelated positions.

Additionally, there could be no corroboration of the measurement of the quantity of air entering the duct because the air discharged from the last aperture could be obtained only by finding the difference between the incoming air quantity and the sum of the other aperture air quantites. A final difficulty was that as the air flowing along the duct diminished in magnitude the manometer readings were correspondingly reduced with a consequent increase in experimental error in recording the manometer values. Inevitably, the conclusion reached from a number of tests on the above lines was that this was not a reliable way of obtaining individual aperture air flows and it was decided that some other method would have to be evolved and to this end a hot-wire anemometer was procured, the use of which is described in the next Section.

SECTION 4. HOT-WIRE ANEMOMETER EXPERIMENTAL TECHNIQUE.

4.1 Calibration of the hot-wire probes.

Four hot-wire probes were supplied with the DISA anemometer and for identification purposes these were labelled P1, P2, P3 and P4, because although nominally identical each probe had in fact its own particular voltage-velocity characteristic. Initially it was decided to calibrate only the probe P1 since it was thought that with careful handling this would last through the entire series of tests. Of course, it was realised from the beginning that because of the extreme fragility of the hot-wire, which was only 5 microns in diameter, accidental breakage was always a possibility and that, therefore, the other probes might eventually have to be calibrated and used.

Although the probe P1 was to be used for measurements in the small-scale air duct it was considered preferable to calibrate it in a separate low-speed wind tunnel because it was known that the air flow in the working section of the tunnel was quite parallel and fig.11 indicates how this was done. The calibration consisted of two separate tests: one to determine the voltage-velocity characteristic of the probe with the hot-wire at 90° to the air stream; and the other, for several chosen fixed air speeds, to turn the probe through 180° in 5° steps and record the corresponding variation in voltage.

For the former test the probe P1 was inserted through the ceiling of the wind tunnel with the hot-wire $3\frac{1}{2}$" below the tunnel ceiling and at 90° to the air flow as shown by fig.11. The tip of the Prandtl tube was then positioned in line with, and $1\frac{1}{4}$" downstream of, the hot-wire. Voltages were then recorded on the Universal Avometer and air velocity pressure heads on the 'Airflow' manometer.

By adjustment of the tunnel fan suction damper various air speeds were obtained from about 13 ft/sec. to 95 ft/sec. and the corresponding

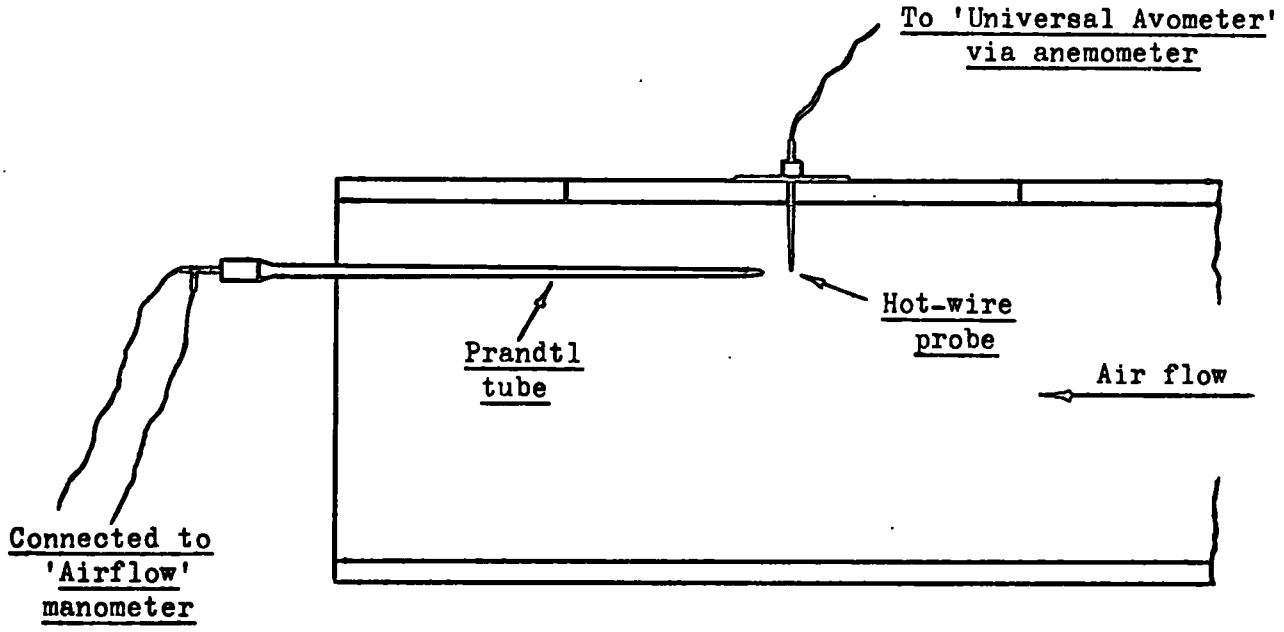

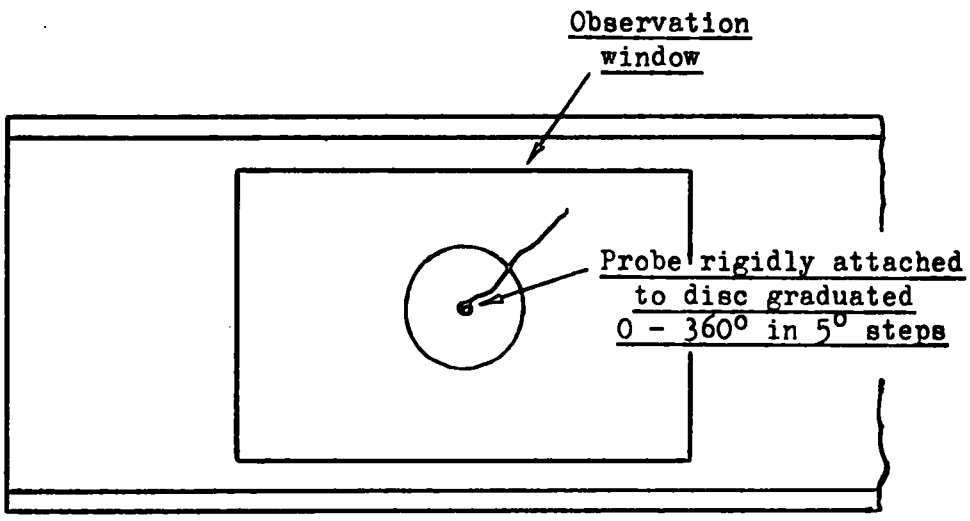

Plan on low-speed wind tunnel

FIG.11 CALIBRATION OF HOT-WIRE PROBE IN LOW-SPEED WIND TUNNEL.

voltages were recorded with the hot-wire at first 90° (and then 270° to the air stream to see if there was any variation in the voltages thus obtained). As might have been anticipated there was virtually no difference between the voltages obtained at 90° and at 270°. A note was also made of the voltage reading with the fan switched off. The results are given in Table 1 from which the graph shown by fig.12 was plotted. This graph verified the theoretical relationship that the square of the voltage is directly proportional to the square-root of the air velocity and also allowed an extrapolation to be made to lower air speeds than those which could be obtained in the low-speed wind tunnel. Because this graph was not convenient to use the graph shown by fig.13 was constructed and to obtain consistency of readings Table 2 was drawn up. As an additional check the probe P1 was subsequently placed in the small-scale air duct and re-calibrated against the pitot-static tube. The points thus obtained are also shown by fig.12 and it can be seen that they lie almost exactly on the first calibration curve. This suggested that it might not be necessary to use the low-speed wind tunnel for calibrating probes, the calibration in the small-scale air duct itself being evidently sufficiently accurate and certainly more convenient to carry out.

Table 3 shows the results of the second calibration test where the probe was turned through 180° at various selected fixed air speeds. From these results the graphs of voltage variation against angle of hot-wire were obtained as shown by fig.14. These graphs enabled the graphs shown by fig.15 to be plotted, which in turn provided the graphs shown by fig.16. Hence, to calculate the normal air velocity component at any chosen point in an aperture it was only necessary to record the voltage, first with the hot-wire vertical, and then with the hot-wire

TABLE 1.

VOLTAGE - VELOCITY CHARACTERISTIC OF HOT-WIRE PROBE P1.

Air velocity $U = 66.7 \sqrt{\frac{30.0}{B} \times \frac{T}{528} \times h}$

h = velocity head ins.w.g.

At test { Barometer B = 29.78 ins.Hg.
Air temp. T = 536°R

Hence $U = 67.4 \sqrt{h}$ ft/sec.

Volts V			Manometer	V^2	Air vel.	$\sqrt{U}$
90°	270°	Average	h ins.w.g.		U ft/sec.	
1.81	1.81	1.81	0.0345	3.28	12.5	3.54
1.825	1.82	1.823	0.0355	3.32	12.7	3.56
1.865	1.86	1.863	0.057	3.47	16.1	4.01
1.915	1.915	1.915	0.083	3.67	19.4	4.41
1.92	1.92	1.92	0.0915	3.69	20.4	4.52
1.955	1.955	1.955	0.131	3.82	24.4	4.94
2.00	2.00	2.00	0.166	4.00	27.4	5.24
2.01	2.01	2.01	0.195	4.04	29.8	5.46
2.05	2.05	2.05	0.253	4.20	33.9	5.82
2.09	2.095	2.093	0.342	4.38	39.4	6.28
2.10	2.10	2.10	0.348	4.41	39.8	6.31
2.13	2.13	2.13	0.446	4.54	45.0	6.71
2.155	2.16	2.158	0.558	4.66	50.4	7.10
2.20	2.20	2.20	0.715	4.84	57.1	7.55
2.22	2.22	2.22	0.768	4.93	59.0	7.68
2.235	2.24	2.238	0.880	5.01	63.3	7.96
2.26	2.265	2.263	1.05	5.12	69.1	8.31
2.295	2.295	2.295	1.23	5.27	74.7	8.64
2.315	2.32	2.318	1.43	5.37	80.5	8.97
2.35	2.355	2.353	1.77	5.54	89.6	9.47
2.37	2.375	2.373	1.98	5.63	94.8	9.74
2.38	2.385	2.383	2.11	5.68	97.9	9.89

Voltage at zero air flow 1.40 volts.

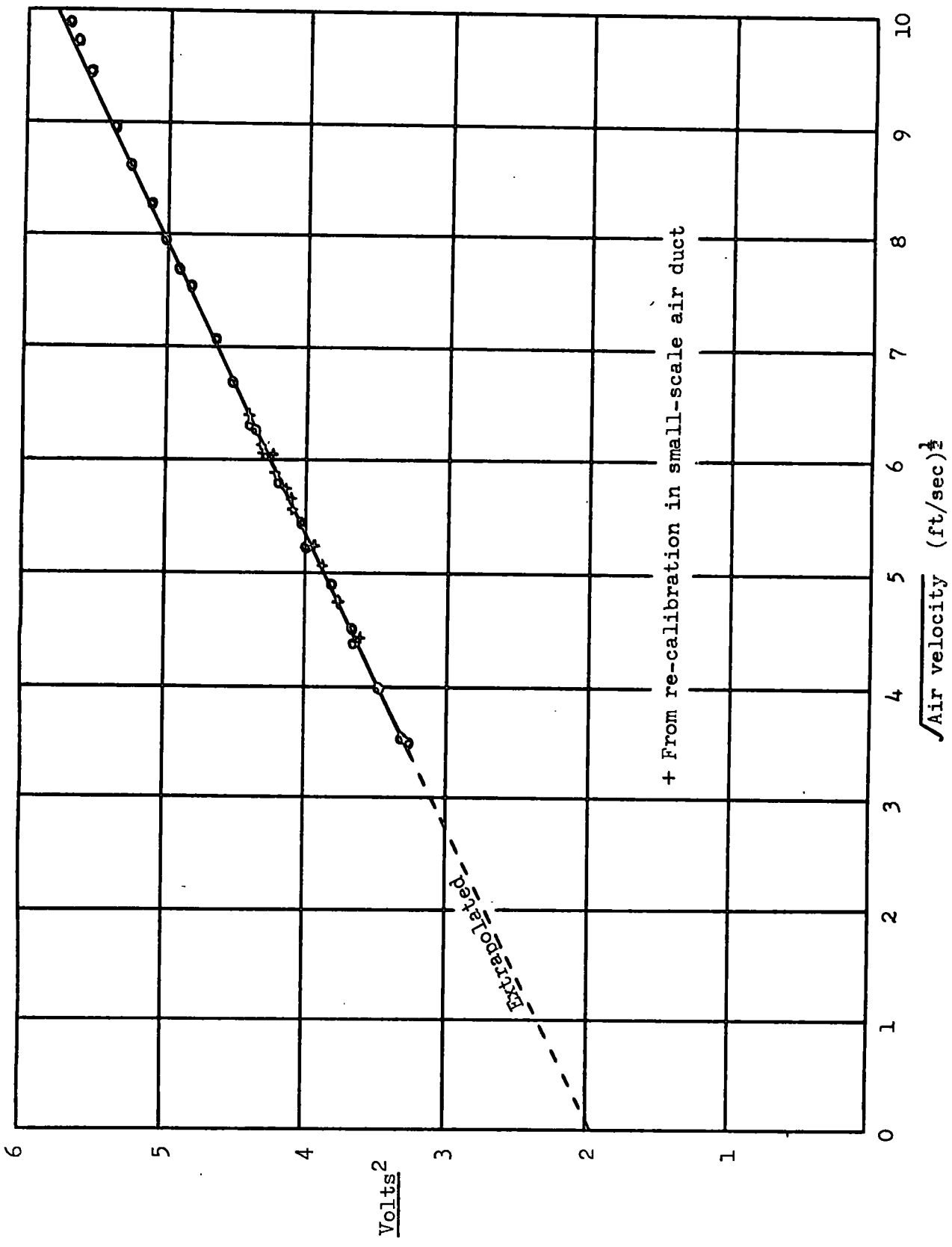

FIG.12 VOLTAGE - VELOCITY CHARACTERISTIC OF HOT-WIRE PROBE P.1.

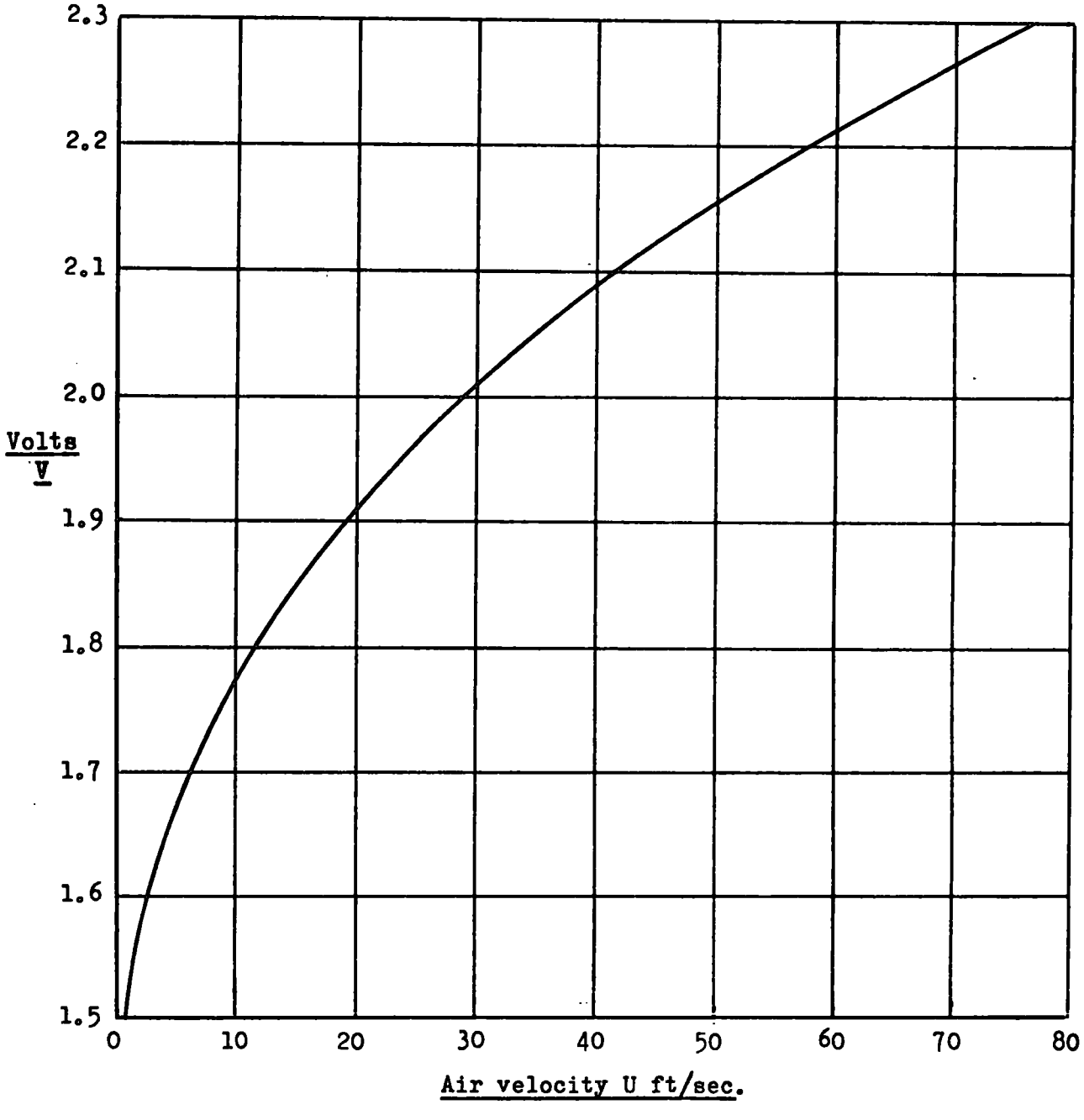

FIG.13 VOLTAGE - VELOCITY CHARACTERISTIC OF HOT-WIRE PROBE P.1.

TABLE 2.

VOLTAGE - VELOCITY CHARACTERISTIC OF HOT-WIRE PROBE P1.

Volts	Vel.	Volts	Vel.	Volts	Vel.	Volts	Vel.
1.500	0.70	1.600	2.55	1.700	6.00	1.800	11.35
1.505	0.75	1.605	2.70	1.705	6.25	1.805	11.65
1.510	0.80	1.610	2.85	1.710	6.50	1.810	12.00
1.515	0.85	1.615	3.00	1.715	6.75	1.815	12.30
1.520	0.90	1.620	3.10	1.720	7.00	1.820	12.65
1.525	1.00	1.625	3.25	1.725	7.25	1.825	13.00
1.530	1.05	1.630	3.45	1.730	7.45	1.830	13.30
1.535	1.15	1.635	3.55	1.735	7.70	1.835	13.65
1.540	1.25	1.640	3.70	1.740	8.00	1.840	14.00
1.545	1.35	1.645	3.90	1.745	8.20	1.845	14.35
1.550	1.45	1.650	4.10	1.750	8.45	1.850	14.70
1.555	1.50	1.655	4.30	1.755	8.75	1.855	15.10
1.560	1.60	1.660	4.50	1.760	9.00	1.860	15.45
1.565	1.70	1.665	4.70	1.765	9.03	1.865	15.80
1.570	1.80	1.670	4.90	1.770	9.55	1.870	16.20
1.575	1.95	1.675	5.05	1.775	9.85	1.875	16.70
1.580	2.05	1.680	5.20	1.780	10.15	1.880	17.05
1.585	2.20	1.685	5.40	1.785	10.45	1.885	17.50
1.590	2.30	1.690	5.60	1.790	10.70	1.890	17.95
1.595	2.45	1.695	5.80	1.795	11.00	1.895	18.40
1.900	18.85	2.000	28.75	2.100	41.20	2.200	57.25
1.905	19.30	2.005	29.30	2.105	42.00	2.205	58.15
1.910	19.70	2.010	29.80	2.110	42.80	2.210	59.00
1.915	20.20	2.015	30.40	2.115	43.60	2.215	59.85
1.920	20.65	2.020	31.00	2.120	44.40	2.220	60.70
1.925	21.10	2.025	31.60	2.125	45.10	2.225	61.60
1.930	21.55	2.030	32.20	2.130	45.80	2.230	62.50
1.935	22.05	2.035	32.85	2.135	46.60	2.235	63.45
1.940	22.55	2.040	33.45	2.140	47.40	2.240	64.40
1.945	23.00	2.045	34.00	2.145	48.20	2.245	65.35
1.950	23.50	2.050	34.60	2.150	49.00	2.250	66.30
1.955	24.00	2.055	35.20	2.155	49.80	2.255	67.25
1.960	24.45	2.060	35.85	2.160	50.55	2.260	68.20
1.965	25.00	2.065	36.50	2.165	51.40	2.265	69.25
1.970	25.50	2.070	37.10	2.170	52.20	2.270	70.30
1.975	26.00	2.075	37.80	2.175	53.00	2.275	71.35
1.980	26.55	2.080	38.50	2.180	53.80	2.280	72.40
1.985	27.10	2.085	39.15	2.185	54.65	2.285	73.45
1.990	27.60	2.090	39.80	2.190	55.50	2.290	74.50
1.995	28.20	2.095	40.50	2.195	56.40	2.295	75.55

Velocities given above are in ft/sec.

Voltage at zero air flow 1.40 volts.

TABLE 3.

VOLTAGE - ANGLE CHARACTERISTIC OF HOT-WIRE PROBE P.1.

	Angle θ°	0°	5°	10°	15°	20°	25°	30°	35°	40°
(a)	Volts Ve	1.575	1.585	1.605	1.635	1.660	1.685	1.705	1.725	1.740
(b)	Volts Ve	1.620	1.635	1.660	1.695	1.730	1.760	1.785	1.810	1.830
(c)	Volts Ve	1.665	1.680	1.715	1.755	1.795	1.830	1.860	1.885	1.905
(d)	Volts Ve	1.700	1.730	1.775	1.825	1.870	1.905	1.940	1.965	1.995
(e)	Volts Ve	1.740	1.775	1.840	1.900	1.950	1.995	2.035	2.075	2.100
(f)	Volts Ve	1.760	1.815	1.895	1.960	2.020	2.075	2.115	2.155	2.185
	Angle θ°	45°	50°	55°	60°	65°	70°	75°	80°	85°
(a)	Volts Ve	1.760	1.775	1.785	1.795	1.805	1.810	1.815	1.820	1.825
(b)	Volts Ve	1.845	1.860	1.870	1.885	1.895	1.900	1.905	1.910	1.915
(c)	Volts Ve	1.925	1.940	1.955	1.970	1.980	1.990	1.995	2.000	2.005
(d)	Volts Ve	2.020	2.035	2.055	2.070	2.080	2.090	2.095	2.100	2.100
(e)	Volts Ve	2.130	2.150	2.165	2.180	2.195	2.205	2.215	2.220	2.225
(f)	Volts Ve	2.215	2.235	2.255	2.270	2.285	2.295	2.305	2.310	2.315
	Angle θ°	90°	95°	100°	105°	110°	115°	120°	125°	130°
(a)	Volts Ve	1.825	1.820	1.820	1.815	1.810	1.805	1.795	1.785	1.775
(b)	Volts Ve	1.915	1.915	1.910	1.905	1.900	1.895	1.885	1.875	1.860
(c)	Volts Ve	2.005	2.000	2.000	1.995	1.985	1.980	1.965	1.955	1.940
(d)	Volts Ve	2.105	2.105	2.100	2.095	2.090	2.080	2.065	2.055	2.035
(e)	Volts Ve	2.225	2.220	2.215	2.215	2.205	2.195	2.180	2.165	2.145
(f)	Volts Ve	2.315	2.315	2.310	2.305	2.295	2.285	2.270	2.255	2.230
	Angle θ°	135°	140°	145°	150°	155°	160°	165°	170°	175°
(a)	Volts Ve	1.760	1.745	1.730	1.710	1.690	1.665	1.650	1.605	1.585
(b)	Volts Ve	1.845	1.830	1.810	1.785	1.760	1.730	1.700	1.665	1.635
(c)	Volts Ve	1.925	1.905	1.885	1.860	1.830	1.795	1.760	1.715	1.680
(d)	Volts Ve	2.015	1.995	1.965	1.935	1.900	1.865	1.820	1.770	1.725
(e)	Volts Ve	2.125	2.100	2.070	2.035	1.995	1.945	1.895	1.835	1.765
(f)	Volts Ve	2.210	2.180	2.145	2.110	2.070	2.020	1.960	1.890	1.805

	Manometer h ins.w.g.	Air vel. U ft/sec.
(a)	0.0360	12.8
(b)	0.0889	20.1
(c)	0.186	29.1
(d)	0.378	41.5
(e)	0.819	61.0
(f)	1.400	79.7

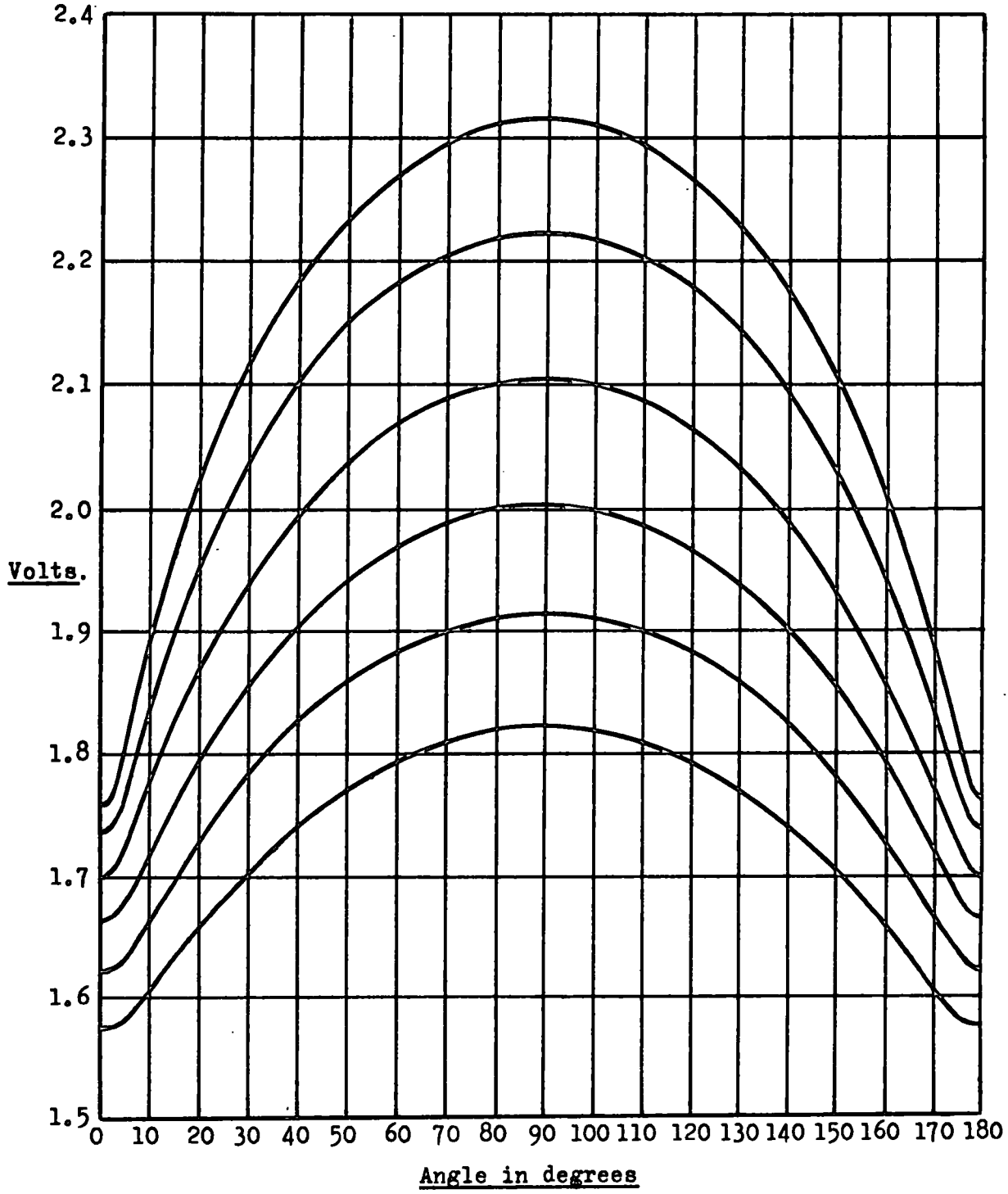

FIG.14 VOLTAGE - ANGLE CHARACTERISTIC OF HOT-WIRE PROBE P.1.

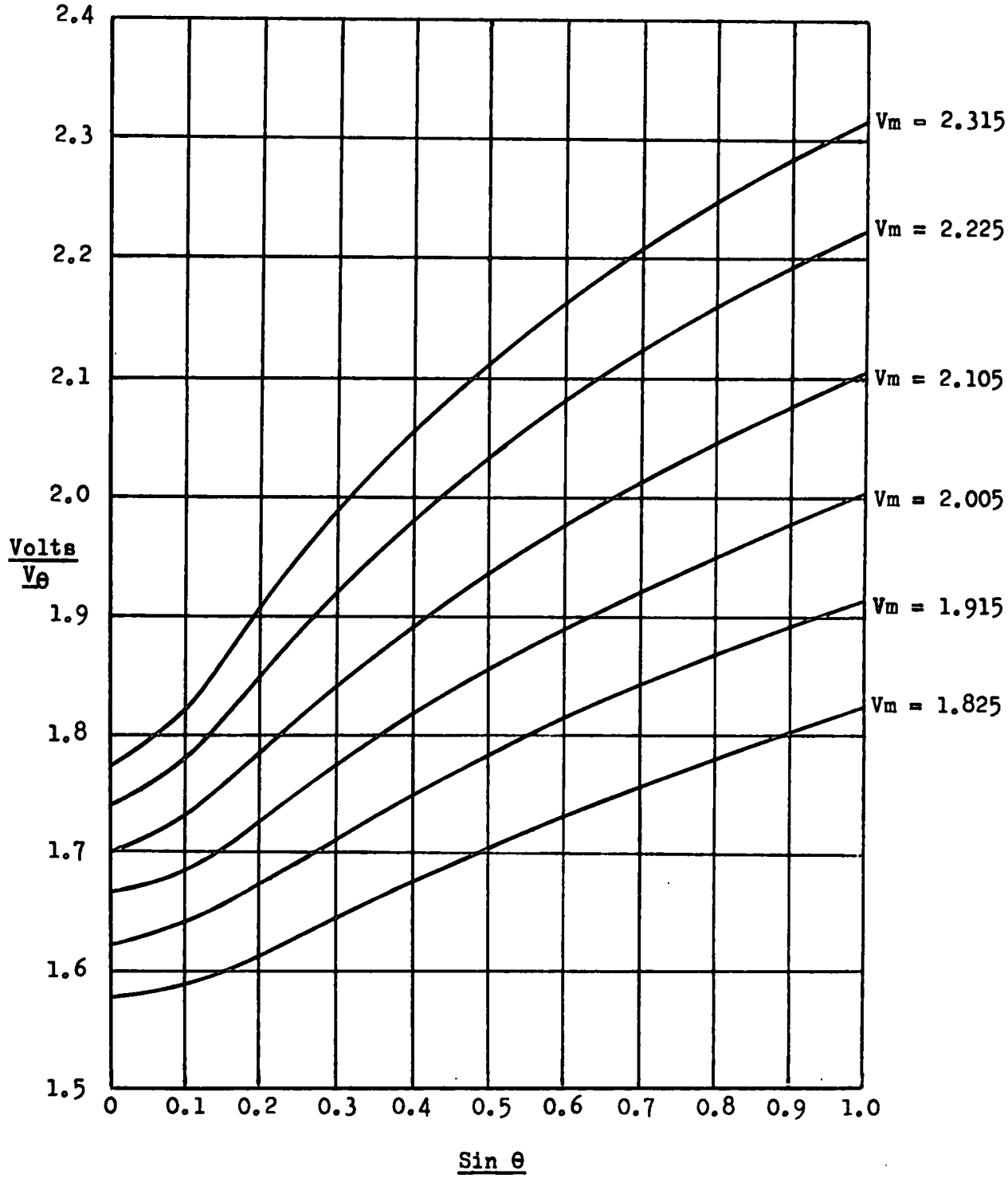

FIG.15 VOLTAGE - ANGLE CHARACTERISTIC OF HOT-WIRE PROBE P.1.

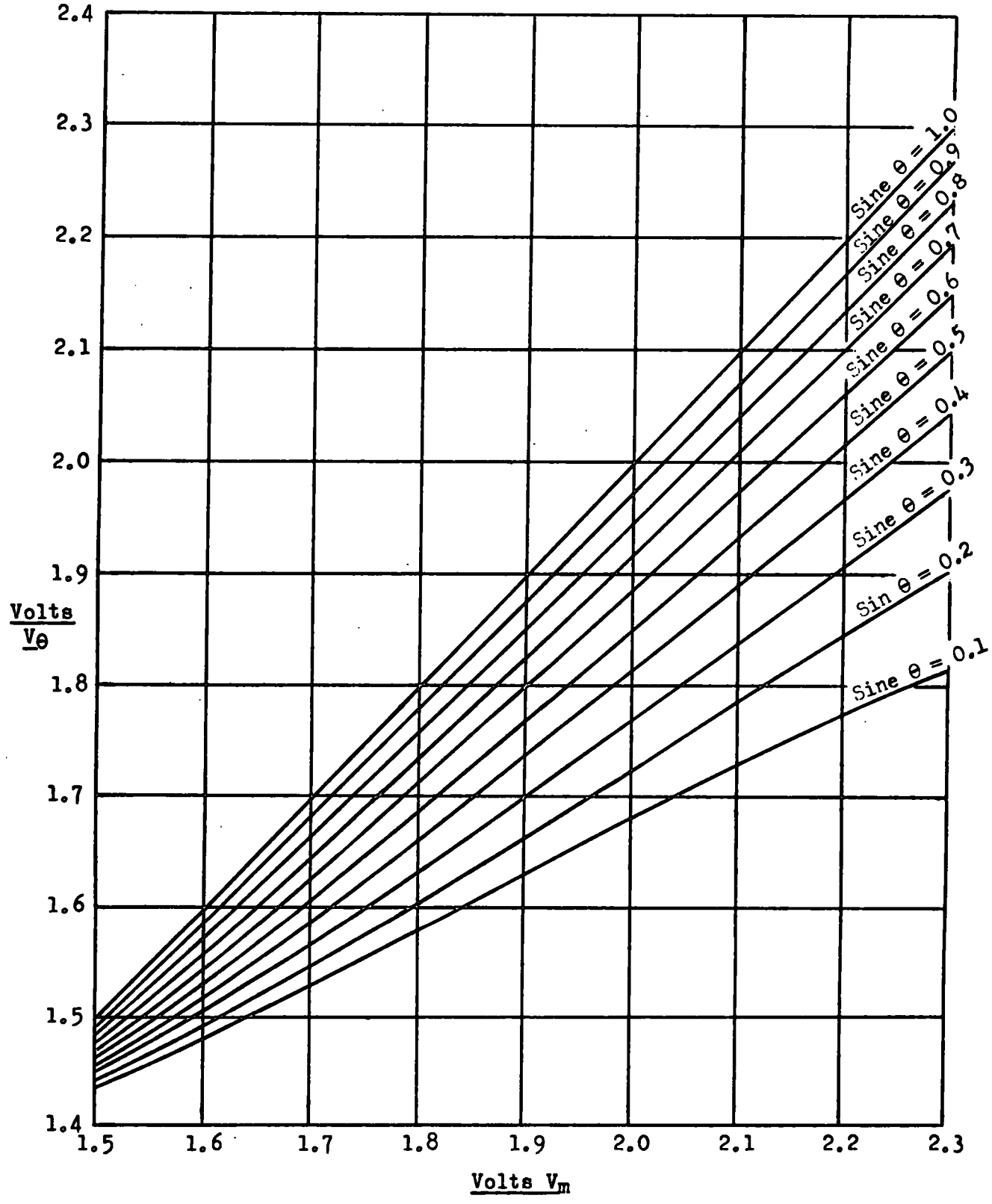

FIG.16 VOLTAGE - ANGLE CHARACTERISTIC OF HOT-WIRE PROBE P.1.

turned through 90° as indicated below.

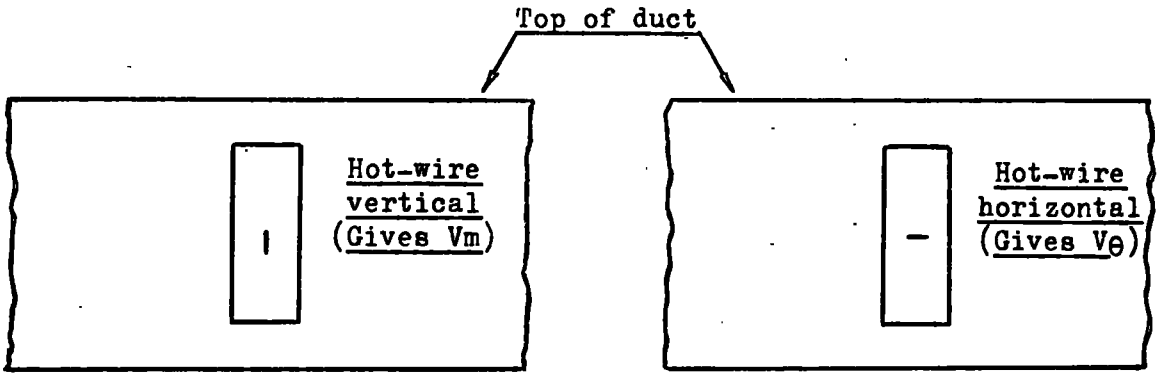

View looking on front of duct

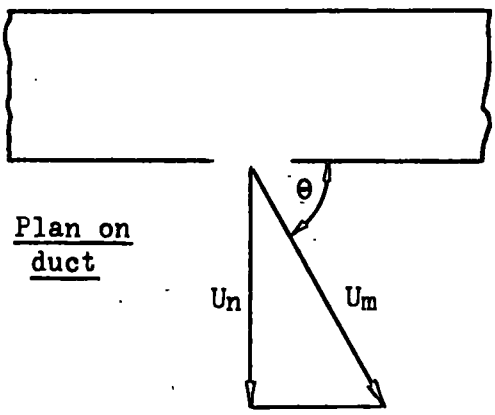

From the first reading the maximum air speed at the chosen point could be obtained by consulting Table 2 and from the second reading the sine of the angle of air issue could be found from fig.16, and hence the component of air velocity normal to the aperture U_n could be easily calculated.

Of course, the validity of this procedure depended upon the absence of any vertical component of air velocity. Fortunately, the bulk of subsequent experimental data showed that the effect of any vertical components of velocity must be very slight indeed because, ultimately, the corroboration between the air volume flow entering the duct and the outflow through the apertures as measured using the above method was extremely good, the discrepancies being customarily

less than 2%.

4.2. Measurement of the volume flow of air through an aperture.

In considering how to measure accurately the air issuing from an aperture it was apparent that several horizontal traverses at suitably different heights in the aperture would be desirable in case there was any vertical variation in the air flow, although it was not anticipated that there would be any appreciable variation, except perhaps towards the top and bottom of the aperture. For a horizontal traverse with the hot-wire probe the screw operated probe holder shown by Plate 3 was used. To achieve a high order of accuracy in plotting the velocity variation across an aperture a 5/16" screw was chosen having 22 threads per inch which allowed 44 readings per inch to be taken, 22 with the hot-wire vertical and 22 with it horizontal.

As an exploratory test apertures N^{os} 2, 7 and 12 were arbitrarily chosen and each set at 6" by 1½", the remaining apertures being covered. Then, for a constant supply of air into the duct, the air discharged from N^{o}2 aperture was measured using five horizontal traverses as shown by fig.17, the resulting velocity contours of which are as shown by figs.18 and 19. As may be seen, it was only near to the top and bottom of the aperture that the flow pattern changed significantly, the discharge in the vicinity of these extremities being somewhat greater proportionally than from the rest of the aperture. Calculations disclosed however that there was only approximately a 1% difference between the aperture air flow deduced from the half-height traverse alone and that found using the more comprehensive five-row traverse. Several further similar tests using different aperture combinations and different aperture sizes showed that the single traverse consistently gave the air volume flow to within usually less than 1½% of the more

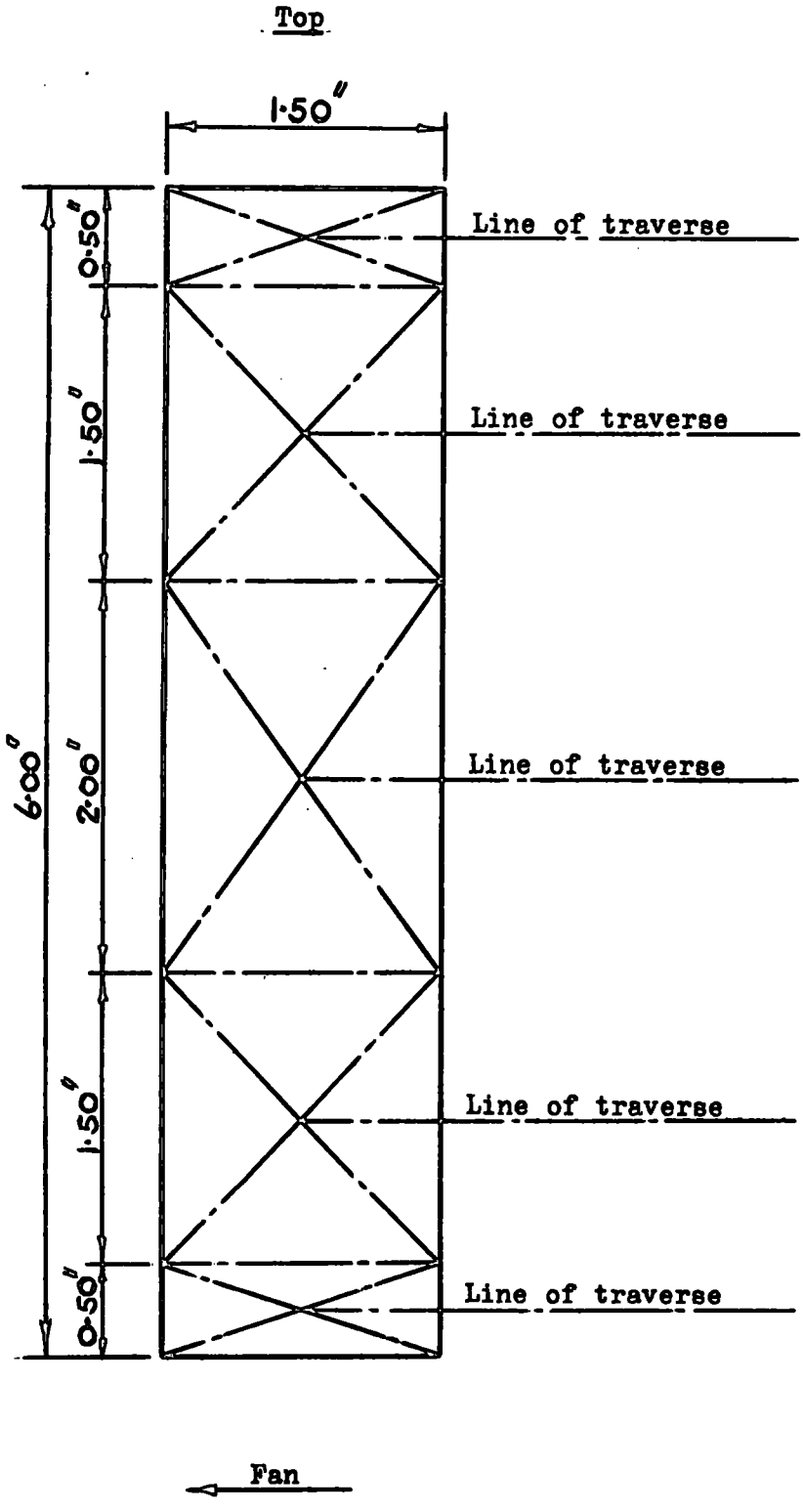

FIG.17 5 - ROW HOT-WIRE PROBE TRAVERSE OF No 2 APERTURE.

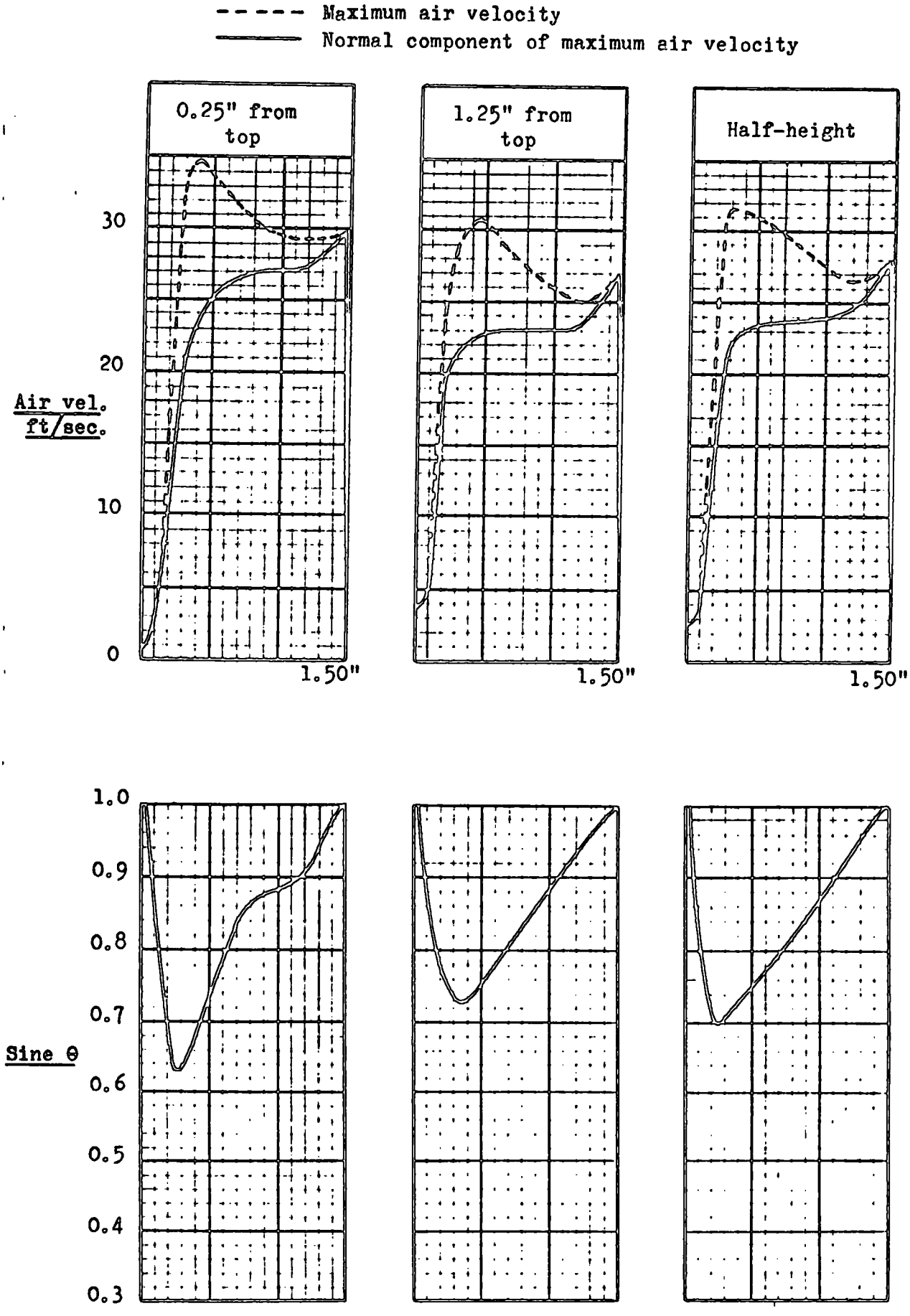

FIG.18 AIR FLOW PATTERNS FOR A 5-ROW TRAVERSE OF NO2 APERTURE.

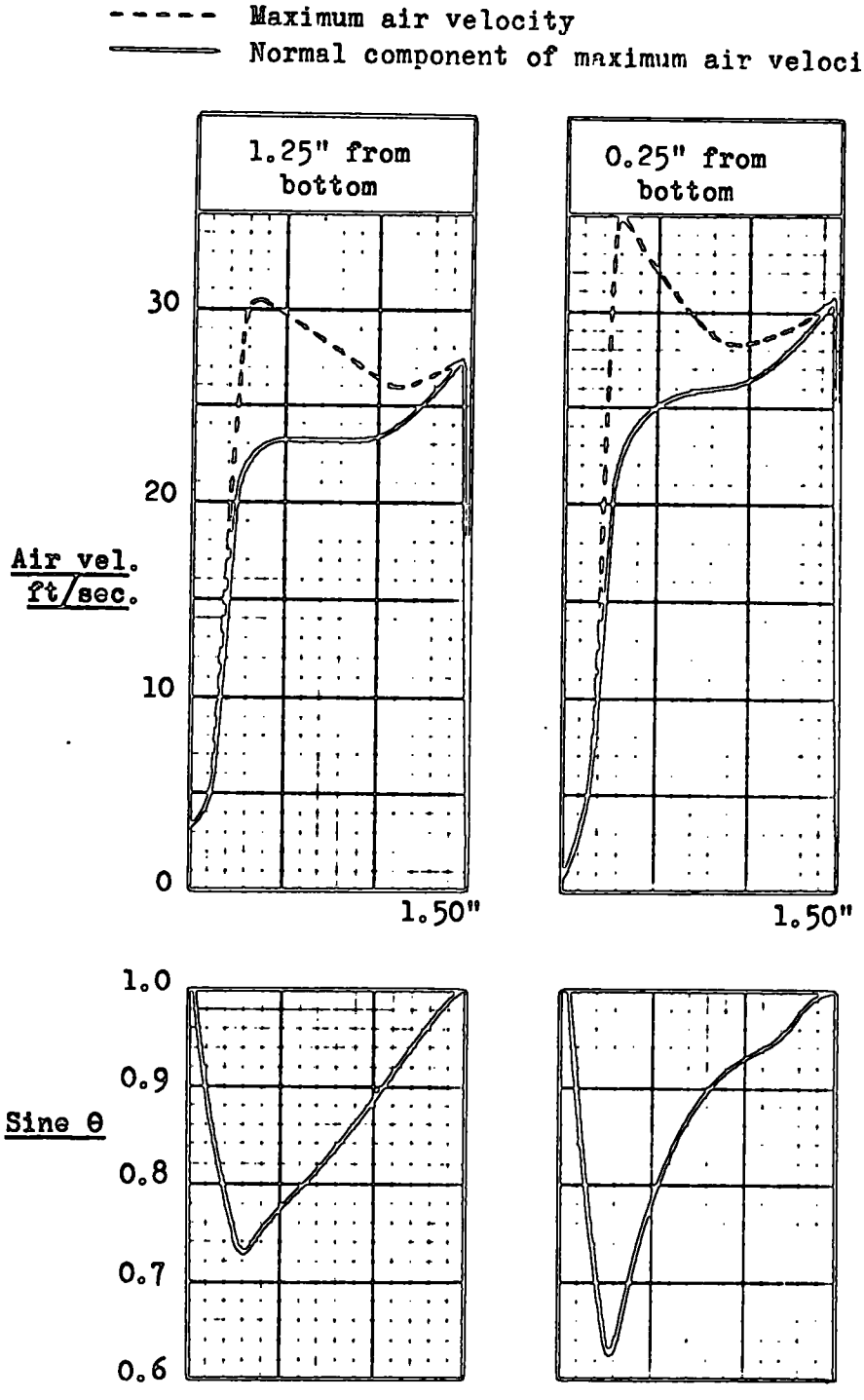

Traverse	'A'	Average vel. ft/sec.	'B'	Air flow $ft^3/sec.$
0.25" from top	3.37	22.5	0.75	0.117
1.25" from top	3.10	20.7	2.25	0.323
Half-height	3.15	21.0	3.00	0.438
1.25" from bottom	3.16	21.1	2.25	0.330
0.25" from bottom	3.35	22.3	0.75	0.116
		Total	9.00	1.324

Column 'A' Area under the normal velocity curve in^2.
Column 'B' Area of aperture section associated with traverse in^2.

Average velocity = 21.2 ft/sec.

$$\text{Ratio} : \frac{\text{Average velocity}}{\text{Half-height velocity}} = \frac{21.2}{21.0} = 1.01$$

FIG.19 AIR FLOW PATTERNS FOR A 5-ROW TRAVERSE OF N°2 APERTURE.

accurately obtained value, the single traverse always giving the lower value. This was most encouraging because the time necessary to carry out five-row traverses on, say, four apertures set at 6" by 3" would have been prohibitive, requiring in fact roughly 2,400 separate voltage readings. It was decided therefore that for future tests a single half-height traverse of an aperture would provide an acceptably accurate method of obtaining the air discharged through the aperture provided that the average velocity calculated from the single traverse was multiplied by 1.01.

4.3 Contamination of the hot-wire probes.

Following the above mentioned tests a preliminary programme was inaugurated using the recently calibrated new probe P1 which attempted to establish the general way in which the air entering the duct distributed itself between two, three, four and twelve apertures open various amounts. At the outset it was realised that if any reliance was to be placed on the findings a simple requirement would have to be fulfilled, namely, that the sum of the measured individual aperture air flows would have to equal the air volume flow entering the duct. If this apparently simple requirement could not be met it would suggest that there was some error in the measuring techniques employed, however, if it could be met consistently it would suggest that the measuring techniques were satisfactory as the probability of obtaining corroboration repeatedly by chance would be so remote as to be negligible.

It was soon evident that this requirement was not being met because it was found that with succeeding tests the discrepancy between the two measured flows progressively increased until eventually the total aperture air flow was being measured as up to 12% less than the incoming air. Considerable confidence was placed in the reliability

of the pitot-static tube traversing method as a means of assessing the volume flow of air entering the duct, so consequently it was felt that the error must be associated with the hot-wire anemometer. Examination of the hot-wire under a powerful magnifying glass revealed that the platinum-coated wire was contaminated with dirt and soot particles and this explained why the false voltage readings had been obtained.

Conditions in the vicinity of the test rig had previously been considered to be quite clean and it had not been thought necessary to fit an air filter upstream of the fan inlet flange. On reflection, however, it was realised that although the air entering the fan was quite clean by normal standards, an air suction filter ought to have been fitted. Ideally, the filter would be capable of extracting virtually all of the dust particles from the incoming air without giving rise to an unduly high pressure drop. Unfortunately, limitations of space in the region of the fan excluded the possibility of installing such a filter, so a compromise was reached by fitting two layers of fine gauze over the fan inlet flange.

Because the smaller dust particles in the incoming air would probably not be extracted by the simple filter arrangement described above, it was recognised that the hot-wire would still become contaminated, but necessarily at a considerably slower rate than before. Hence, it seemed reasonable to assume that if a test were begun with a clean hot-wire it would not be particularly contaminated at the end of the test, say, four hours later. This presupposed that it would be a relatively easy task to clean the probe at the beginning of each test.

Experience showed however that this was not the case. First attempts at cleaning were made by immersing the hot-wire in various solvents, such as petrol, carbon tetrachloride, etc., and gently moving

it to and fro for several minutes, but no cleaning effect at all occurred. Similarly, there was no success with detergent solutions, both hot and cold. Finally, a number of attempts were made revolving the probe at 3,000 r.p.m. while immersed in a solvent but again with no success, the hot-wire being eventually broken by this harsh treatment. It was finally concluded that the particles adhering to the wire did so very tenaciously indeed, to an extent, in fact, which made cleaning by solvents apparently impossible.

Confirmation of this conclusion came from the manufacturers of the hot-wire anemometer who stated that contamination of probes was one of the most fundamental difficulties to be overcome by the users of such instruments. In their experience the type of dirt deposited on a probe varied from one area to another, and even from one laboratory to another, and a solvent which might be partially successful in one case could easily be completely ineffective in another. Their final advice was that the ultra-sonic method of cleaning was probably the best way to attempt to clean probes.

As no ultra-sonic cleaning equipment was available it was clear that the problem of probe contamination would have to be solved in some other way. Of course, the main objection to probe contamination, provided that it was a reasonably gradual process, was simply that as time progressed the voltage-velocity relationship of the original calibration changed. An acceptable solution of the problem appeared to be the calibration of the probe at the beginning of a test and then, several hours later, at the end of the test. As explained in Section 4.1 it was not necessary to use the comparatively large low-speed wind tunnel to calibrate the probe, the small-scale air duct itself being quite suitable.

Nevertheless, as a precaution against possible error it was deemed

sensible to carry out the first calibration of the new probe P2 in the low-speed wind tunnel and, as in the case of the probe P1, carry out a subsequent calibration in the small-scale air duct. This was done, and as expected the two voltage-velocity calibration curves were almost identical, thus confirming the reliability of the latter calibration.

Although it would not take too long to establish the voltage-velocity relationship of the probe P2 in the duct it was realised that it would not be feasible to try to determine the voltage-angle relationship necessary to give the sine of the angle of the air issuing from an aperture. Fortunately, the initial calibration of the probe P2 showed that although its voltage-velocity characteristic was significantly different from its predecessor's, the voltage-angle relationship was virtually the same provided that cognizance was taken of any slight difference in the voltage at zero air flow, since this provided the origin of the graphs used to determine the sine of the angle of the issuing air. Opportunity was taken from time to time, using the progressively contaminated probe, to verify the above statement and no contradiction of it was found.

It was now believed that a technique had been evolved whereby the air discharged from an aperture could be measured with satisfactory accuracy. That is, the probe would be calibrated in the duct at the beginning and end of testing and the test results would be accepted only if the two calibrations were practically identical. Furthermore, in traversing an aperture the probe would be progressively turned in a clockwise direction only, so that what small contamination did occur would be spread as evenly as possible along the length of the wire. For example, at a particular measuring point the hot-wire would be placed vertical and the voltage recorded, then the wire would be turned

through 90° and the lower voltage registered. The traversing screw would then be turned through one complete revolution and the new value of the lower voltage noted, then the wire would again be turned clockwise through 90° and the higher voltage recorded, and so on right across the aperture.

Past experience had shown that if this procedure was not followed the wire, due to the oblique angle of the issuing air, would become unevenly contaminated along its length so that if the voltage was recorded with the wire vertical, a significantly different value of voltage would be recorded when the wire was turned through 180°. As a further safeguard against inaccuracy it was decided that the aperture air flow which had been measured first would be re-measured finally, and if it agreed with the original measurement this would be taken as a confirmation that the results of the entire test were acceptable, but if not, the results would be discarded.

In subsequent tests the above procedure was followed, but although it was found that the calibration curves at the start and end of a test were substantially the same, and that the re-measurement of the first aperture air flow coincided with the original measurement, the total air flow from the apertures was still being measured as less than that entering the duct. Happily, the explanation for this was not difficult to find. In calibrating the probe in the small-scale air duct at the T plane (and for that matter in the low-speed wind tunnel) it had been necessary to introduce the probe vertically through the ceiling of the duct, but of course in measuring the air issuing from an aperture the probe stem was horizontal.

Hence, in operation at an aperture, the hot-wire was not being contaminated evenly around its circumference so that when calibrated with the stem vertical in the air duct misleading results were obtained.

A simple remedy was to remove the blank end of the duct at the beginning and end of a test and calibrate the hot-wire probe in the same attitude as it was being used to measure aperture air flows. When this was done no further trouble was encountered and the agreement between the air volume flow entering the duct and that measured leaving through the apertures was consistently extraordinarily close, the discrepancy being generally less than 2%. An opportunity was also taken to check the voltage-angle characteristic of the probe at the duct end position but no significant change had occurred.

SECTION 5. SELECTION OF MAIN TEST PROGRAMME.

5.1. Preliminary tests.

Initial exploratory tests with an arbitrary choice of aperture numbers, sizes, spacings, etc., had indicated a pronounced tendency for the apertures situated furthest away from the fan end of the duct to discharge the greatest quantities of air with the most upstream aperture being distinctly starved of air. Of course this was not unexpected because each time air left the duct through an aperture there was, in accordance with Bernoulli's theorem, a corresponding increase in the static pressure downstream of the aperture and it was plausible to suppose that the quantity of air discharged through an opening in the duct would in some way be related to the pressure differential between the duct and the surrounding atmosphere.

Table 4 shows the results of several tests which, in general, bear out the above contention except that with relatively narrow openings there was a predisposition for the very last aperture to discharge slightly less, instead of more, than its predecessor. It was decided that it would be worthwhile to investigate, in some depth, the extent to which the disparity in aperture air flows was influenced by various factors, such as the magnitude of the air flow entering the duct, the number and size of openings along the duct, etc., but as mentioned earlier it was recognised that the number of variants would have to be severely limited if any kind of discernible air distribution pattern was to emerge.

After due consideration it was resolved that the main test programme would consist basically of investigating how a constant volume flow rate of air entering the duct would be distributed through a fixed number of apertures, evenly pitched along the duct, when the areas of the apertures were varied over a comparatively wide range.

TABLE 4.

RESULTS OF PRELIMINARY TESTS.

TEST DETAILS				
	Apertures open	Aperture size	Aperture air flow $ft^3/sec.$	Aperture flow %
Test 1	N° 8	6" x 2"	3.70	47.0%
	N° 11	6" x 2"	4.18	53.0%
			7.88	100.0%
Test 2	N° 5	6" x 2"	2.39	27.7%
	N° 8	6" x 2"	3.00	34.8%
	N° 11	6" x 2"	3.24	37.5%
			8.63	100.0%
Test 3	N° 2	6" x 1"	2.36	31.9%
	N° 6	6" x 1"	2.44	33.0%
	N° 11	6" x 1"	2.60	35.1%
			7.40	100.0%
Test 4	N° 2	6" x 1"	1.25	14.7%
	N° 4	6" x 1"	1.32	15.6%
	N° 6	6" x 1"	1.40	16.5%
	N° 8	6" x 1"	1.48	17.4%
	N° 10	6" x 1"	1.54	18.1%
	N° 12	6" x 1"	1.50	17.7%
			8.49	100.0%

If the information yielded from such a programme was insufficient to enable any general conclusions to be drawn about the air distribution characteristics of the duct then supplementary programmes would be evolved as required to investigate further any other aspects which were of special interest. The reasons for the choice of number, disposition and sizes of the apertures used in the main programme, together with the selected constant air flow rate, are outlined below.

5.2. Number of openings along the duct.

Consideration of the time required to successfully carry out a test was the primary factor in selecting the number of openings along the duct. A single test entailed firstly, the measurement of the air flow entering the duct by conducting a pitot-static tube traverse at the T plane, followed by the calibration of the hot-wire probe in the duct. Secondly, the measurement of the aperture air flows by recording 44 voltage readings per inch of aperture width, care being taken to re-measure finally the aperture air flow measured initially. Thirdly, the re-calibration of the hot-wire probe to check that it had not become unacceptably contaminated during the test and, lastly, the record of the variation of static pressure along the duct.

After contemplation it was clear that the air flow from not more than four openings could be satisfactorily measured in a test of several hours duration so this number was chosen. On reflection this seemed to be a reasonable choice because it was not untypical of the number of openings often encountered in the blind ducts of many actual ventilating systems.

5.3. Disposition of the four openings.

This was a fairly straightforward decision. Because of the proximity of N°1 aperture to the T plane it was deemed advisable to blank off this opening for all tests and thus eliminate the slight chance of it

causing the air flow at the above mentioned pitot-static tube traversing plane to deviate from parallel flow. In addition, in case of any air buffeting effect at the end of the duct, N°12 aperture was also permanently sealed off. Moreover, it seemed preferable to locate the openings at equal intervals along the duct, rather than have them asymmetrically pitched so, utilising as much of the length of the duct as possible, apertures N^{os} 2, 5, 8 and 11 were chosen, the intermediate apertures being covered with perspex plates.

5.4. Range of aperture areas.

By fixing the number and disposition of the apertures along the duct as indicated above the number of variants had been appreciably reduced. However, there still remained many possible variants with regard to aperture shape and range of areas to be employed. As the maximum size of an aperture was a vertical rectangle 6" by 3" it was obvious that any area smaller than this could be obtained by suitable blanking-off of the unwanted space. For example, some ventilating ducts discharge their air through horizontal rectangular grilles and it would have been quite feasible to simulate this condition by carrying out tests on 3" wide rectangular openings of varying depth. In the event, it was decided to use the full depth of an aperture and vary the width.

Because of possible breakage of the delicate hot-wire of the probe it was necessary to allow a clearance of about 0.05" between the wire and the extremities of the aperture width. This meant that the smallest practicable aperture width could not be less than about one inch because otherwise an unacceptable degree of uncertainty would be introduced into the reliability of the resulting air flow measurements.

Consequently, the range of areas to be used was fixed from a minimum of 6" by 1" to a maximum of 6" by 3". Of course, for any given

test it would have been possible to set apertures N^{os} 2, 5, 8 and 11 to different areas, for example, they could have been arranged in decreasing arithmetical or geometrical progression, but on balance it appeared preferable to set them all to the same area. Increments in aperture width of 0.500" were chosen, with the proviso that 0.250" would be used wherever this was considered desirable.

5.5. Constant volume flow rate of air entering the duct.

With all twelve apertures fully open, and the fan suction damper removed, the greatest delivery from the fan was slightly less than 10 ft^3/sec., corresponding to an everage duct entry velocity of approximately 45 ft/sec. Setting the four selected apertures to their mimimum areas of 6 in^2 each resulted in the flow rate being diminished to a little over 7 ft^3/sec. with the fan suction damper almost fully open. This latter figure was chosen for inclusion in the main test programme despite the fact that the related duct entry velocity of roughly 33 ft/sec. was higher than that usually associated with low-velocity ventilating systems.

There were two reasons for choosing this rather high inlet velocity. The first was that since the air velocity obtained from the anemometer was proportional to the fourth power of the voltage, and since the voltage would be read to the nearest two-hundreth of a volt irrespective of its actual magnitude, then the percentage error in the velocity, being inversely proportional to the voltage, would diminish as the voltage was increased, as shown below.

$$U \propto V^4$$

$$\frac{dU}{U} \propto 4.\frac{dV}{V}$$

The second reason was that if the air velocities through the apertures became too low then there would be some difficulty in

obtaining with sufficient exactitude the sine of the angle of air issue from the voltage-angle characteristic of the hot-wire probe shown by fig.16. In any case, if specific data were subsequently required for a lower duct air entry velocity then particular tests would be incorporated in a supplementary programme.

SECTION 6. MAIN TEST PROGRAMME RESULTS.

6.1. Air flow patterns.

Figs.20 to 28 show the velocity contours and variation in the sine of the angle of air issue for the range of aperture areas decided in the previous section. In all cases the traverse with the probe was made with the hot-wire $\frac{1}{8}$" inward from the front faces of the $\frac{1}{4}$" thick perspex plates forming the aperture sides. Although interest was primarily in the normal components U_n of the air velocity, shown by full lines, the actual maximum air velocity U_m was also plotted, shown by dotted lines.

In some cases there was a certain amount of doubt about the reliability of the value of sine θ near to the upstream edge of an aperture, due to air turbulence in that region. Any such uncertainties are shown by dotted lines, instead of full lines, on the angle of air issue graphs. However, as can be seen from the various air flow patterns, the maximum air velocities are generally very low at an aperture's upstream edge, so that any small errors in evaluating the sine of the angle of the issuing air do not materially affect the average normal air velocity $\bar{U}_n$.

6.2. Variation of static pressure along the duct.

Table 5 shows the static gauge pressures recorded at the 15 tapping points along the top of the duct for various conditions. The upper figures give the pressure in ins.w.g. which, in the lower figures, have been converted to ft. of air at 80°F. A visual representation of the variation in the static pressure is given by fig.29.

6.3. Average normal velocity $\bar{U}_n$.

Areas under the normal air velocity curves were found using a planimeter, several careful measurements per curve being made to obtain reliable mean values. It was estimated that these areas were measured

to an accuracy of appreciably better than $\pm 1\%$. For any given aperture the average normal air velocity U_n was found by dividing the area under the normal air velocity curve by the breadth of the opening and multiplying by the vertical scale of the graph, the resulting figure being finally multiplied by 1.01 in accordance with the reason given in Section 4.2.

6.4. Typical experimental results.

A typical set of experimental results is given in Table 6, where each aperture was set at 6" by 2". Values of U_m were obtained from figures, appropiate to the hot-wire probe used for the test, compiled in the style of Table 2. The sine of the angle of air issue was found from a suitable graph similar to fig.16 which enabled the normal component U_n of the issuing air to be determined.

6.5. Summary of results.

Table 7 shows the summary of the results and fig.30 indicates the variation with aperture area of the proportional distribution of the constant volume air flow entering the duct to the four apertures. In Table 7, the static gauge pressures shown in columns (g) and (h) were measured at the following tapping points (see fig.1) : N°2 aperture, 10 & 14: N°5 aperture, 14 & 17: N°8 aperture, 17 & 20: N°11 aperture, 20 & 24.

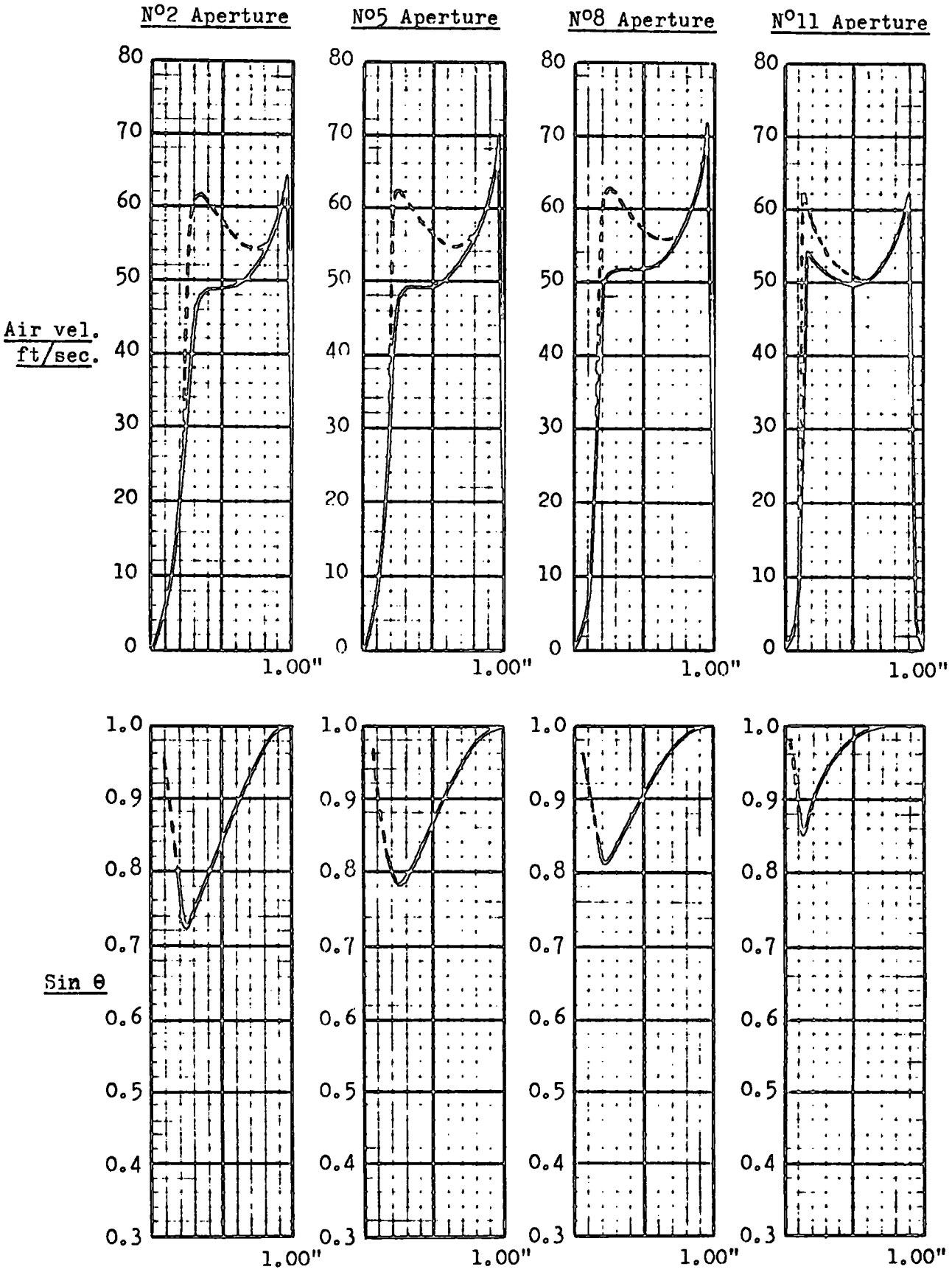

FIG.20. APERTURE AIR FLOW PATTERNS.

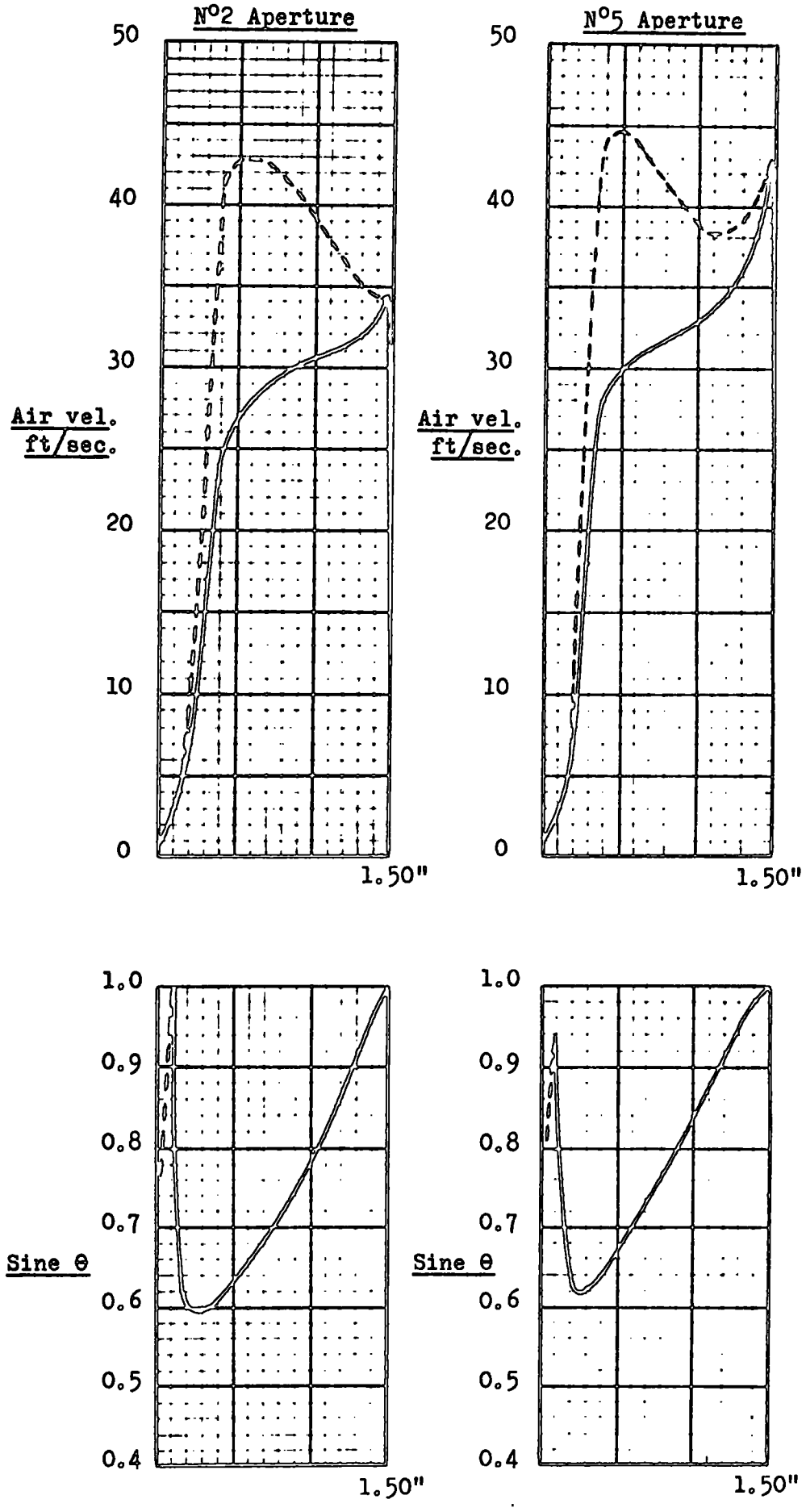

FIG.21 APERTURE AIR FLOW PATTERNS.

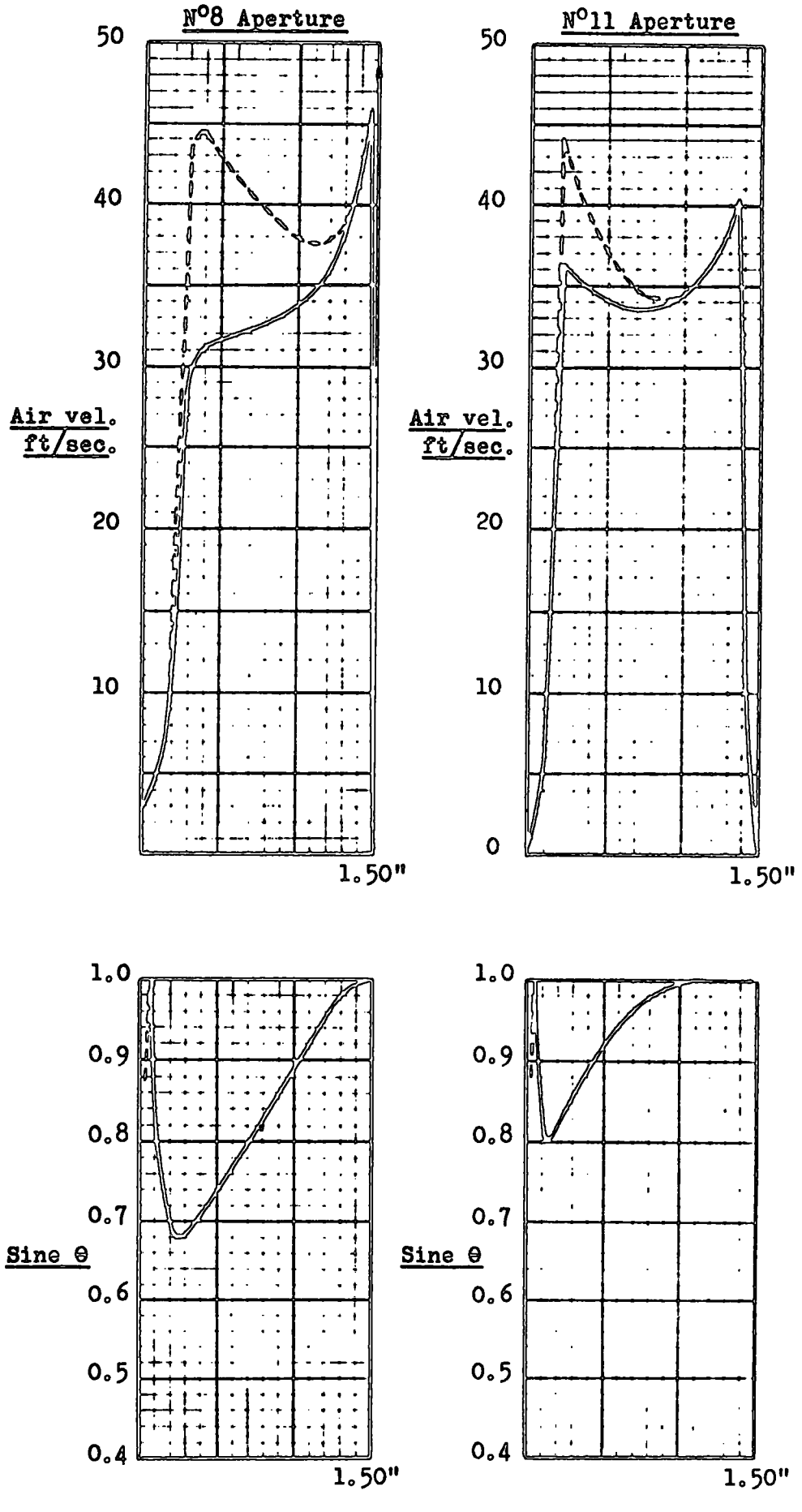

FIG.22 APERTURE AIR FLOW PATTERNS.

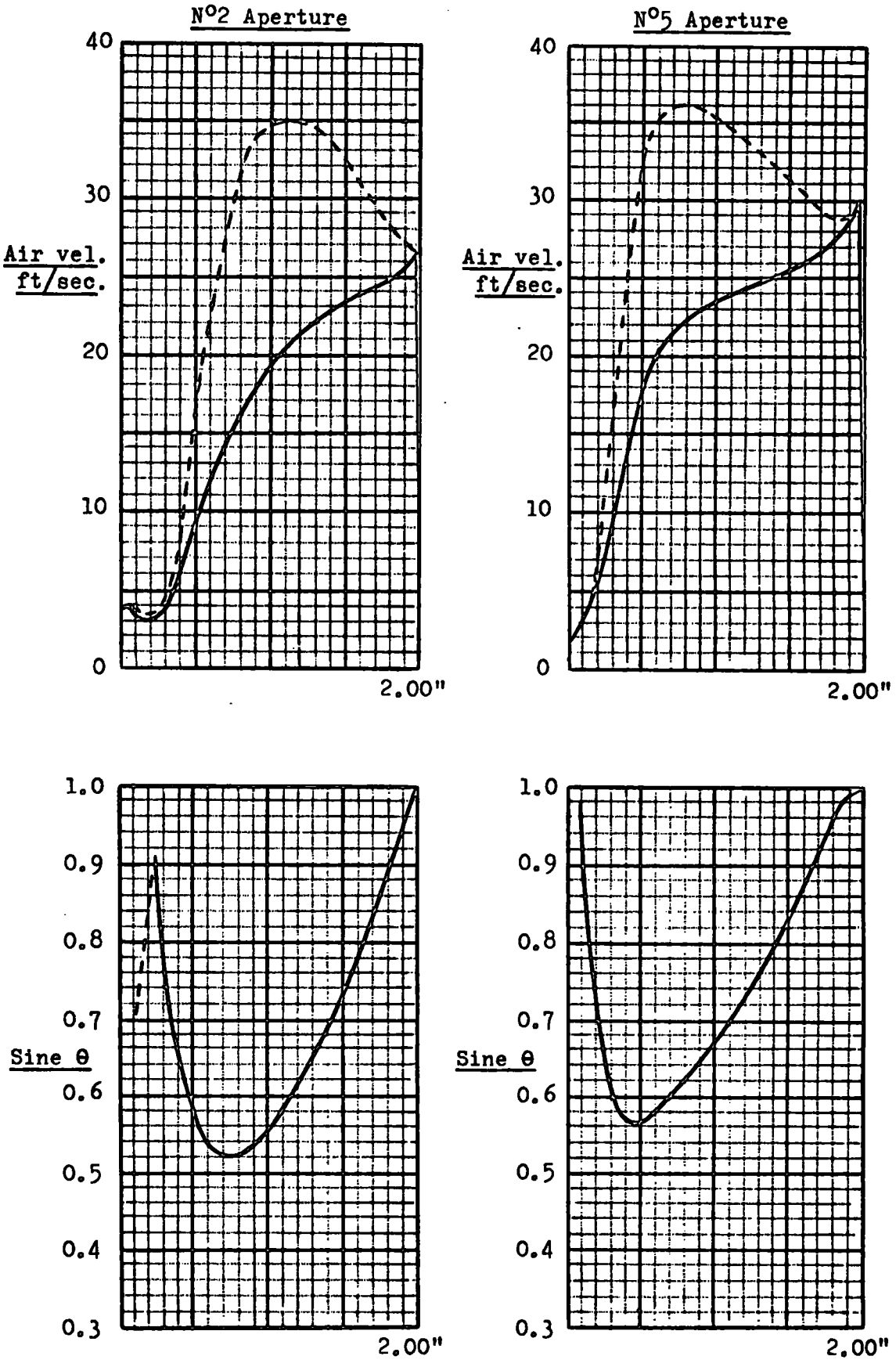

FIG.23 APERTURE AIR FLOW PATTERNS.

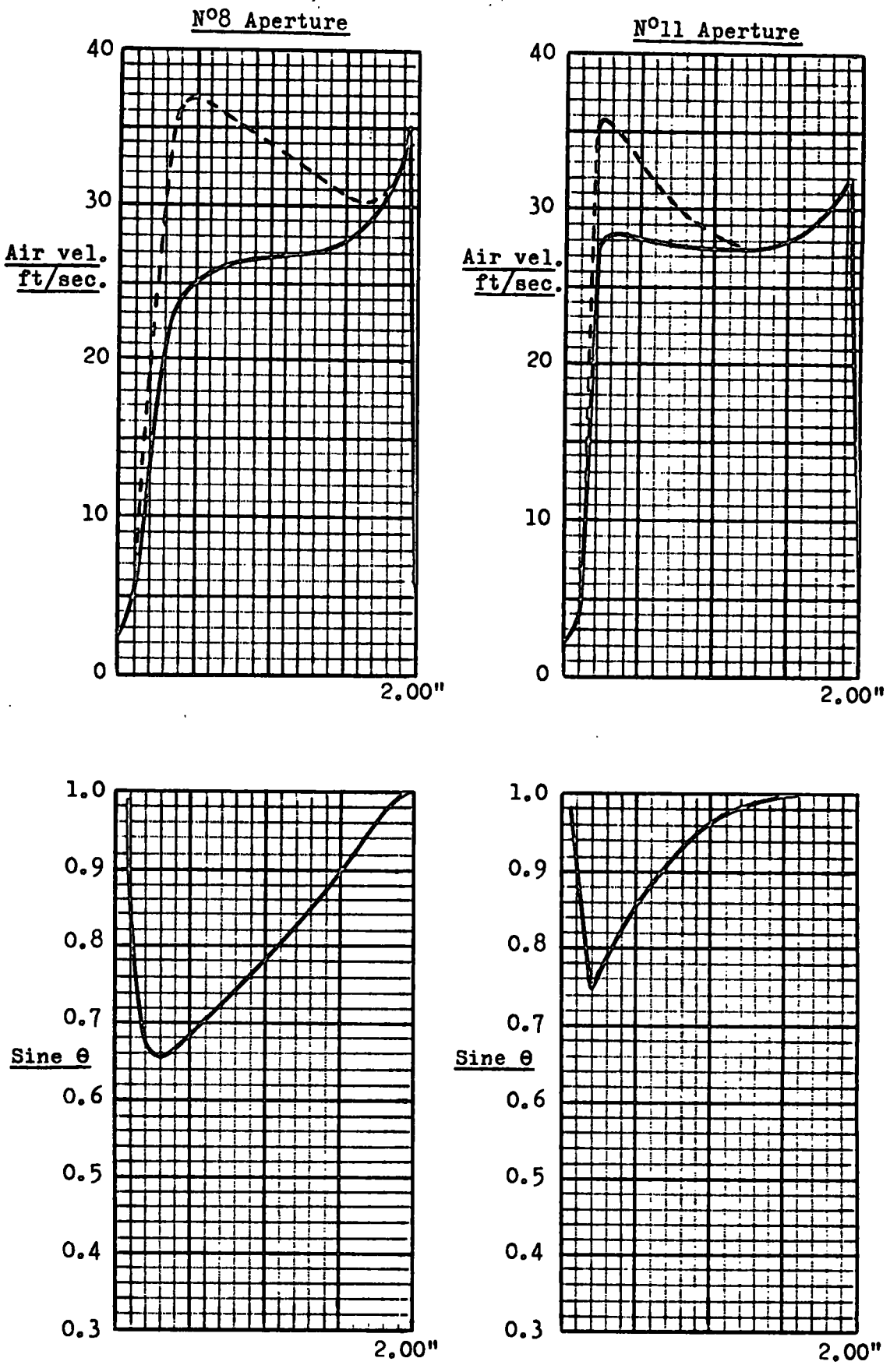

FIG.24 APERTURE AIR FLOW PATTERNS.

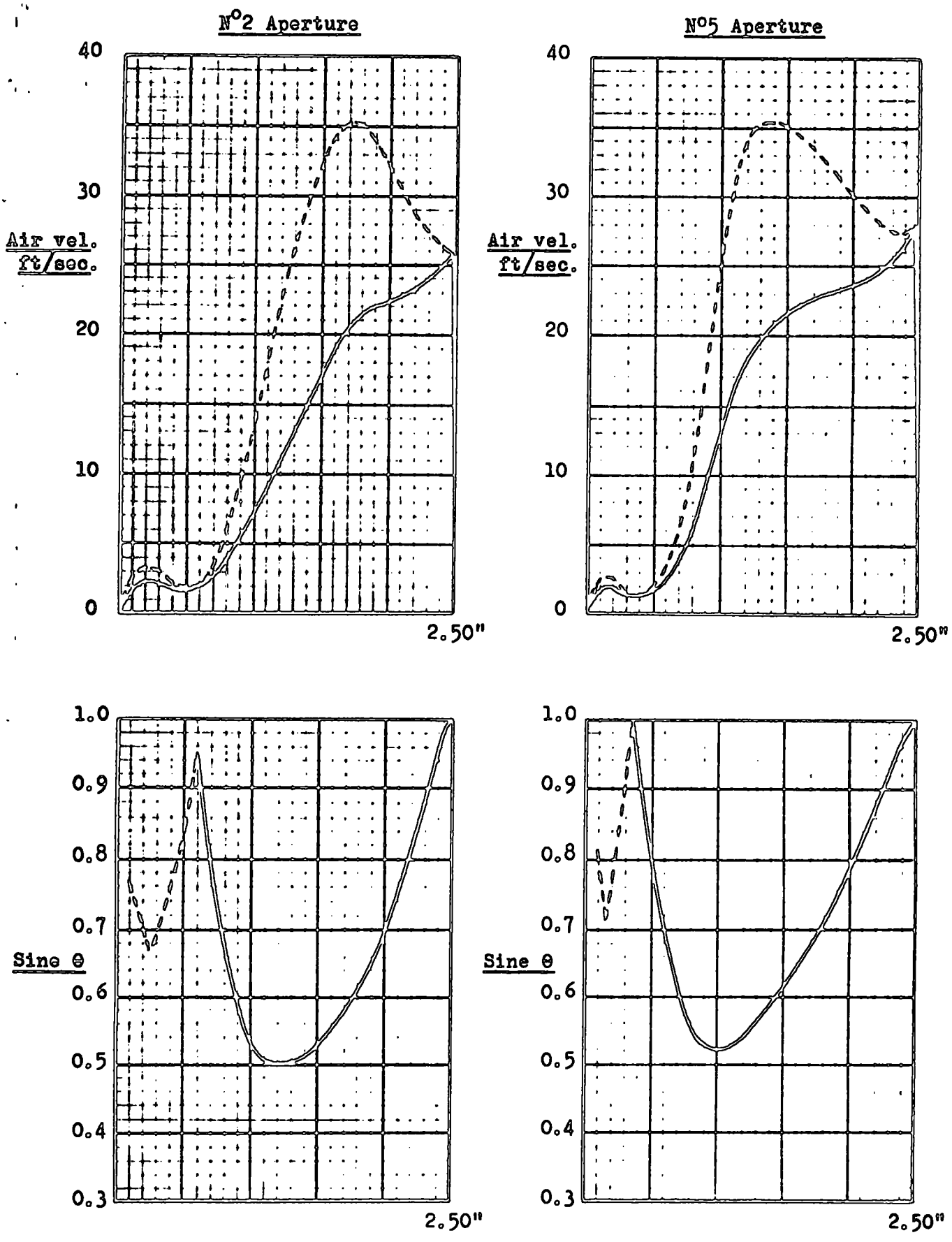

FIG.25 APERTURE AIR FLOW PATTERNS.

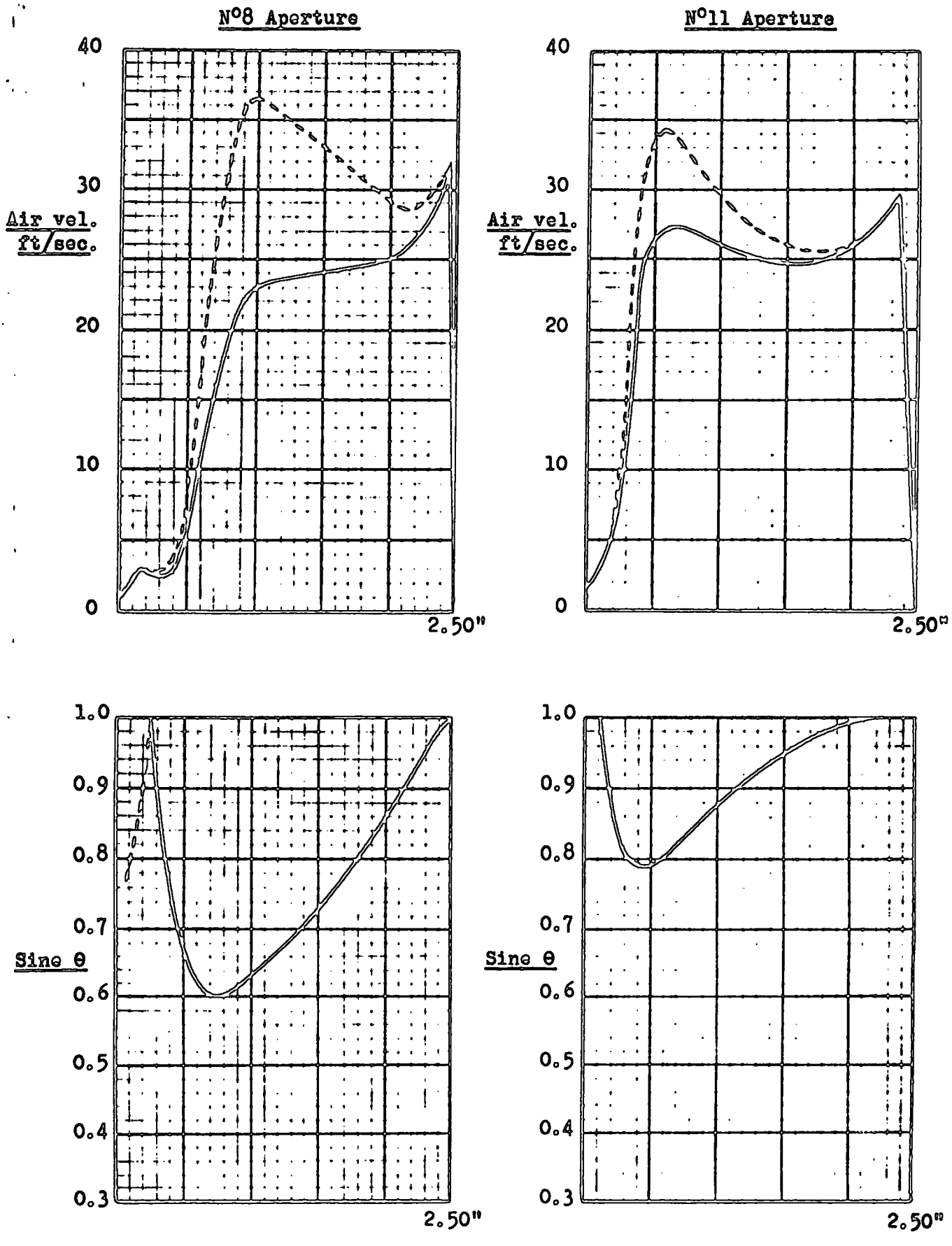

FIG.26 APERTURE AIR FLOW PATTERNS.

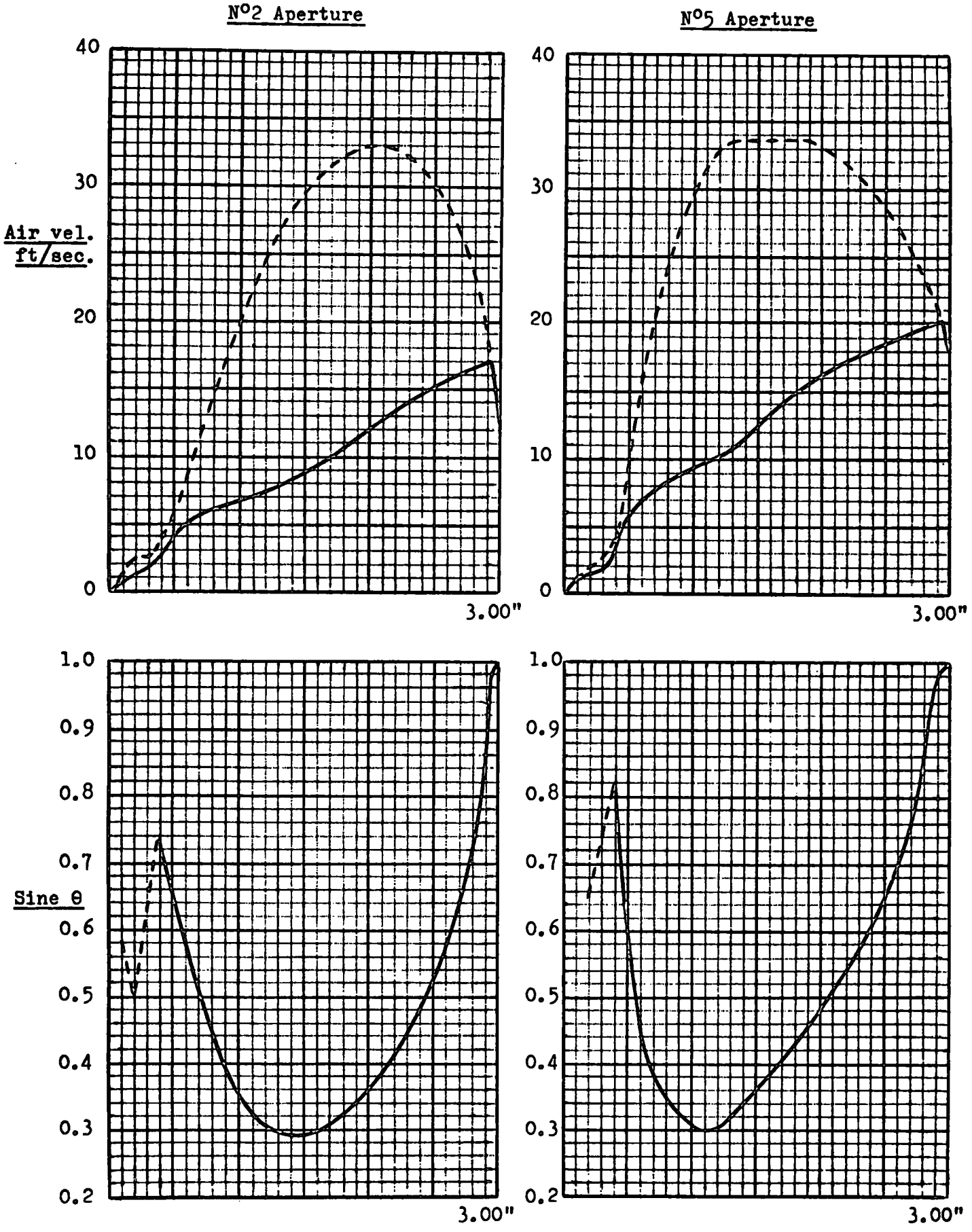

FIG.27 APERTURE AIR FLOW PATTERNS.

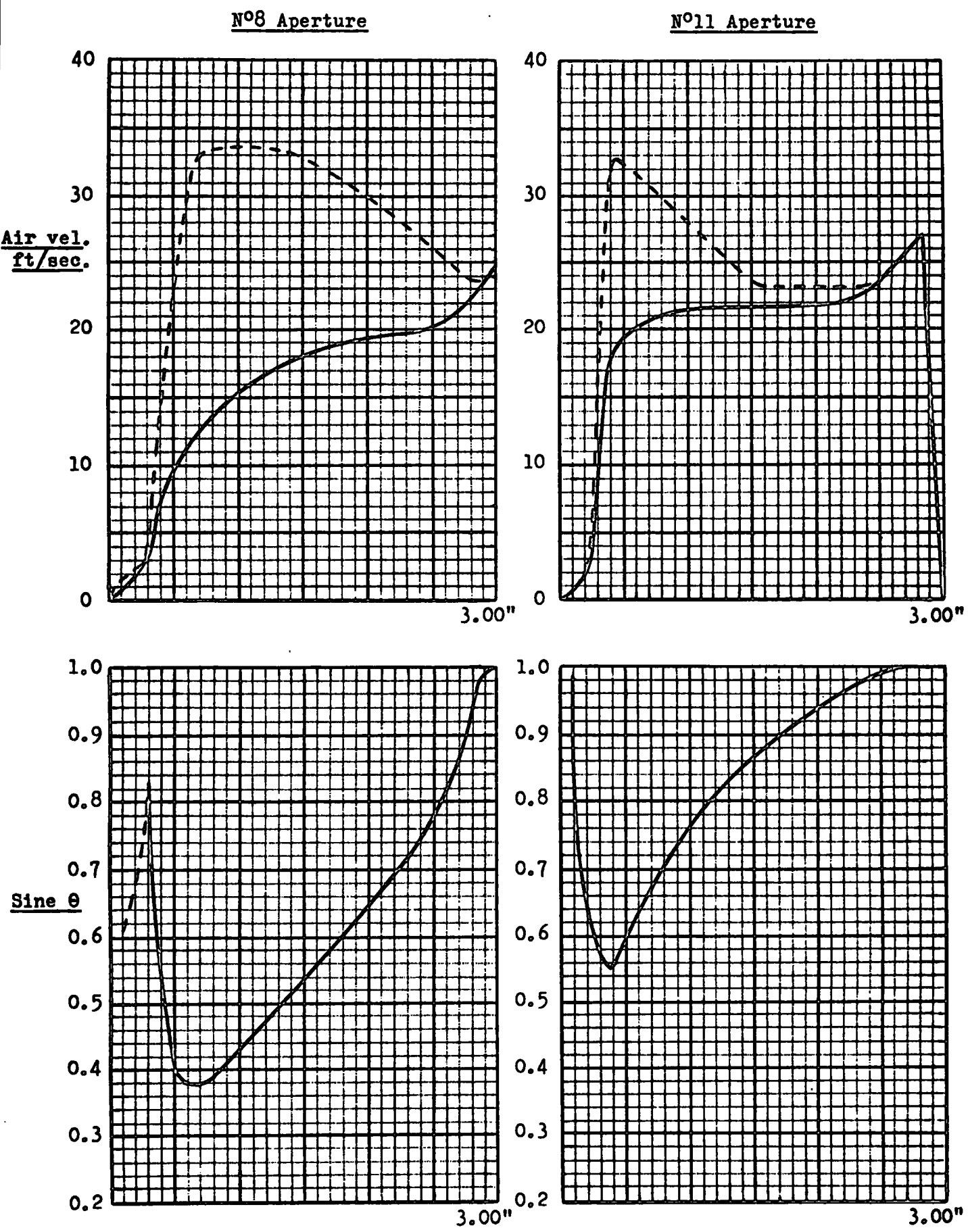

FIG.28 APERTURE AIR FLOW PATTERNS.

TABLE 5.

VARIATION OF STATIC PRESSURE ALONG DUCT.

Aperture size	Static pressure tapping points							
	10	11	12	13	14	15	16	17
6" x 1"	0.789 55.8	0.778 55.0	0.853 60.3	0.857 60.6	0.853 60.3	0.843 59.6	0.899 63.6	0.907 64.1
6" x 1½"	0.300 21.2	0.288 20.4	0.366 25.9	0.366 25.9	0.358 25.3	0.347 24.5	0.405 28.6	0.409 28.9
6" x 2"	0.141 9.97	0.128 9.06	0.198 14.0	0.198 14.0	0.190 13.4	0.178 12.6	0.242 17.1	0.245 17.3
6" x 2½"	0.120 8.48	0.108 7.60	0.166 11.7	0.166 11.7	0.156 11.0	0.146 10.3	0.207 14.6	0.207 14.6
6" x 3"	0.103 7.25	0.090 6.36	0.146 10.3	0.146 10.3	0.137 9.69	0.126 8.91	0.188 13.3	0.188 13.3

Aperture size	Static pressure tapping points						
	18	19	20	21	22	23	24
6" x 1"	0.899 63.6	0.921 65.1	0.925 65.4	0.930 65.7	0.928 65.6	0.933 66.0	0.933 66.0
6" x 1½"	0.405 28.6	0.430 30.4	0.433 30.6	0.438 31.0	0.438 31.0	0.443 31.3	0.446 31.5
6" x 2"	0.236 16.7	0.267 18.9	0.274 19.4	0.274 19.4	0.282 19.9	0.289 20.4	0.290 20.5
6" x 2½"	0.200 14.1	0.240 17.0	0.248 17.5	0.250 17.7	0.252 17.8	0.263 18.6	0.266 18.8
6" x 3"	0.180 12.7	0.220 15.6	0.226 16.0	0.230 16.3	0.232 16.4	0.243 17.2	0.248 17.5

Upper figures are in inches w.g.

Lower figures are in ft. of air at 80°F.

1 in.w.g. = 70.7 ft. of air at 80°F and 14.7 psia.

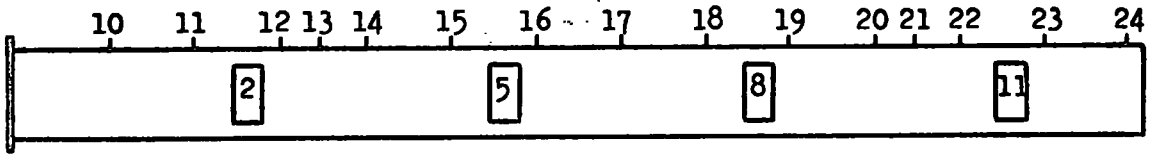

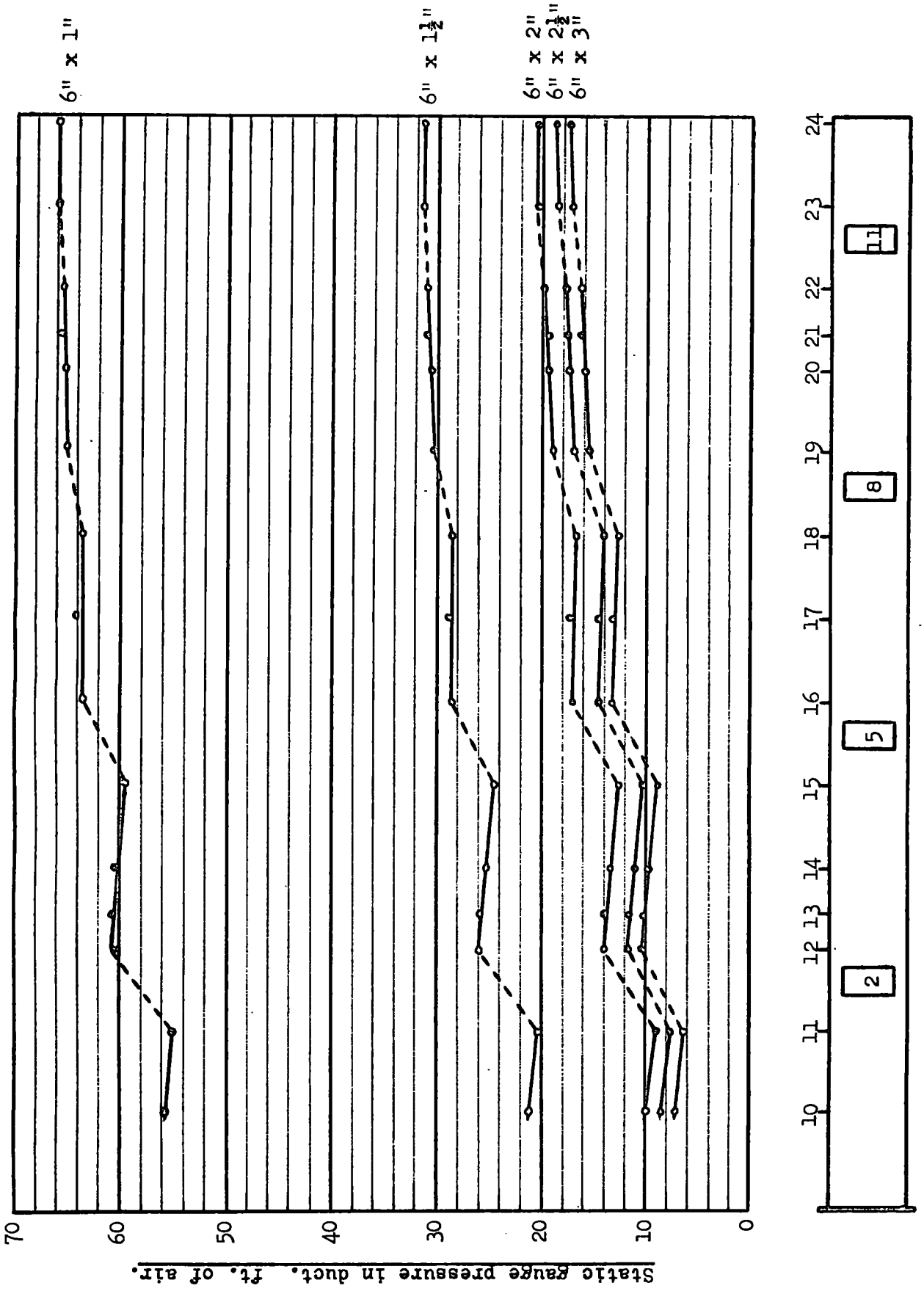

FIG.29 VARIATION OF STATIC PRESSURE ALONG AIR DUCT.

TABLE 6.

EXPERIMENTAL RESULTS FOR APERTURES 2,5,8 & 11, 6" by 2".

Points 1 to 43 represent probe locations at half aperture height, from upstream to downstream edge of aperture, 0.125" inward from outside faces of aperture cover plates.

Probe location		1	2	3	4	5	6	7	8	9
N°2 Aperture	V_m	1.575	1.590	1.570	1.550	1.560	1.590	1.610	1.660	1.735
	V_e		1.550	1.545	1.535	1.550	1.575	1.600	1.620	1.650
	U_m	3.8	4.4	3.6	3.0	3.4	4.4	5.1	7.3	11.7
	Sin θ		0.70	0.80	0.89	0.91	0.90	0.925	0.75	0.55
	U_n	3.8	3.1	2.9	2.7	3.1	4.0	4.7	5.5	6.4
Probe location		10	11	12	13	14	15	16	17	18
N°2 Aperture	V_m	1.765	1.780	1.820	1.860	1.890	1.905	1.925	1.940	1.955
	V_e	1.680	1.705	1.720	1.735	1.765	1.780	1.790	1.805	1.820
	U_m	13.7	14.7	18.0	21.7	24.8	26.4	28.7	30.5	32.2
	Sin θ	0.585	0.64	0.55	0.495	0.525	0.53	0.51	0.525	0.535
	U_n	8.0	9.4	9.9	10.7	13.0	14.0	14.7	16.0	17.2
Probe location		19	20	21	22	23	24	25	26	27
N°2 Aperture	V_m	1.965	1.970	1.975	1.975	1.975	1.975	1.975	1.975	1.975
	V_e	1.825	1.835	1.845	1.850	1.855	1.855	1.860	1.865	1.865
	U_m	33.5	34.1	34.8	34.8	34.8	34.8	34.8	34.8	34.8
	Sin θ	0.525	0.54	0.55	0.57	0.585	0.585	0.600	0.620	0.620
	U_n	17.6	18.4	19.1	19.8	20.4	20.4	20.9	21.6	21.6
Probe location		28	29	30	31	32	33	34	35	36
N°2 Aperture	V_m	1.970	1.965	1.965	1.965	1.960	1.955	1.950	1.945	1.940
	V_e	1.875	1.875	1.875	1.875	1.875	1.880	1.880	1.885	1.885
	U_m	34.1	33.5	33.5	33.5	32.8	32.2	31.6	31.1	30.5
	Sin θ	0.665	0.68	0.68	0.68	0.695	0.725	0.745	0.775	0.79
	U_n	22.7	22.8	22.8	22.8	22.8	23.3	23.6	24.1	24.1
Probe location		37	38	39	40	41	42	43		
N°2 Aperture	V_m	1.930	1.925	1.920	1.915	1.915	1.910	1.905		
	V_e	1.885	1.885	1.885	1.890	1.895	1.900			
	U_m	29.3	28.7	28.0	27.5	27.5	26.9	26.4		
	Sin θ	0.825	0.85	0.86	0.90	0.92	0.955			
	U_n	24.2	24.4	24.1	24.7	25.3	25.7	26.4		

V_m = Reading in volts with hot-wire vertical.

V_e = Reading in volts with hot-wire horizontal.

U_m = Maximum air velocity ft/sec.

U_n = Normal component of maximum air velocity ft/sec.

$U_n = U_m \times \text{Sin } \theta$.

Fig.23 shows the air flow patterns for N°2 aperture plotted from the above results.

TABLE 6. (Cont'd.)

EXPERIMENTAL RESULTS FOR APERTURES 2,5,8 & 11, 6" by 2".

Points 1 to 43 represent probe locations at half aperture height, from upstream to downstream edge of aperture, 0.125" inward from outside faces of aperture cover plates.

Probe location		1	2	3	4	5	6	7	8	9
N°5 Aperture	V_m	1.520	1.540	1.580	1.660	1.710	1.775	1.835	1.890	1.915
	V_e		1.535	1.570	1.625	1.675	1.690	1.735	1.770	1.810
	U_m	2.2	2.7	4.0	7.3	10.0	14.4	19.3	24.8	27.5
	Sin θ		0.975	0.925	0.78	0.80	0.595	0.57	0.54	0.60
	U_n	2.2	2.6	3.7	5.7	8.0	8.6	11.0	13.4	16.5

Probe location		10	11	12	13	14	15	16	17	18
N°5 Aperture	V_m	1.940	1.965	1.975	1.980	1.985	1.985	1.985	1.985	1.985
	V_e	1.825	1.835	1.850	1.860	1.865	1.870	1.870	1.870	1.875
	U_m	30.5	33.5	34.8	35.4	36.1	36.1	36.1	36.1	36.1
	Sin θ	0.585	0.55	0.57	0.59	0.59	0.605	0.605	0.605	0.625
	U_n	17.9	18.4	19.8	20.9	21.3	21.8	21.8	21.8	22.6

Probe location		19	20	21	22	23	24	25	26	27
N°5 Aperture	V_m	1.980	1.975	1.975	1.975	1.975	1.970	1.970	1.970	1.965
	V_e	1.875	1.880	1.885	1.885	1.885	1.885	1.885	1.890	1.890
	U_m	35.4	34.8	34.8	34.8	34.8	34.1	34.1	34.1	33.5
	Sin θ	0.64	0.665	0.685	0.685	0.685	0.70	0.70	0.715	0.73
	U_n	22.6	23.1	23.8	23.8	23.8	23.9	23.9	24.4	24.5

Probe location		28	29	30	31	32	33	34	35	36
N°5 Aperture	V_m	1.965	1.960	1.960	1.950	1.950	1.950	1.940	1.935	1.935
	V_e	1.890	1.890	1.895	1.900	1.895	1.895	1.900	1.900	1.900
	U_m	33.5	32.8	32.8	31.6	31.6	31.6	30.5	29.9	29.9
	Sin θ	0.73	0.745	0.76	0.81	0.795	0.795	0.85	0.865	0.865
	U_n	24.5	24.5	24.9	25.6	25.1	25.1	25.9	25.9	25.9

Probe location		37	38	39	40	41	42	43
N°5 Aperture	V_m	1.935	1.930	1.925	1.925	1.925	1.930	1.935
	V_e	1.900	1.905	1.910	1.915	1.925	1.930	
	U_m	29.9	29.3	28.7	28.7	28.7	29.3	29.9
	Sin θ	0.865	0.90	0.94	0.96	1.00	1.00	
	U_n	25.9	26.4	27.0	27.6	28.7	29.3	29.9

V_m = Reading in volts with hot-wire vertical.

V_e = Reading in volts with hot-wire horizontal.

U_m = Maximum air velocity ft/sec.

U_n = Normal component of maximum air velocity ft/sec.

$U_n = U_m \times \sin \theta$.

Fig.23 shows the air flow patterns for N°5 aperture plotted from the above results.

TABLE 6. (Cont'd.)

Points 1 to 43 represent probe locations at half aperture height, from upstream to downstream edge of aperture, 0.125" inward from outside faces of aperture cover plates.

Probe location		1	2	3	4	5	6	7	8	9
N°8 Aperture	V_m	1.550	1.565	1.725	1.825	1.870	1.935	1.970	1.985	1.990
	V_e		1.565	1.655	1.755	1.815	1.840	1.870	1.890	1.890
	U_m	3.0	3.5	11.0	18.4	22.7	29.9	34.1	36.1	36.7
	Sin θ		1.00	0.625	0.69	0.77	0.65	0.65	0.675	0.655
	U_n	3.0	3.5	6.9	12.7	17.5	19.4	22.2	24.4	24.1
Probe location		10	11	12	13	14	15	16	17	18
N°8 Aperture	V_m	1.990	1.990	1.990	1.985	1.985	1.985	1.980	1.980	1.980
	V_e	1.895	1.900	1.900	1.900	1.905	1.905	1.905	1.905	1.905
	U_m	36.7	36.7	36.7	36.1	36.1	36.1	35.4	35.4	35.4
	Sin θ	0.675	0.695	0.695	0.70	0.72	0.72	0.735	0.735	0.735
	U_n	24.8	25.5	25.5	25.3	26.0	26.0	26.0	26.0	26.0
Probe location		19	20	21	22	23	24	25	26	27
N°8 Aperture	V_m	1.975	1.970	1.970	1.970	1.965	1.965	1.965	1.960	1.955
	V_e	1.910	1.910	1.910	1.910	1.910	1.910	1.910	1.910	1.910
	U_m	34.8	34.1	34.1	34.1	33.5	33.5	33.5	32.8	32.2
	Sin θ	0.765	0.785	0.785	0.785	0.80	0.80	0.80	0.81	0.83
	U_n	26.6	26.8	26.8	26.8	26.8	26.8	26.8	26.6	26.7
Probe location		28	29	30	31	32	33	34	35	36
N°8 Aperture	V_m	1.955	1.950	1.950	1.945	1.940	1.940	1.940	1.940	1.940
	V_e	1.910	1.910	1.910	1.910	1.910	1.915	1.915	1.920	1.920
	U_m	32.2	31.6	31.6	31.1	30.5	30.5	30.5	30.5	30.5
	Sin θ	0.83	0.85	0.85	0.865	0.89	0.90	0.90	0.92	0.92
	U_n	26.7	26.9	26.9	26.9	27.2	27.5	27.5	28.1	28.1
Probe location		37	38	39	40	41	42	43		
N°8 Aperture	V_m	1.940	1.940	1.940	1.950	1.960	1.970	1.960		
	V_e	1.925	1.925	1.935	1.945	1.960	1.970			
	U_m	30.5	30.5	30.5	31.6	32.8	34.1	32.8		
	Sin θ	0.945	0.945	0.985	0.985	1.00	1.00			
	U_n	28.9	28.9	30.1	31.2	32.8	34.1	32.8		

V_m = Reading in volts with hot-wire vertical.

V_e = Reading in volts with hot-wire horizontal.

U_m = Maximum air velocity ft/sec.

U_n = Normal component of maximum air velocity ft/sec.

$U_n = U_m \times \text{Sin } \theta$.

Fig.24 shows the air flow patterns for N°8 aperture plotted from the above results.

TABLE 6. (Cont'd.)

EXPERIMENTAL RESULTS FOR APERTURES 2,5,8 & 11, 6" by 2".

Points 1 to 43 represent probe locations at half aperture height, from upstream to downstream edge of aperture, 0.125" inward from outside faces of aperture cover plates.

Probe location		1	2	3	4	5	6	7	8	9
N°11 Aperture	V_m	1.550	1.600	1.730	1.950	1.980	1.980	1.980	1.980	1.965
	V_e		1.590	1.800	1.860	1.920	1.925	1.925	1.925	1.925
	U_m	3.0	4.7	11.3	31.6	35.4	35.4	35.4	35.4	33.5
	Sin θ		0.94	1.00	0.67	0.785	0.80	0.80	0.80	0.85
	U_n	3.0	4.4	11.3	21.2	27.8	28.3	28.3	28.3	28.5
Probe location		10	11	12	13	14	15	16	17	18
N°11 Aperture	V_m	1.960	1.960	1.950	1.950	1.945	1.935	1.935	1.935	1.930
	V_e	1.920	1.920	1.920	1.920	1.915	1.915	1.915	1.915	1.910
	U_m	32.8	32.8	31.6	31.6	31.1	29.9	29.9	29.9	29.3
	Sin θ	0.85	0.85	0.885	0.885	0.885	0.925	0.925	0.925	0.925
	U_n	27.8	27.8	28.0	28.0	27.5	27.7	27.7	27.7	27.1
Probe location		19	20	21	22	23	24	25	26	27
N°11 Aperture	V_m	1.925	1.925	1.925	1.925	1.920	1.920	1.920	1.915	1.915
	V_e	1.910	1.910	1.915	1.910	1.915	1.915	1.915	1.910	1.910
	U_m	28.7	28.7	28.7	28.7	28.0	28.0	28.0	27.5	27.5
	Sin θ	0.94	0.94	0.96	0.94	0.985	0.985	0.985	0.985	0.985
	U_n	27.0	27.0	27.6	27.0	27.6	27.6	27.6	27.1	27.1
Probe location		28	29	30	31	32	33	34	35	36
N°11 Aperture	V_m	1.915	1.920	1.920	1.920	1.920	1.920	1.925	1.925	1.925
	V_e	1.915	1.915	1.915	1.915	1.915	1.915	1.920	1.920	1.920
	U_m	27.5	28.0	28.0	28.0	28.0	28.0	28.7	28.7	28.7
	Sin θ	1.00	0.985	0.985	0.985	0.985	0.985	0.985	0.985	0.985
	U_n	27.5	27.6	27.6	27.6	27.6	27.6	28.3	28.3	28.3
Probe location		37	38	39	40	41	42	43		
N°11 Aperture	V_m	1.935	1.940	1.950	1.950	1.960	1.870	1.570		
	V_e	1.925	1.935	1.940	1.945	1.950	1.900			
	U_m	29.9	30.5	31.6	31.6	32.8	22.7	3.6		
	Sin θ	0.96	0.985	0.96	0.985	0.96	1.00	1.00		
	U_n	28.7	30.0	30.3	31.1	31.5	22.7	3.6		

V_m = Reading in volts with hot-wire vertical.

V_e = Reading in volts with hot-wire horizontal.

U_m = Maximum air velocity ft/sec.

U_n = Normal component of maximum air velocity ft/sec.

$U_n = U_m \times \text{Sin } \theta$.

Fig.24 shows the air flow patterns for N°11 aperture plotted from the above results.

TABLE 7.

SUMMARY OF RESULTS.

Column (a) : Area under aperture normal velocity curve. in^2.

Column (b) : Average aperture normal velocity $\bar{U}_n$. ft/sec.

Column (c) : Aperture air discharge q. ft^3/sec.

Column (d) : Aperture air discharge expressed as a proportion of the air entering the duct.

Column (e) : Average velocity in duct upstream of aperture. ft/sec.

Column (f) : Average velocity in duct downstream of aperture. ft/sec.

Column (g) : Static gauge pressure at aperture upstream tapping point. ft. of air at 80°F.

Column (h) : Static gauge pressure at aperture downstream tapping point. ft. of air at 80°F.

N°2 Aperture								
Aperture size	(a)	(b)	(c)	(d)	(e)	(f)	(g)	(h)
6" x 1"	1.91	38.6	1.61	0.226	32.8	25.4	55.8	60.3
6" x 1½"	3.71	25.0	1.56	0.220	32.7	25.5	21.2	25.3
6" x 2"	3.31	16.7	1.39	0.192	33.4	27.0	9.97	13.4
6" x 2½"	3.06	12.4	1.29	0.180	33.1	27.1	8.48	11.0
6" x 3"	2.76	9.29	1.16	0.163	32.7	27.4	7.25	9.69

N°5 Aperture								
Aperture size	(a)	(b)	(c)	(d)	(e)	(f)	(g)	(h)
6" x 1"	2.16	43.6	1.82	0.256	25.4	17.0	60.3	64.1
6" x 1½"	4.19	28.2	1.76	0.248	25.5	17.4	25.3	28.9
6" x 2"	4.06	20.5	1.71	0.236	27.0	19.1	13.4	17.3
6" x 2½"	3.68	14.9	1.55	0.216	27.1	20.0	11.0	14.6
6" x 3"	3.60	12.1	1.51	0.212	27.4	20.4	9.69	13.2

N°8 Aperture								
Aperture size	(a)	(b)	(c)	(d)	(e)	(f)	(g)	(h)
6" x 1"	2.22	44.8	1.87	0.262	17.0	8.40	64.1	65.4
6" x 1½"	4.47	30.1	1.88	0.265	17.4	8.73	28.9	30.6
6" x 2"	4.84	24.4	2.03	0.280	19.1	9.75	17.3	19.4
6" x 2½"	4.68	18.9	1.97	0.274	20.0	10.9	14.6	17.5
6" x 3"	4.72	15.9	1.99	0.281	20.4	11.3	13.2	16.0

N°11 Aperture								
Aperture size	(a)	(b)	(c)	(d)	(e)	(f)	(g)	(h)
6" x 1"	2.16	43.6	1.82	0.256	8.40	—	65.4	66.0
6" x 1½"	4.52	30.4	1.90	0.267	8.73	—	30.6	31.5
6" x 2"	5.04	25.4	2.12	0.292	9.75	—	19.4	20.5
6" x 2½"	5.64	22.8	2.37	0.330	10.9	—	17.5	18.8
6" x 3"	5.79	19.5	2.44	0.344	11.3	—	16.0	17.5

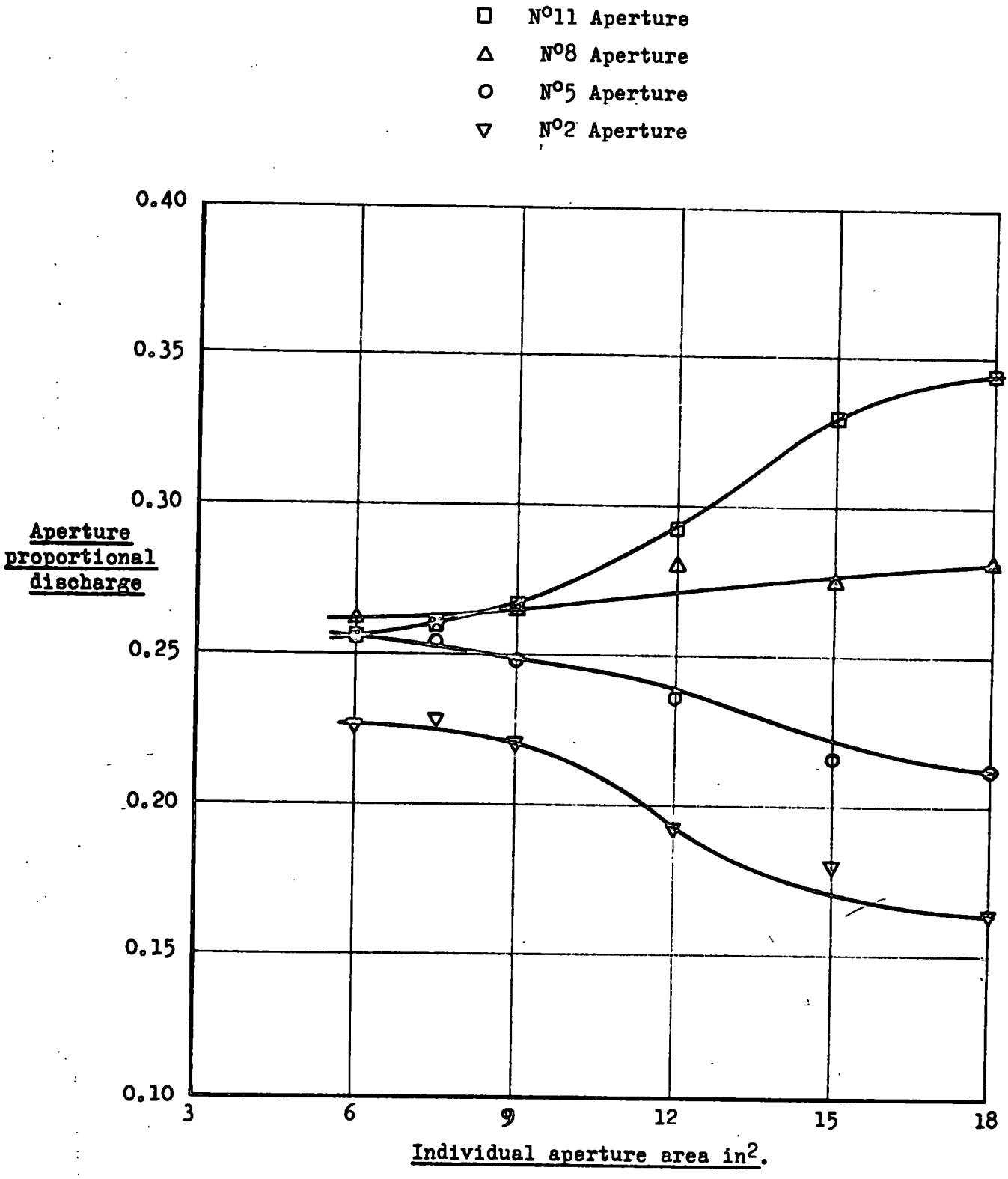

FIG.30 APERTURE AIR DISCHARGE EXPRESSED AS A PROPORTION OF THE AIR ENTERING THE DUCT PLOTTED AGAINST THE VARIATION IN INDIVIDUAL APERTURE AREA.

SECTION 7. SUPPLEMENTARY TEST PROGRAMME WITH RESULTS.

7.1. Aperture proportional discharge at the smaller openings.

Fig.30 shows that as the individual aperture areas were reduced from 9 in^2 to 6 in^2 the pattern of proportional air discharge changed slightly, the discharge from N°11 aperture becoming less than that from N°8 aperture, instead of the other way about. To reduce the effect of experimental points scatter in this region a test was carried out with each of the four apertures set at the intermediate area of 7.5 in^2, the resulting air flow patterns of which are shown by figs.31 and 32. Given below is the relevant data obtained from this test, the proportional air discharges in column (d) being plotted as shown by fig.30.

Column (a) : Area under aperture normal velocity curve. in^2.

Column (b) : Average aperture normal velocity $\bar{U}_n$. ft/sec.

Column (c) : Aperture air discharge q. ft^3/sec.

Column (d) : Aperture air discharge expressed as a proportion of the air entering the duct.

Column (e) : Average velocity in duct upstream of aperture. ft/sec.

Column (f) : Average velocity in duct downstream of aperture. ft/sec.

Column (g) : Static gauge pressure at aperture upstream tapping point. ft. of air at 80°F.

Column (h) : Static gauge pressure at aperture downstream tapping point. ft. of air at 80°F.

Apertures 2,5,8 & 11, 6" x 1.25"								
Aperture	(a)	(b)	(c)	(d)	(e)	(f)	(g)	(h)
N°2	3.87	31.3	1.63	0.229	32.9	25.4	32.6	36.8
N°5	4.30	34.8	1.81	0.254	25.4	17.0	36.8	40.3
N°8	4.37	35.3	1.84	0.258	17.0	8.53	40.3	42.1
N°11	4.39	35.5	1.85	0.259	8.53	——	42.1	43.1

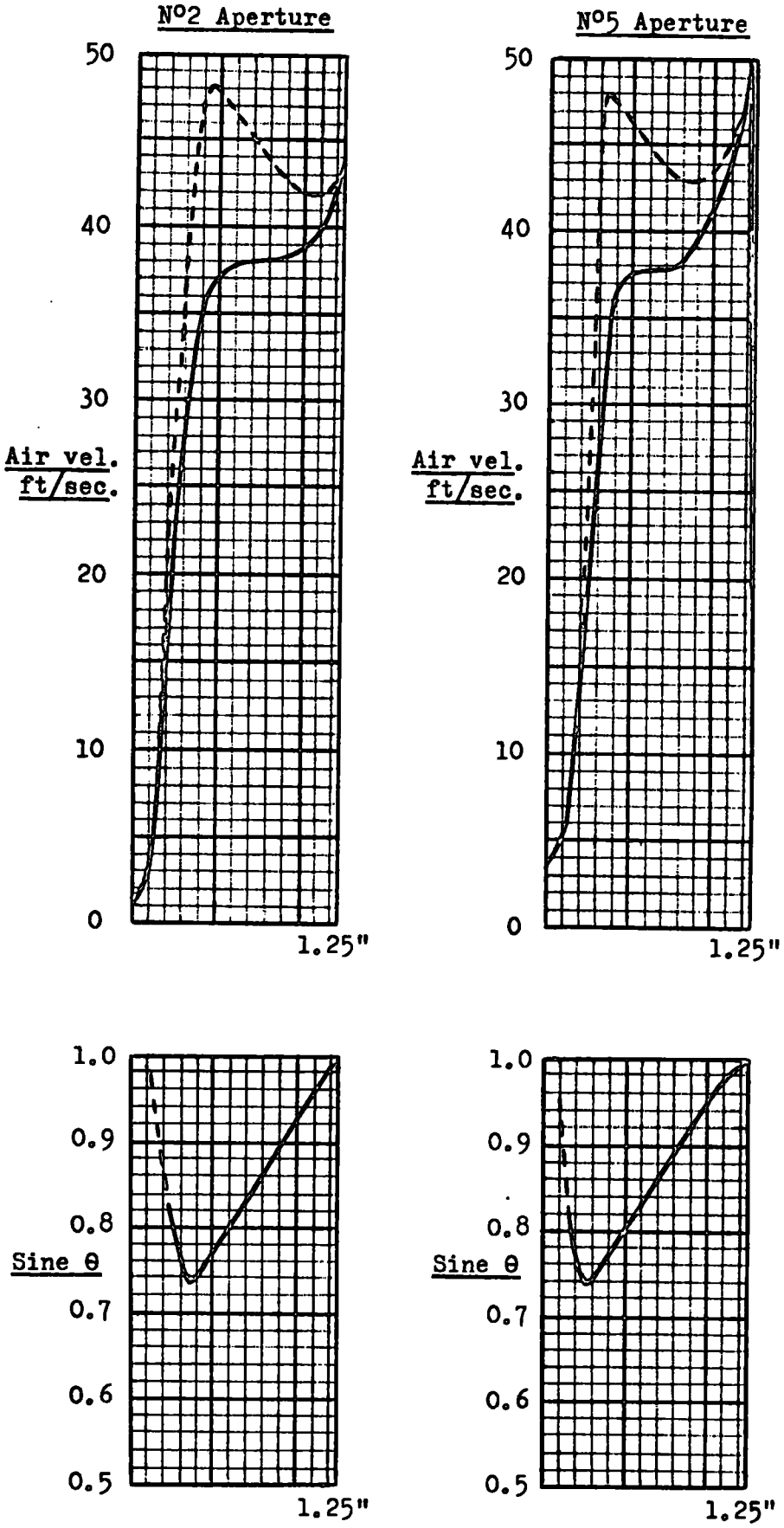

FIG.31 APERTURE AIR FLOW PATTERNS.

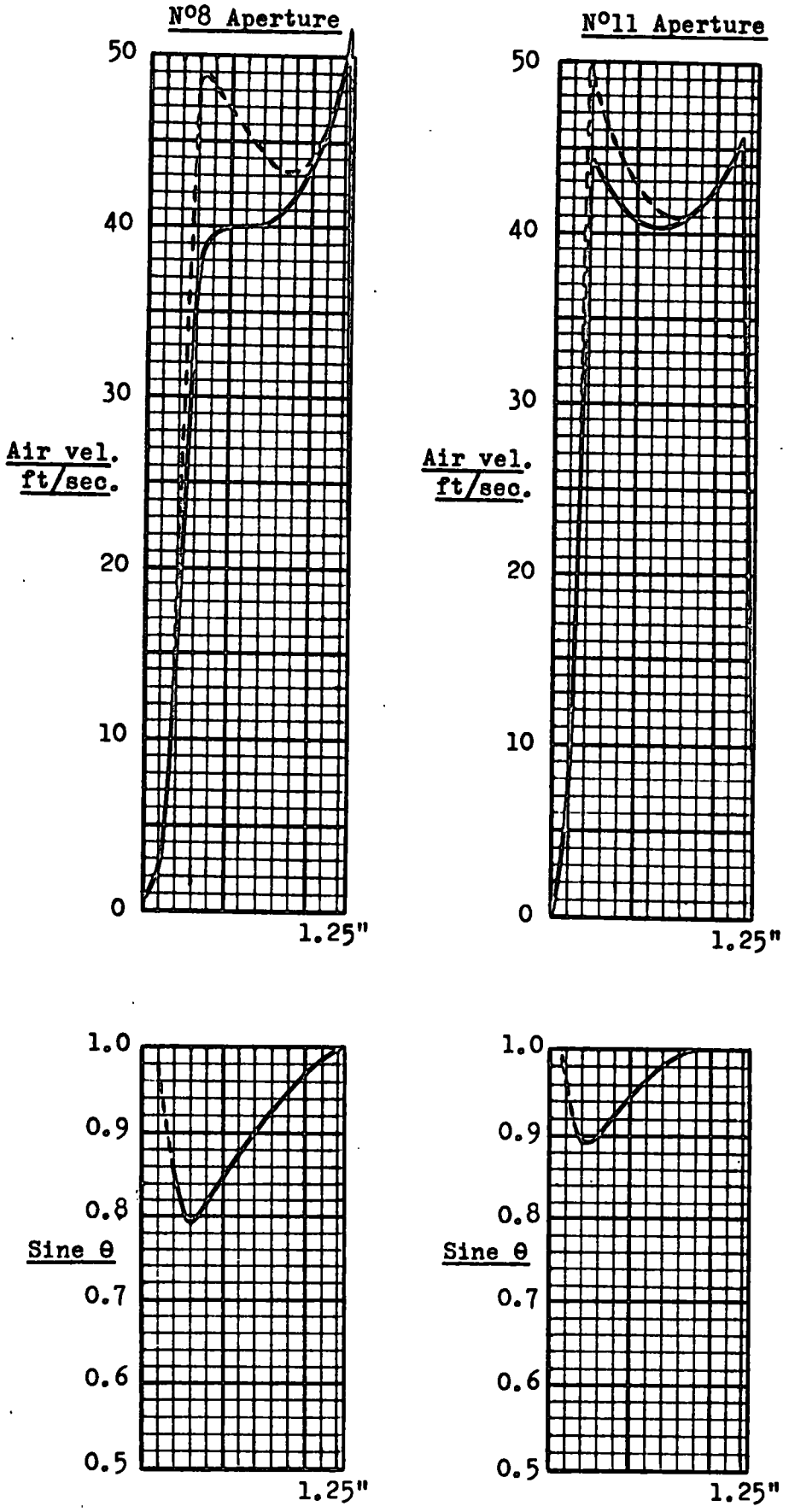

FIG.32 APERTURE AIR FLOW PATTERNS.

7.2 Variation of static pressure across the aperture.

Early tests with the pitot-static tube had suggested that the static pressure varied in a complex manner across the aperture width. Apart from the intrinsic interest in knowing in detail what form this variation would take for various openings, it was felt that such knowledge might be indispensable to an adequate understanding of the air distribution characteristics of the duct. Consequently, tests were carried out with the same range of aperture areas and total air flow as outlined in Section 5.

In all cases the pitot-static tube was in the horizontal plane with the tube head at half aperture height and the static pressure holes situated 0.125" inward from the front faces of the perspex aperture cover plates. Readings were taken at every 0.1" across the aperture width, the values of which are given in Table 8 and are plotted as shown by figs.33 to 37.

Care was taken at every location to align the head of the pitot-static tube with the issuing air, thereby eliminating the possibility of the horizontal static pressure holes experiencing a component of the air velocity. As a further safeguard these holes were masked and the readings repeated, but no significant changes were recorded.

TABLE 8.

VARIATION OF STATIC PRESSURE ACROSS APERTURE WIDTH.

Pitot-static tube location indicates position of static pressure holes at half aperture height commencing from upstream edge of aperture.

Apertures 6" x 1"									
Location	0.15"	0.2"	0.3"	0.4"	0.5"	0.6"	0.7"	0.8"	0.9"
N°2 Aperture	-.030 -2.1	-.026 -1.8	0.018 1.3	0.072 5.1	0.177 12.5	0.233 16.5	0.277 19.6	0.266 18.8	0.229 16.2
N°5 Aperture	-.045 -3.2	-.020 -1.4	0.026 1.8	0.135 9.5	0.207 14.6	0.232 16.4	0.272 19.2	0.229 16.2	0.122 8.6
N°8 Aperture	-.048 -3.4	-.007 -0.5	0.075 5.3	0.190 13.4	0.213 15.1	0.259 18.3	0.236 16.7	0.143 10.1	0.051 3.6
N°11 Aperture	-.028 -2.0	0.054 3.8	0.174 12.3	0.245 17.3	0.266 18.8	0.238 16.8	0.202 14.3	0.123 8.7	-.028 -2.0

Apertures 6" x 1½"									
Location	0.2"	0.3"	0.4"	0.5"	0.6"	0.7"	0.8"	0.9"	1.0"
N°2 Aperture	-.018 -1.3	-.014 -1.0	0.006 0.4	0.028 2.0	0.065 4.6	0.103 7.3	0.129 9.1	0.167 11.8	0.202 14.3
N°5 Aperture	-.013 -0.9	-.006 -0.4	0.013 0.9	0.054 3.8	0.111 7.8	0.136 9.6	0.164 11.6	0.180 12.6	0.187 13.2
N°8 Aperture	-.013 -0.9	-.003 -0.2	0.033 2.3	0.067 4.7	0.093 6.6	0.123 8.7	0.150 10.6	0.158 11.2	0.171 12.1
N°11 Aperture	0.017 1.2	0.065 4.6	0.115 8.1	0.154 10.9	0.160 11.3	0.168 11.9	0.177 12.5	0.178 12.6	0.177 12.5

Apertures 6" x 1½"				
Location	1.1"	1.2"	1.3"	1.4"
N°2 Aperture	0.228 16.1	0.236 16.7	0.213 15.1	0.206 14.6
N°5 Aperture	0.184 13.0	0.174 12.3	0.154 10.9	0.147 10.4
N°8 Aperture	0.178 12.6	0.162 11.5	0.135 9.5	0.107 7.6
N°11 Aperture	0.150 10.6	0.115 8.1	0.027 1.9	0.016 1.1

Upper figures are in inches w.g.

Lower figures are in ft. of air at 80°F.

1 in.w.g. = 70.7 ft. of air at 80°F. and 14.7 psia.

TABLE 8 (Cont'd.)

VARIATION OF STATIC PRESSURE ACROSS APERTURE WIDTH.

Pitot-static tube location indicates position of static pressure holes at half aperture height commencing from upstream edge of aperture.

Apertures 6" x 2"										
Location	0.1"	0.2"	0.3"	0.4"	0.5"	0.6"	0.7"	0.8"	0.9"	1.0"
N°2 Aperture	-.004 -0.3	-.008 -0.6	-.014 -1.0	-.018 -1.3	-.024 -1.7	-.026 -1.8	-.026 -1.8	-.028 -2.0	-.008 -0.6	0.002 0.1
N°5 Aperture	-.006 -0.4	-.008 -0.6	-.016 -1.1	-.010 -0.7	-.008 -0.6	0.006 0.4	0.016 1.1	0.041 2.9	0.054 3.8	0.067 4.7
N°8 Aperture	-.013 -0.9	-.013 -0.9	-.018 -1.3	-.008 -0.6	0.010 0.7	0.032 2.2	0.045 3.2	0.055 3.9	0.082 5.8	0.089 6.3
N°11 Aperture	-.014 -1.0	0.002 0.1	0.027 1.9	0.051 3.6	0.066 4.7	0.086 6.1	0.096 6.8	0.103 7.3	0.109 7.7	0.113 8.0

Apertures 6" x 2"									
Location	1.1"	1.2"	1.3"	1.4"	1.5"	1.6"	1.7"	1.8"	1.9"
N°2 Aperture	0.024 1.7	0.045 3.2	0.069 4.9	0.099 7.0	0.113 8.0	0.129 9.1	0.127 9.0	0.127 9.0	0.127 9.0
N°5 Aperture	0.085 6.0	0.105 7.4	0.116 8.2	0.130 9.2	0.130 9.2	0.132 9.3	0.126 8.9	0.115 8.1	0.074 5.2
N°8 Aperture	0.105 7.4	0.117 8.3	0.123 8.7	0.129 9.1	0.129 9.1	0.125 8.8	0.112 7.9	0.088 6.2	0.065 4.6
N°11 Aperture	0.110 7.8	0.113 8.0	0.105 7.4	0.095 6.7	0.082 5.8	0.074 5.2	0.045 3.2	0.011 0.8	-.010 -0.7

Upper figures are in inches w.g.

Lower figures are in ft. of air at 80°F.

1 in.w.g. = 70.7 ft. of air at 80°F and 14.7 psia.

TABLE 8. (Cont'd.)

VARIATION OF STATIC PRESSURE ACROSS APERTURE WIDTH.

Pitot-static tube location indicates position of static pressure holes at half aperture height commencing from upstream edge of aperture.

Apertures 6" x 2½"								
Location	0.2"	0.3"	0.4"	0.5"	0.6"	0.7"	0.8"	0.9"
N°2 Aperture	-.008 -0.6	-.008 -0.6	-.008 -0.6	-.010 -0.7	-.010 -0.7	-.016 -1.1	-.020 -1.4	-.028 -2.0
N°5 Aperture	-.008 -0.6	-.010 -0.7	-.010 -0.7	-.014 -1.0	-.014 -1.0	-.034 -2.4	-.050 -3.5	-.048 -3.4
N°8 Aperture	-.016 -1.1	-.018 -1.3	-.018 -1.3	-.023 -1.6	-.024 -1.7	-.020 -1.4	-.010 -0.7	0.004 0.3
N°11 Aperture	-.010 -0.7	0.004 0.3	0.020 1.4	0.035 2.5	0.050 3.5	0.065 4.6	0.072 5.1	0.081 5.7

Apertures 6" x 2½"								
Location	1.0"	1.1"	1.2"	1.3"	1.4"	1.5"	1.6"	1.7"
N°2 Aperture	-.028 -2.0	-.027 -1.9	-.023 -1.6	-.013 -0.9	-.003 -0.2	0.008 0.6	0.025 1.8	0.048 3.4
N°5 Aperture	-.021 -1.5	-.016 -1.1	-.006 -0.4	0.006 0.4	0.034 2.4	0.047 3.3	0.076 5.4	0.093 6.6
N°8 Aperture	0.023 1.6	0.025 1.8	0.054 3.8	0.065 4.6	0.089 6.3	0.093 6.6	0.109 7.7	0.115 8.1
N°11 Aperture	0.089 6.3	0.089 6.3	0.095 6.7	0.093 6.6	0.093 6.6	0.093 6.6	0.093 6.6	0.083 5.9

Apertures 6" x 2½"							
Location	1.8"	1.9"	2.0"	2.1"	2.2"	2.3"	2.35"
N°2 Aperture	0.088 6.2	0.102 7.2	0.129 9.1	0.132 9.3	0.133 9.4	0.125 8.8	0.117 8.3
N°5 Aperture	0.113 8.0	0.129 9.1	0.141 10.0	0.141 10.0	0.127 9.0	0.134 9.5	0.126 8.9
N°8 Aperture	0.127 9.0	0.132 9.3	0.137 9.7	0.130 9.2	0.125 8.8	0.120 8.5	0.095 6.7
N°11 Aperture	0.077 5.4	0.071 5.0	0.061 4.3	0.047 3.3	0.028 2.0	0.010 0.7	-.003 -0.2

Upper figures are in inches w.g.

Lower figures are in ft. of air at 80°F.

1 in.w.g. = 70.7 ft. of air at 80°F and 14.7 psia.

TABLE 8. (Cont'd.)

VARIATION OF STATIC PRESSURE ACROSS APERTURE WIDTH.

Pitot-static tube location indicates position of static pressure holes at half aperture height commencing from upstream edge of aperture.

Apertures 6" x 3"										
Location	0.2"	0.3"	0.4"	0.5"	0.6"	0.7"	0.8"	0.9"	1.0"	1.1"
N°2 Aperture	-.003 -0.2	-.006 -0.4	-.011 -0.8	-.014 -1.0	-.021 -1.5	-.025 -1.8	-.030 -2.1	-.020 -1.4	-.018 -1.3	-.016 -1.1
N°5 Aperture	-.003 -0.2	-.006 -0.4	-.010 -0.7	-.009 -0.6	-.007 -0.5	-.007 -0.5	-.007 -0.5	-.007 -0.5	-.004 -0.3	-.003 -0.2
N°8 Aperture	-.004 -0.3	-.011 -0.8	-.018 -1.3	-.010 -0.7	-.008 -0.6	-.004 -0.3	0.011 0.8	0.014 1.0	0.021 1.5	0.030 2.1
N°11 Aperture	-.010 -0.7	-.020 -1.4	-.016 -1.1	0.006 0.4	0.034 2.4	0.042 3.0	0.059 4.2	0.069 4.9	0.078 5.5	0.082 5.8

Apertures 6" x 3"										
Location	1.2"	1.3"	1.4"	1.5"	1.6"	1.7"	1.8"	1.9"	2.0"	2.1"
N°2 Aperture	-.014 -1.0	-.011 -0.8	-.010 -0.7	-.009 -0.6	0.000 0.0	0.042 0.3	0.011 0.8	0.014 1.0	0.030 2.1	0.047 3.3
N°5 Aperture	0.003 0.2	0.009 0.6	0.017 1.2	0.025 1.8	0.034 2.4	0.040 2.8	0.050 3.5	0.061 4.3	0.069 4.9	0.079 5.6
N°8 Aperture	0.038 2.7	0.047 3.3	0.055 3.9	0.064 4.5	0.071 5.0	0.079 5.6	0.085 6.0	0.091 6.4	0.096 6.8	0.103 7.3
N°11 Aperture	0.086 6.1	0.091 6.4	0.093 6.6	0.098 6.9	0.099 7.0	0.099 7.0	0.098 6.9	0.093 6.6	0.091 6.4	0.091 6.4

Apertures 6" x 3"								
Location	2.2"	2.3"	2.4"	2.5"	2.6"	2.7"	2.8"	2.9"
N°2 Aperture	0.057 4.0	0.071 5.0	0.083 5.9	0.100 7.1	0.105 7.4	0.109 7.7	0.099 7.0	0.102 7.2
N°5 Aperture	0.093 6.6	0.105 7.4	0.116 8.2	0.125 8.8	0.126 8.9	0.109 7.7	0.081 5.7	0.064 4.5
N°8 Aperture	0.110 7.8	0.113 8.0	0.115 8.1	0.115 8.1	0.115 8.1	0.112 7.9	0.093 6.6	0.081 5.7
N°11 Aperture	0.089 6.3	0.088 6.2	0.075 5.3	0.068 4.8	0.059 4.2	0.038 2.7	0.017 1.2	0.004 0.3

Upper figures are in inches w.g.

Lower figures are in ft. of air at 80°F.

1 in.w.g. = 70.7 ft. of air at 80°F and 14.7 psia.

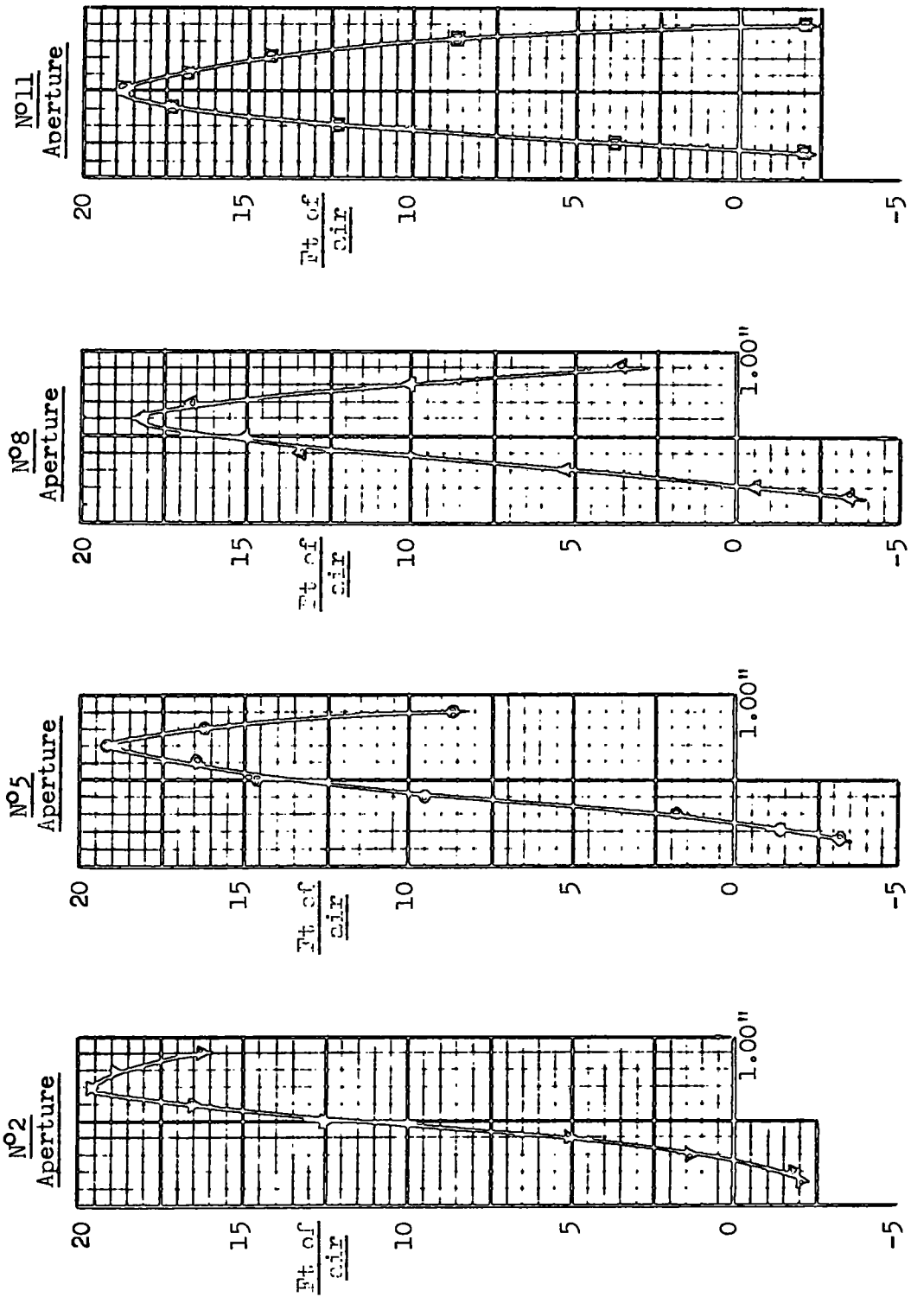

FIG.33 VARIATION OF STATIC PRESSURE ACROSS APERTURES.

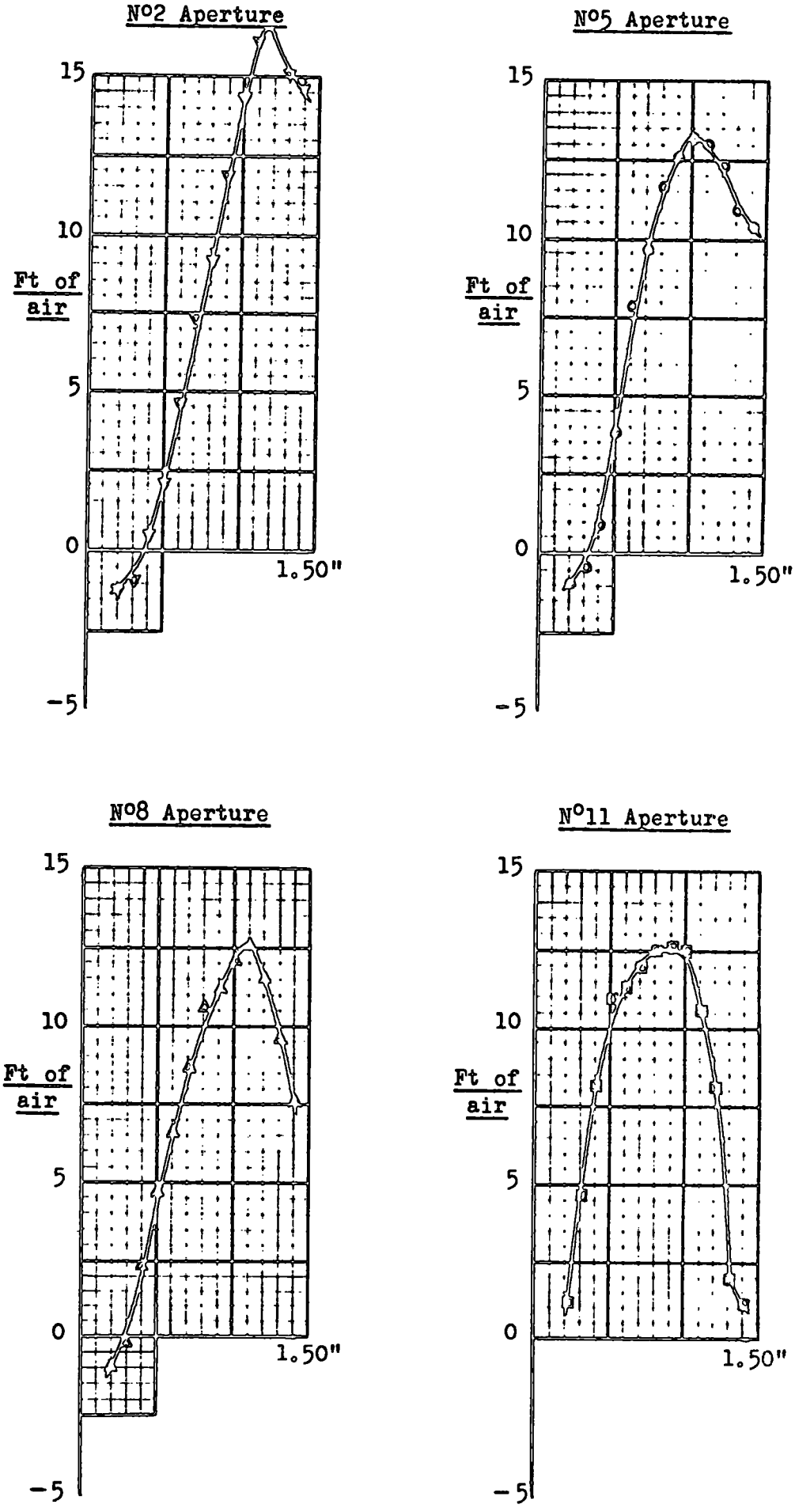

FIG.34 VARIATION OF STATIC PRESSURE ACROSS APERTURES.

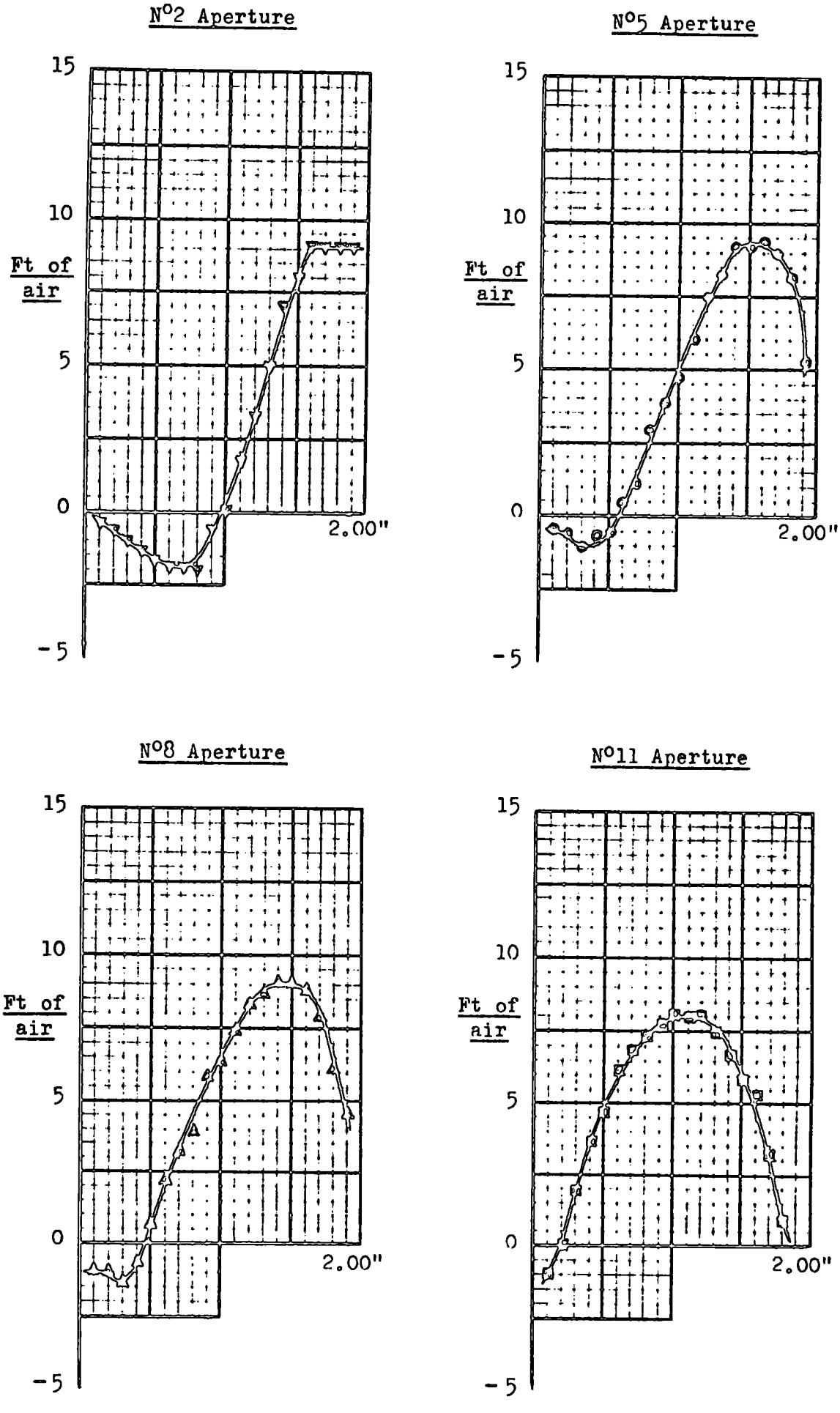

FIG.35 VARIATION OF STATIC PRESSURE ACROSS APERTURES.

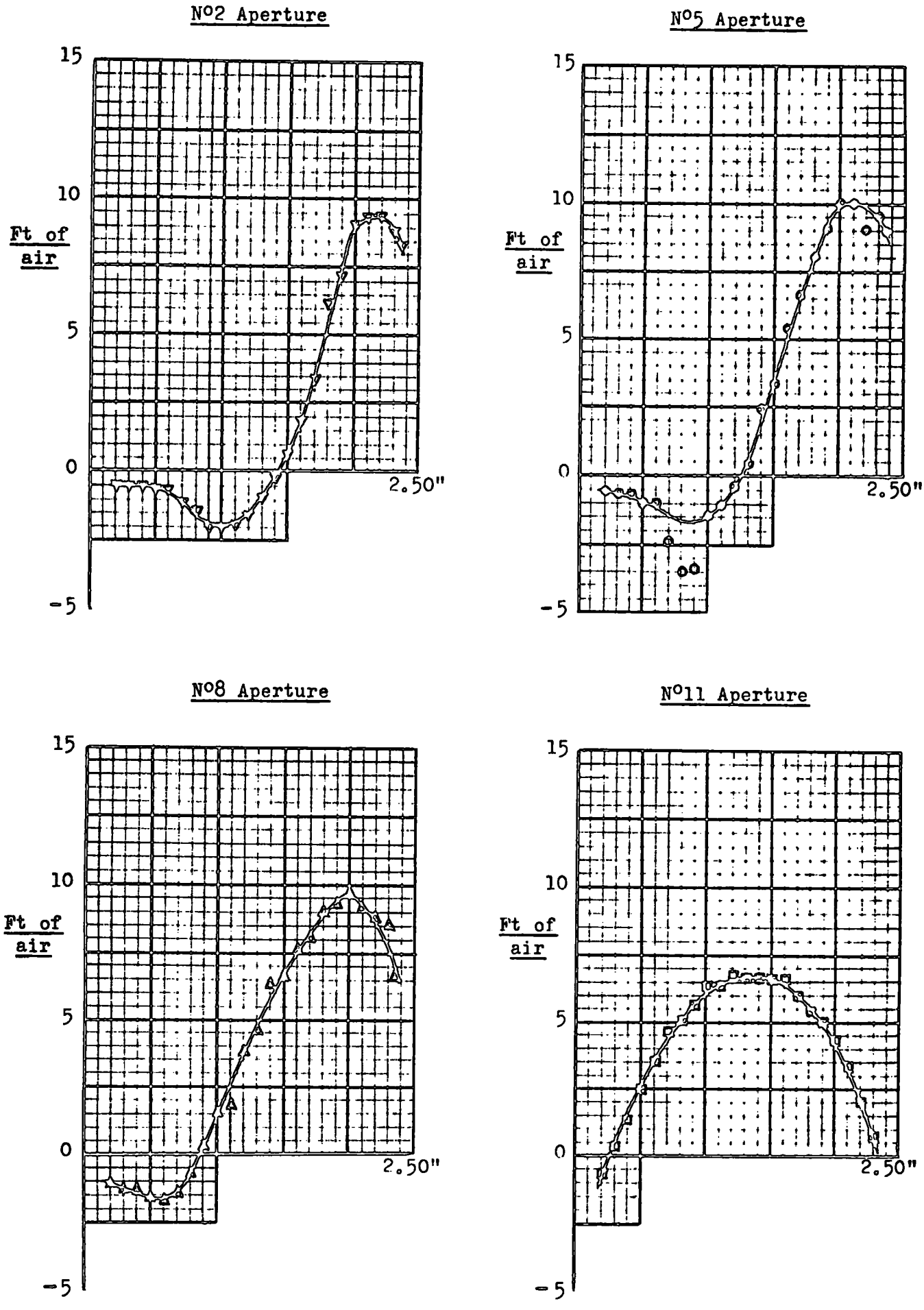

FIG.36 VARIATION OF STATIC PRESSURE ACROSS APERTURES.

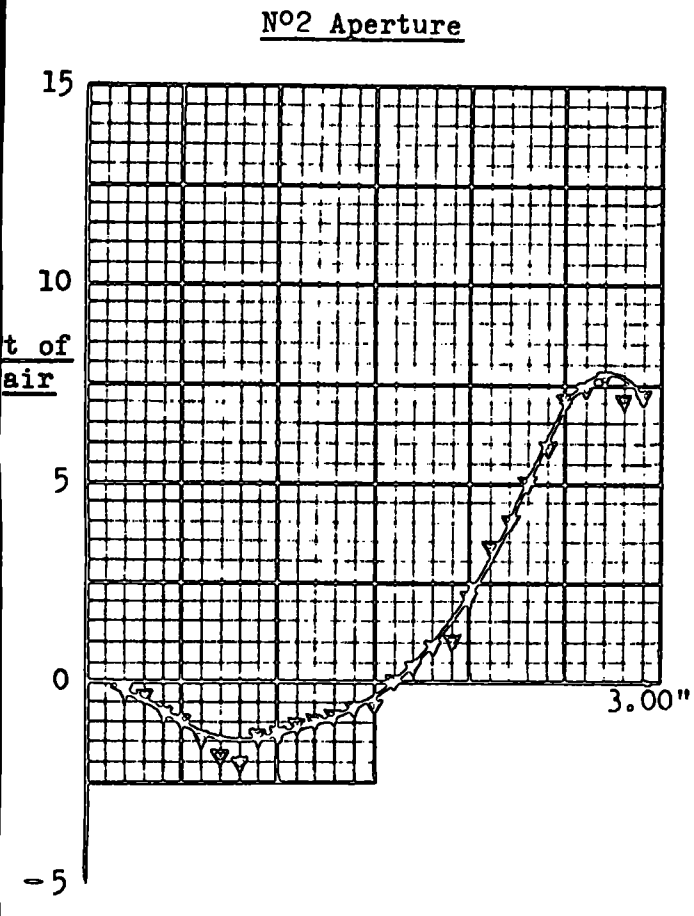

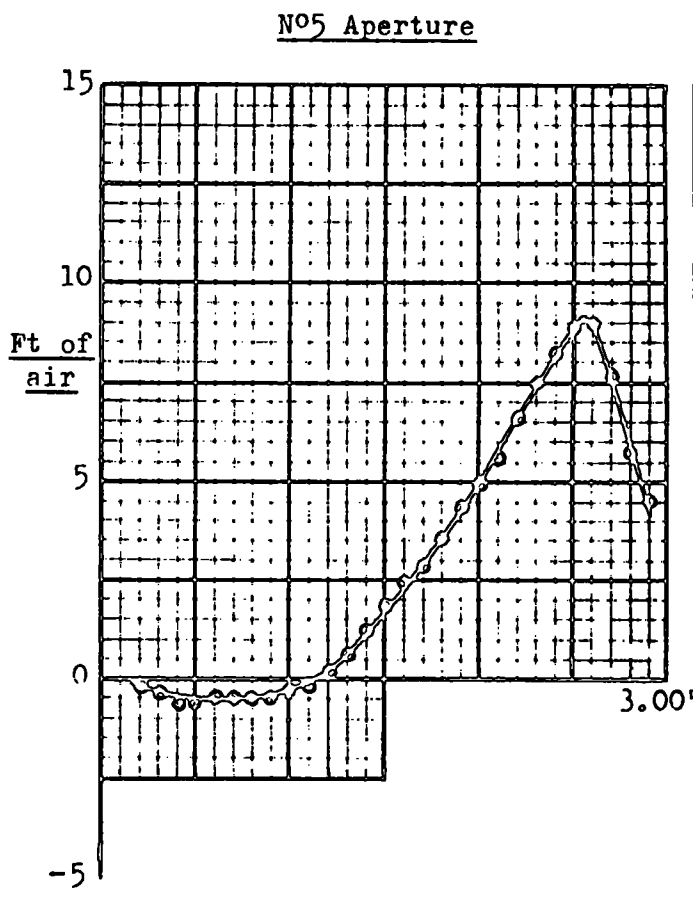

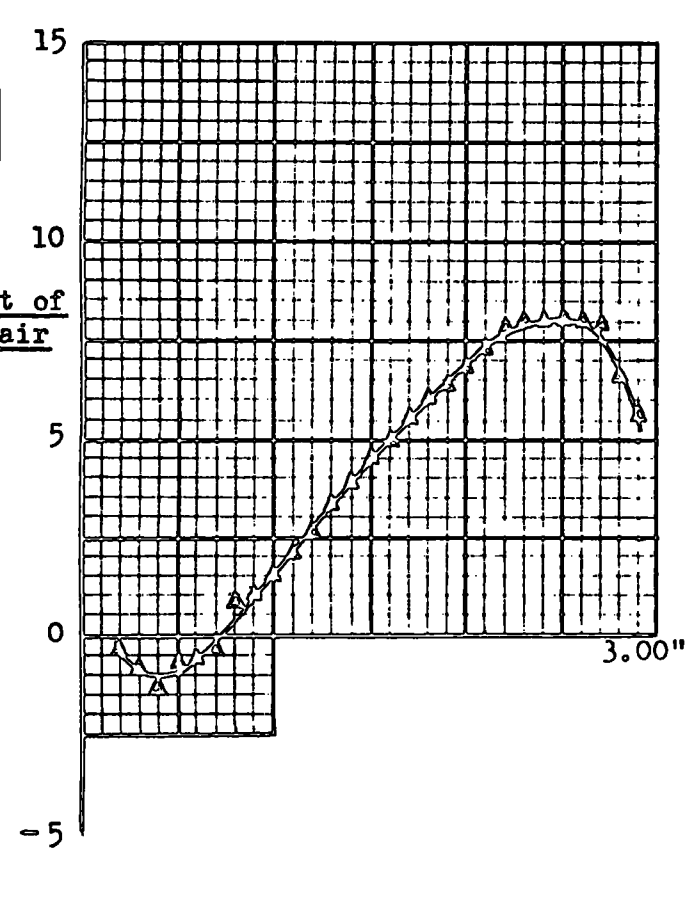

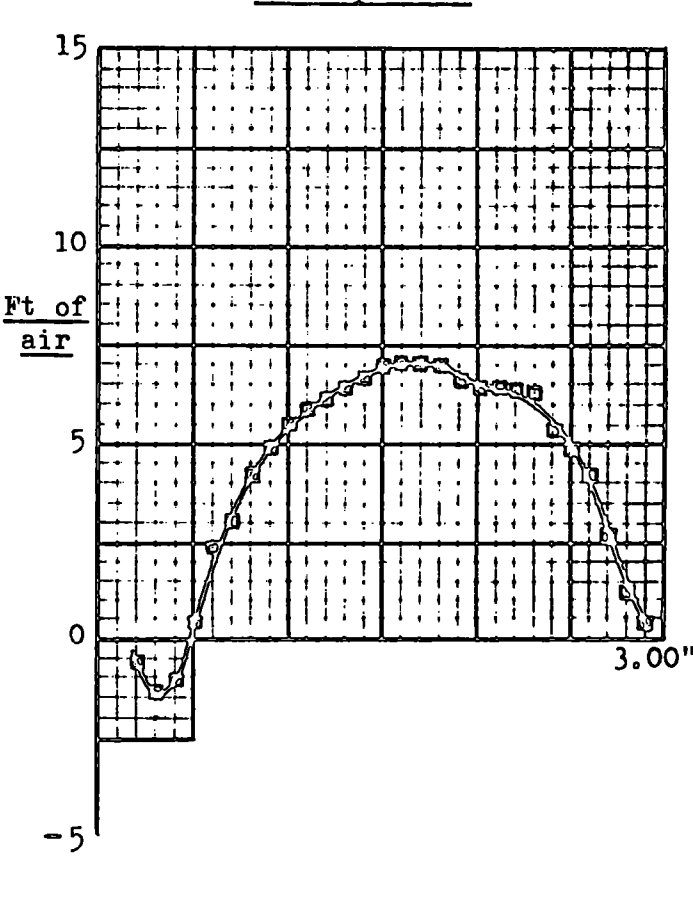

FIG.37 VARIATION OF STATIC PRESSURE ACROSS APERTURES.

SECTION 8. ANALYSIS OF EXPERIMENTAL RESULTS.

8.1. General comments.

A detailed inspection of the experimental results inevitably leads to the conclusion that the complexities associated with both the air flowing in the duct and the air leaving through the apertures preclude any sort of exact analysis of the duct's air distribution characteristics. For example, consider the air discharged through a single aperture as indicated below and assume for simplicity that the flow is two dimensional and incompressible.

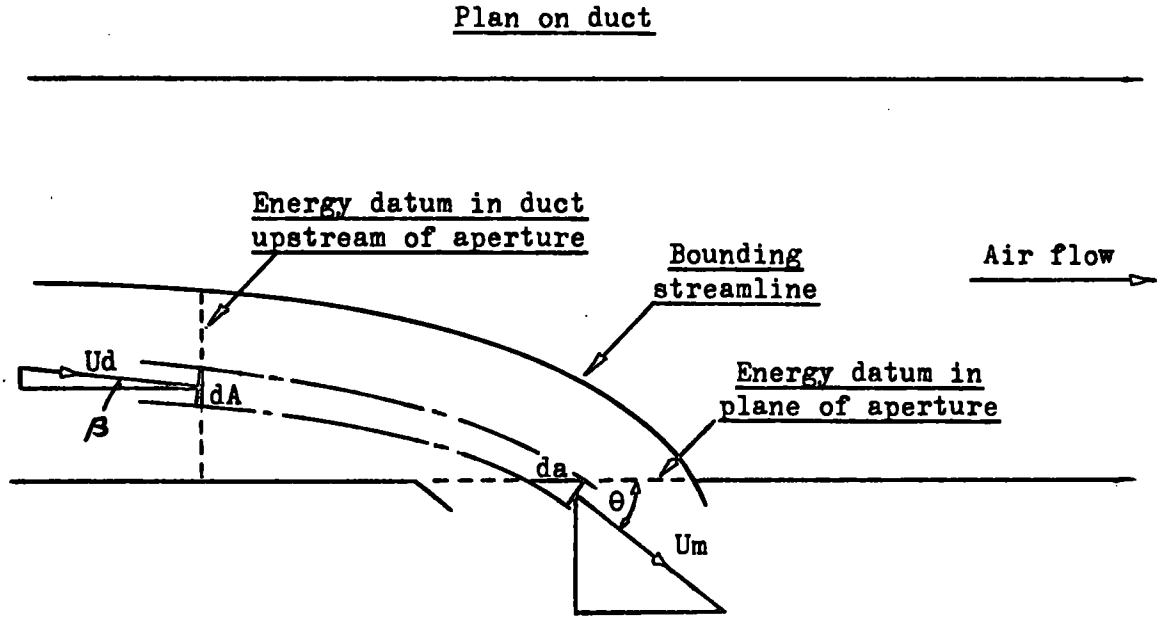

For the element of flow shown let U_d and h_d be the velocity and static pressure at the energy datum in the duct, and U_m and h_a be the velocity and static pressure at the energy datum in the plane of the aperture. Also, let any energy loss between the two datum sections be expressed as $k.\frac{U_m^2}{2g}$.

Then application of Bernoulli's Theorem to the two sections of area A and a respectively yields the following equation :

$$\rho \int_A U_d . \cos\beta \left\{ \frac{U_d^2}{2g} + h_d \right\} dA = \rho \int_a U_m . \sin\theta \left\{ (1+k) . \frac{U_m^2}{2g} + h_a \right\} da$$

It is evident, because of the complicated way in which U_d, $\cos\beta$ & h_d vary in the duct, and U_m, $\sin\theta$ & h_a across the plane of the aperture, that the use of the above equation to assist in an accurate prediction of the air discharge through the aperture is not feasible. A similar comment applies to the use of the momentum equation.

8.2. Proportional aperture air discharge.

The essence of good ventilation is the provision of adequate quantities of fresh air at specified locations. Since the final dispersal of the air is commonly from a terminal duct with side outlets it is obvious that in such cases the attainment of good ventilation will be facilitated by a general knowledge of the proportional air distribution characteristic of this type of duct and consequently a prominent result of this investigation is that illustrated by fig.30.

Basically, this shows that if all the apertures are open the same amount then the further downstream an aperture is situated the greater is the volume flow of air it discharges. The disparity between the aperture air flows is fairly small at the relatively narrow openings with associated high duct static pressures, but becomes quite pronounced at the wider openings with associated smaller duct static pressures.

Of course, this general effect was to be expected for a duct where the outlets are relatively close together and frictional losses are comparatively small because after each discharge through an outlet there is static pressure regain in the duct downstream of the opening and it is reasonable to assume that the greater the duct static gauge pressure in the vicinity of an outlet the greater will be the air discharged through it.

8.3. Frictional head energy loss per unit mass along duct.

Application of Bernoulli's Theorem to planes in the duct coincident with the most upstream and downstream pressure tapping points, 10 and 24 respectively, gives the following equation :

$$h_{10} + \frac{U_{10}^2}{2g} = h_B + \frac{U_B^2}{2g} + h_L$$

where h_{10} = Static pressure at upstream plane. ft. of air.

U_{10} = Air velocity at upstream plane. ft/sec.

h_B = Static pressure at downstream plane (bulkhead). ft. of air.

U_B = Air velocity at downstream plane (bulkhead). ft/sec.

h_L = Head lost between planes due to friction. ft. of air.

$$\text{As } U_B = 0, \quad h_L = \left(h_{10} + \frac{U_{10}^2}{2g} \right) - h_B \qquad \text{——————} (1)$$

At the upstream plane it is assumed that the air flow is reasonably uniform so that no kinetic energy correction factor need be placed before the $\frac{U_{10}^2}{2g}$ term and also that the value of h_{10} recorded at the static pressure tapping point is typical of the static pressure at any point in the entire plane. As the air in the vicinity of the bulkhead is stagnant h_B is, of course, a true record of the static pressure there.

In determining the aperture proportional air discharges slight variations occurred in the value of the average duct entry velocity as shown in Table 7, column (e) which, although not affecting the validity of the various proportions obtained, could introduce slight but undesirable inaccuracies into the values of static pressure recorded along the duct. Consequently, the figures given in Table 5 represent re-measured values of static pressure where the average inlet velocity was carefully maintained constant at 32.8 ft/sec.

Hence (1) becomes $h_L = (h_{10} + 16.7) - h_8$ (2)

Substitution in (2) of the experimental values of h_{10} and h_8 from Table 5 gives the required values of h_L as shown below.

Aperture size	6" x 1"	6" x 1½"	6" x 2"	6" x 2½"	6" x 3"
Total aperture area in^2.	24	36	48	60	72
h_{10} ft.	55.8	21.2	9.97	8.48	7.25
h_8 ft.	66.0	31.5	20.5	18.8	17.5
h_L ft.	6.5	6.4	6.2	6.4	6.5

Inspection of the bottom row of the above table reveals the fact that the heads lost in frictional effects along the duct are approximately the same at 6.4 ft., irrespective of the total area for air flow available at the apertures. Insufficient experimental data prohibits the accurate allocation of the individual duct losses in the vicinity of each aperture but an estimate of these losses can be made as indicated below by considering the average air velocities in the duct upstream and downstream of the apertures in conjunction with the static pressures upstream and downstream of the apertures.

To simplify the procedure the losses will be allocated to the equal lengths of duct lying between the pairs of static pressure tapping points 10 & 14, 14 & 17, 17 & 20, and 20 & 24.

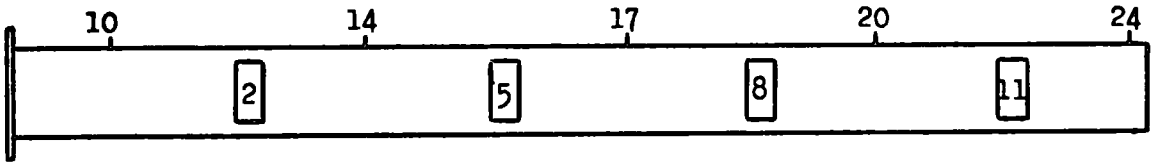

TABLE 9.

ENERGY LOSSES ALONG DUCT.

Column (a) : Static gauge pressure at upstream tapping point. (See Table 5) ft. of air.

Column (b) : Average velocity in duct upstream of aperture. $\bar{U}_{du}$ ft/sec.

Column (c) : Average velocity in duct downstream of aperture. $\bar{U}_{dd}$ ft/sec.

Column (d) : $\frac{\bar{U}_{du}^2}{2g} - \frac{\bar{U}_{dd}^2}{2g}$ ft. of air.

Column (e) : (a) + (d)

Column (f) : Static gauge pressure at downstream tapping point. (See Table 5) ft. of air.

Column (g) : Energy loss (e) − (f) ft.lbf/lb.

Column (h) : Energy loss expressed as a proportion of the upstream average kinetic energy term $\frac{\bar{U}_{du}^2}{2g}$

Energy loss between static pressure tapping points 10 and 14								
Aperture size	(a)	(b)	(c)	(d)	(e)	(f)	(g)	(h)
6" x 1"	55.8	32.8	25.4	6.68	62.5	60.3	2.2	0.13
6" x 1½"	21.2	32.8	25.6	6.53	27.7	25.3	2.4	0.14
6" x 2"	9.97	32.8	26.5	5.80	15.8	13.4	2.4	0.14
6" x 2½"	8.48	32.8	27.2	5.22	13.7	11.0	2.7	0.16
6" x 3"	7.25	32.8	27.4	5.05	12.3	9.69	2.6	0.16
Energy loss between static pressure tapping points 14 and 17								
Aperture size	(a)	(b)	(c)	(d)	(e)	(f)	(g)	(h)
6" x 1"	60.3	25.4	17.0	5.53	65.8	64.1	1.7	0.17
6" x 1½"	25.3	25.6	17.5	5.45	30.8	28.9	1.9	0.19
6" x 2"	13.4	26.5	18.7	5.48	18.9	17.3	1.6	0.15
6" x 2½"	11.0	27.2	20.0	5.32	16.3	14.6	1.7	0.15
6" x 3"	9.69	27.4	20.4	5.19	14.9	13.2	1.7	0.15
Energy loss between static pressure tapping points 17 and 20								
Aperture size	(a)	(b)	(c)	(d)	(e)	(f)	(g)	(h)
6" x 1"	64.1	17.0	8.40	3.39	67.5	65.4	2.1	0.47
6" x 1½"	28.9	17.5	8.75	3.54	32.4	30.6	1.8	0.38
6" x 2"	17.3	18.7	9.75	3.96	21.3	19.4	1.9	0.35
6" x 2½"	14.6	20.0	10.9	4.35	19.0	17.5	1.5	0.24
6" x 3"	13.2	20.4	11.3	4.48	17.7	16.0	1.7	0.26
Energy loss between static pressure tapping points 20 and 24								
Aperture size	(a)	(b)	(c)	(d)	(e)	(f)	(g)	(h)
6" x 1"	65.4	8.40	----	1.10	66.5	66.0	0.5	0.46
6" x 1½"	30.6	8.75	----	1.19	31.8	31.5	0.3	0.25
6" x 2"	19.4	9.75	----	1.48	20.9	20.5	0.4	0.27
6" x 2½"	17.5	10.9	----	1.82	19.3	18.8	0.5	0.27
6" x 3"	16.0	11.3	----	1.98	18.0	17.5	0.5	0.25

In general, the duct air flow will be non-uniform and a suitable kinetic energy correction factor Ke, ranging usually from 1.0 to about 1.15, should be placed before each $\frac{U^2}{2g}$ term. However, since the considerable amount of data needed to establish the true factors is not in existence it will be assumed that no serious error will be incurred by taking Ke = 1.0 throughout. Moreover, at any given plane in the duct there will be a variation of static pressure, but again as a simplification it will be assumed that the static pressures recorded at the tappings along the top of the duct are typical of their respective sections.

Columns (g) and (h) of Table 9 show the estimated energy losses for each length of duct where the average values of duct air velocity in the table have been deduced from the 'smoothed' curves of fig.30.

8.4 Friction factor f.

In the foregoing section it was found convenient to allocate estimated losses to four equal lengths of the duct, the justification for this being that the disturbed flow conditions downstream of N°2 aperture precluded the possiblity of accurate calculations. Between the static pressure tapping points 10 and 11, however, the flow is reasonably uniform and a question arises as to whether the pressure drop here could be predicted using accepted methods of calculating f. Since the average duct inlet velocity is constant at 32.8 ft/sec. it would be expected that the pressure drop between tapping points 10 and 11 would be approximately the same irrespective of the size of the openings along the duct and this is largely borne out by the figures given below which have been abstracted from Table 5.

Aperture size	h_{10} ft. air	h_{11} ft. air	$h_{10} - h_{11}$ ft. air
6" x 1"	55.8	55.0	0.80
6" x 1½"	21.2	20.4	0.80
6" x 2"	9.97	9.06	0.91
6" x 2½"	8.48	7.60	0.88
6" x 3"	7.25	6.36	0.89

The pressure drop in ft. may be expressed as $h = \frac{f.L.}{De} \frac{U^2}{2g}$ ——— (3)

(neglecting the kinetic energy term correction factor associated with any non-uniformity of flow)

where De = equivalent dia. of duct = $4.\frac{A}{P} = \frac{4(8.0 \times 3.9)}{12 \times 2(8.0+3.9)}$ = 0.437 ft.

For smooth surfaces Blasius suggests, for Reynolds Numbers between 5,000 and 100,000, the empirical relationship $f = \frac{0.316}{Re^{0.25}}$

$Re = \frac{U.De}{\nu}$ and for air at 80°F and 14.7 psia the kinematic viscosity $\nu = 1.69 \times 10^{-4}$ ft^2/sec.

Hence $Re = \frac{32.8 \times 0.437}{1.69 \times 10^{-4}}$ = 84,800 which is within the normal range of Reynolds Numbers associated with ventilating systems.

Consequently, f = 0.0186

As the distance between the static pressure tapping points 10 and 11 is 9", the pressure drop suggested by (3) is then :

$$h_L = \frac{0.0186 \times 0.75 \times 32.8^2}{0.437 \times 64.4} = 0.53 \text{ ft.}$$

Whilst this result indicates that the predicted frictional head loss is of the same order as the measured values it suggests that for the small-scale duct it would be unwise to use any friction factors which have not been determined experimentally from the duct itself.

8.5 Correlation of the experimental results.

As pointed out in Section 8.1, the complexity of the air flow

both in the duct and through the apertures precludes the possibility of an exact analysis of the duct's distribution characteristic using energy or momentum equations. Consequently it is necessary to search for some empirical or semi-empirical correlation of the experimental results which might enable useful predictions to be made about the duct's performance under operating conditions other than those hitherto experienced. Preferably, any such correlation obtained should be expressed in non-dimensional terms so that any conclusions reached would not necessarily be confined to the small-scale duct but, ideally, would be applicable to a wide range of terminal ventilating ducts.

Any simple procedure that would allow the determination of aperture areas for given air flow requirements would need to be such that conditions downstream of an aperture, as well as the aperture size itself, could be determinable. For then it would be possible to proceed along the duct, aperture by aperture, determining the required information for each in turn, resulting finally in the complete design. This suggests that two relationships would have to be known : (a) that between the fraction of the upstream flow escaping and the aperture size and (b) that between the fraction escaping and the pressure change across the aperture within the duct.

If these relationships were known then knowledge of conditions upstream of an aperture together with the required fraction of the upstream flow escaping would enable the use of relationship (a) to determine aperture size and of (b) to find the conditions downstream of that aperture which in turn become the upstream conditions of the next aperture (after possibly allowing for friction).

Now it might be expected that some relationship would exist between the momentum of the escaping air normal to the duct and the pressure difference between the duct and the outside atmosphere which

gives rise to the outflow.

i.e. Suppose $\left(\frac{\rho . a . \bar{U}_n}{g}\right) \bar{U}_n = f(\rho . h_u . a)$

Where a = aperture area, $\bar{U}_n$ = average normal velocity of issuing air, and h_u = duct static gauge pressure upstream of aperture.

Division by $\rho . a$ then gives $\frac{\bar{U}_n^2}{g} = f(h_u)$

Now if η is the fraction of the approaching air which escapes through an aperture then $\rho . a . \bar{U}_n = \eta . \rho . A . \bar{U}_{du}$, where A = duct area and $\bar{U}_{du}$ = average velocity in duct upstream of aperture, and consequently $\bar{U}_n = \eta \frac{A . \bar{U}_{du}}{a}$ Hence $\left(\eta \frac{A . \bar{U}_{du}}{a}\right)^2 = f(h_u . g)$ or $h_u . g = \phi\left(\eta \frac{A . \bar{U}_{du}}{a}\right)^2$

This can be conveniently rendered non-dimensional by dividing by $\bar{U}_{du}^2/2$ to give $\frac{h_u}{\bar{U}_{du}^2/2g} = 2\phi\left(\frac{\eta}{a/A}\right)^2$

Also, if b and B are the breadths of the aperture and duct resp., then the equation may be written : $\frac{h_u}{\bar{U}_{du}^2/2g} = 2\phi\left(\frac{\eta}{6b/8B}\right)^2$ for constant heights of aperture and duct of 6" and 8" resp.

Therefore $\frac{h_u}{\bar{U}_{du}^2/2g} = 3.56\,\phi\left(\frac{\eta}{b/B}\right)^2$

Table 10 gives the values of $\frac{h_u}{\bar{U}_{du}^2/2g}$ and $\frac{\eta}{b/B}$ obtained from the experimental results, these parameters being plotted on logarithmic graph paper as shown by fig.38. As may be seen, the points lie approximately on a straight line and a 'least squares error' correlation of the points gives a line whose equation is :

$$\frac{h_u}{\bar{U}_{du}^2/2g} = 4.29\left(\frac{\eta}{b/B}\right)^{1.74}$$

An expression for the pressure change across an aperture along the duct can be written similarly in non-dimensional terms as

$$\frac{h_d - h_u}{U^2/2g}$$

where the velocity U could be either $\bar{U}_{du}$ or $\bar{U}_{dd}$.

In the design procedure that follows it was found more convenient to use $\bar{U}_{dd}$, the average velocity in the duct downstream of an aperture, than $\bar{U}_{du}$, the empirical relationship between the pressure recovery factor and the fraction of the upstream flow which escapes through an aperture being expressed as $\frac{h_d - h_u}{\bar{U}_{dd}^2/2g} = \phi(\eta)$.

where h_d and h_u = duct static gauge pressure downstream and upstream of an aperture respectively.

Table 11 lists the experimentally obtained values and fig.39 shows that when plotted they lie reasonably close to a straight line whose equation is $\frac{h_d - h_u}{\bar{U}_{dd}^2/2g} = 4.06\eta - 0.498$

Since the graphs of figs.38 & 39 essentially embody the duct's distribution characteristic, including the effect of friction, it should be possible to use them to predict the necessary sizes of outlets for these outlets to discharge preselected proportions of the incoming air flow. In addition, the graphs should allow the prediction of static gauge pressures along the duct. A method outlining how this can be done is given in Section 9.

TABLE 10.

CORRELATION OF EXPERIMENTAL RESULTS (1).

Column (a) : Aperture air discharge expressed as a proportion of the air entering the duct.

Column (b) : Static gauge pressure at aperture upstream tapping point. ft. of air at 80°F.

Column (c) : Average velocity in duct upstream of aperture. ft/sec.

Column (d) : $(c)^2/2g$ ft.

Column (e) : Proportion of duct upstream volume flow discharged through aperture.

Column (f) : Breadth of aperture b/breadth of duct B. (B = 3.90")

Column (g) : $(e)/(f) = \frac{\eta}{b/B}$

Column (h) : $(b)/(d) = \frac{h_u}{U_d^2/2g}$

Aperture size	(a)	(b)	(c)	(d)	(e)	(f)	(g)	(h)
N°2 Aperture								
6" x 1"	0.226	55.8	32.8	16.7	0.226	0.256	0.883	3.34
6" x 1¼"	0.225	32.6	32.8	16.7	0.225	0.321	0.702	1.95
6" x 1½"	0.220	21.2	32.8	16.7	0.220	0.385	0.571	1.27
6" x 2"	0.192	9.97	32.8	16.7	0.192	0.513	0.374	0.597
6" x 2½"	0.170	8.48	32.8	16.7	0.170	0.641	0.265	0.508
6" x 3"	0.163	7.25	32.8	16.7	0.163	0.769	0.212	0.434
N°5 Aperture								
6" x 1"	0.256	60.3	25.4	10.0	0.331	0.256	1.29	6.03
6" x 1¼"	0.252	36.8	25.4	10.0	0.325	0.321	1.01	3.68
6" x 1½"	0.248	25.3	25.6	10.2	0.318	0.385	0.826	2.48
6" x 2"	0.237	13.4	26.5	10.9	0.293	0.513	0.571	1.23
6" x 2½"	0.222	11.0	27.2	11.5	0.267	0.641	0.417	0.957
6" x 3"	0.212	9.69	27.5	11.7	0.253	0.769	0.329	0.828
N°8 Aperture								
6" x 1"	0.262	64.1	17.0	4.49	0.506	0.256	1.98	14.3
6" x 1¼"	0.263	40.3	17.2	4.59	0.503	0.321	1.57	8.78
6" x 1½"	0.265	28.9	17.5	4.75	0.498	0.385	1.30	6.08
6" x 2"	0.274	17.3	18.7	5.43	0.480	0.513	0.936	3.19
6" x 2½"	0.278	14.6	19.9	6.15	0.457	0.641	0.713	2.37
6" x 3"	0.281	13.2	20.5	6.53	0.450	0.769	0.585	2.02

TABLE 10 (Cont'd).

CORRELATION OF EXPERIMENTAL RESULTS (1).

Column (a) : Aperture air discharge expressed as a proportion of the air entering the duct.

Column (b) : Static gauge pressure at aperture upstream tapping point. ft. of air.

Column (c) : Average velocity in duct upstream of aperture. ft/sec.

Column (d) : $(c)^2/2g$ ft.

Column (e) : Proportion of duct upstream volume flow discharged through aperture.

Column (f) : Breadth of aperture b/breadth of duct B. (B = 3.90")

Column (g) : $(e)/(f) = \frac{\eta}{b/B}$

Column (h) : $(b)/(d) = \frac{hu}{U_{du}^2/2g}$

N°11 Aperture								
Aperture size	(a)	(b)	(c)	(d)	(e)	(f)	(g)	(h)
6" x 1"	0.256	65.4	8.40	1.10	1.000	0.256	3.91	59.4
6" x 1¼"	0.260	42.1	8.52	1.13	1.000	0.321	3.12	37.3
6" x 1½"	0.267	30.6	8.75	1.19	1.000	0.385	2.60	25.7
6" x 2"	0.297	19.4	9.74	1.47	1.000	0.513	1.95	13.2
6" x 2½"	0.330	17.5	10.8	1.81	1.000	0.641	1.56	9.68
6" x 3"	0.344	16.0	11.3	1.98	1.000	0.769	1.30	8.08

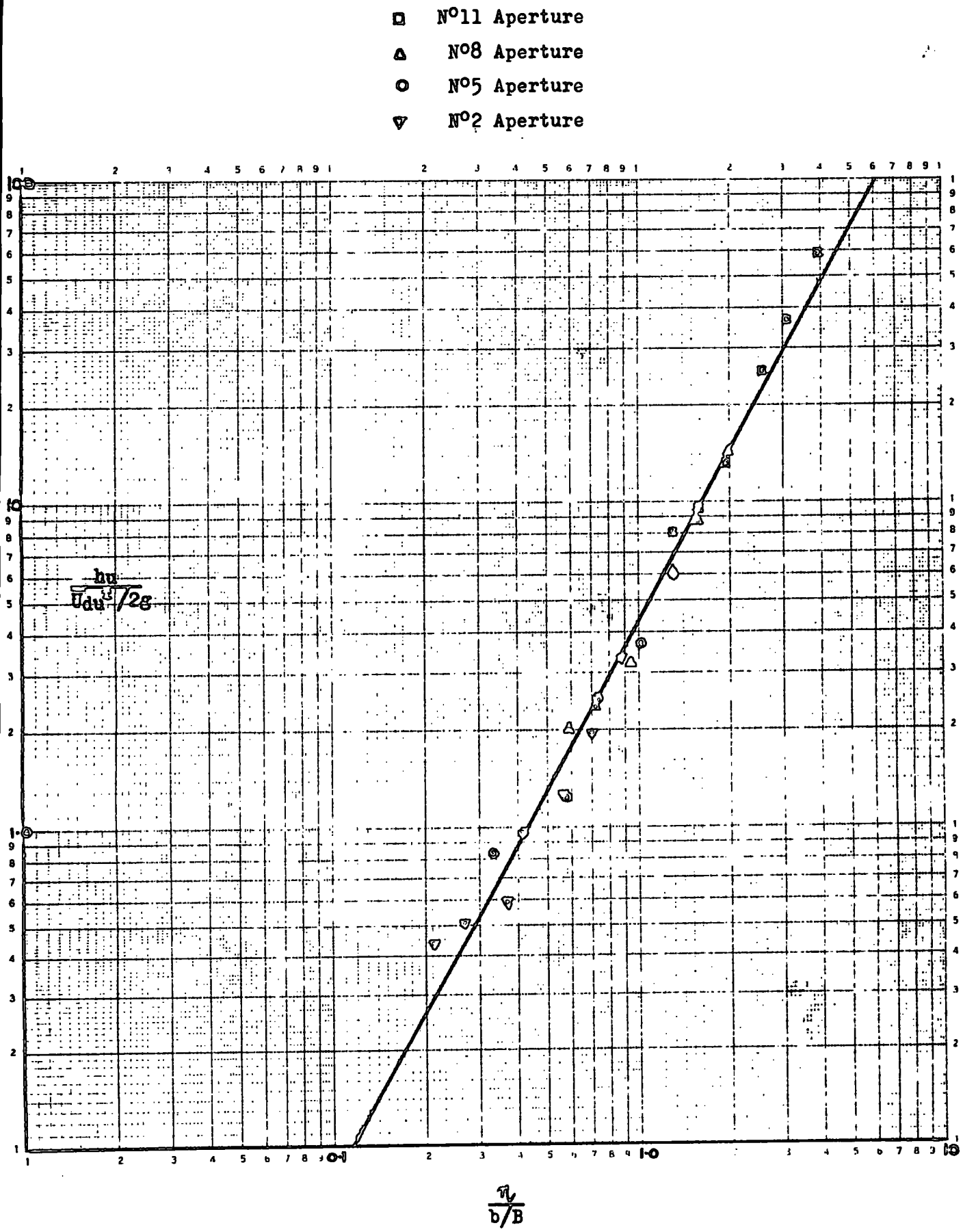

FIG.38 CORRELATION OF EXPERIMENTAL RESULTS (1).

TABLE 11.

CORRELATION OF EXPERIMENTAL RESULTS (2).

Column (a) : Static gauge pressure at aperture downstream tapping point. ft. of air at 80°F.

Column (b) : Static gauge pressure at aperture upstream tapping point. ft. of air at 80°F.

Column (c) : (a) - (b)

Column (d) : Average velocity in duct downstream of aperture. ft/sec. (Abstracted from Table 10)

Column (e) : $(d)^2/2g$ ft.

Column (f) : (c)/(e)

Column (g) : Proportion of duct upstream volume flow discharged through aperture. (Abstracted from Table 10)

Aperture size	(a)	(b)	(c)	(d)	(e)	(f)	(g)
N°2 Aperture							
6" x 1"	60.3	55.8	4.5	25.4	10.0	0.450	0.226
6" x 1¼"	36.8	32.6	4.2	25.4	10.0	0.420	0.225
6" x 1½"	25.3	21.2	4.1	25.6	10.2	0.402	0.220
6" x 2"	13.4	9.97	3.43	26.5	10.9	0.315	0.192
6" x 2½"	11.0	8.48	2.52	27.2	11.5	0.219	0.170
6" x 3"	9.69	7.25	2.44	27.5	11.7	0.209	0.163
N°5 Aperture							
6" x 1"	64.1	60.3	3.8	17.0	4.49	0.846	0.331
6" x 1¼"	40.3	36.8	3.5	17.2	4.59	0.762	0.325
6" x 1½"	28.9	25.3	3.6	17.5	4.75	0.758	0.318
6" x 2"	17.3	13.4	3.9	18.7	5.43	0.718	0.293
6" x 2½"	14.6	11.0	3.6	19.9	6.15	0.585	0.267
6" x 3"	13.2	9.69	3.51	20.5	6.53	0.538	0.253
N°8 Aperture							
6" x 1"	65.4	64.1	1.3	8.40	1.10	1.18	0.506
6" x 1¼"	42.1	40.3	1.8	8.52	1.13	1.59	0.503
6" x 1½"	30.6	28.9	1.7	8.75	1.19	1.43	0.498
6" x 2"	19.4	17.3	2.1	9.74	1.47	1.43	0.480
6" x 2½"	17.5	14.6	2.9	10.8	1.81	1.60	0.457
6" x 3"	16.0	13.2	2.8	11.3	1.98	1.42	0.450
N°11 Aperture							
6" x 1"	66.0	65.4	0.6	0	0	∞	1.000
6" x 1¼"	43.1	42.1	1.0	0	0	∞	1.000
6" x 1½"	31.5	30.6	0.9	0	0	∞	1.000
6" x 2"	20.5	19.4	1.1	0	0	∞	1.000
6" x 2½"	18.8	17.5	1.3	0	0	∞	1.000
6" x 3"	17.5	16.0	1.5	0	0	∞	1.000

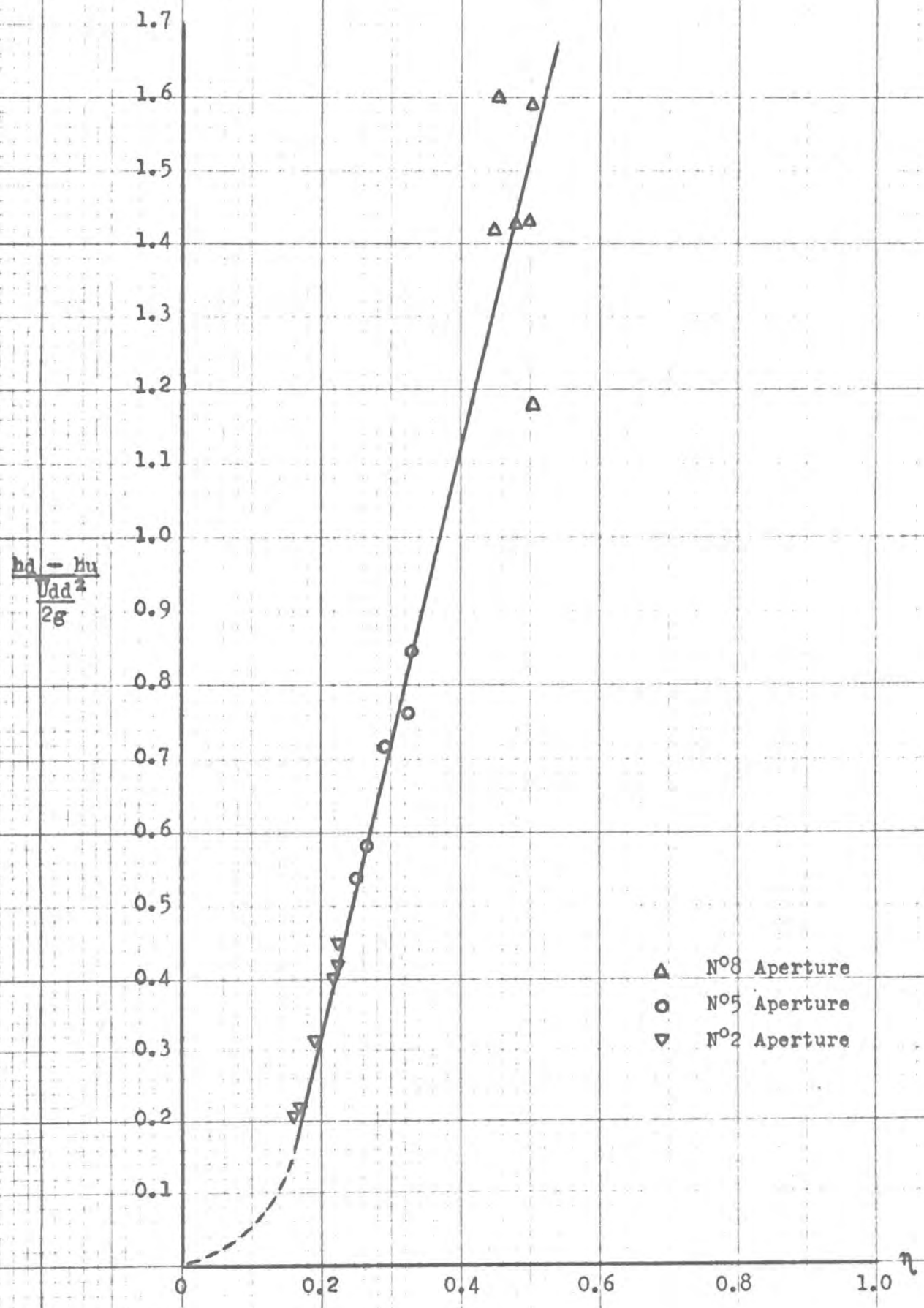

FIG.39 CORRELATION OF EXPERIMENTAL RESULTS (2).

SECTION 9. METHOD OF PREDICTING THE REQUISITE APERTURE AREAS FOR EACH APERTURE TO DISCHARGE A SPECIFIED PROPORTION OF THE TOTAL AIR FLOW.

9.1. Outline of method.

Knowing the desired proportion of the total air flow which each aperture is to discharge, the values of η_2, η_5, η_8 and η_{11} can be easily calculated. In the case of equal aperture air flows η takes the values 0.250, 0.333, 0.500 and 1.000 respectively. Now, a suitable ratio of b/B is selected for the most upstream outlet, N°2 aperture, where b and B are the breadths of aperture and duct respectively. (The choice of b/B will, of course, determine the average normal air velocity through the aperture and also influence the upstream pressure in the duct.)

Hence, for this outlet $\frac{\eta}{b/B}$ can be determined and from fig.38 the corresponding value of $\frac{hu}{\bar{U}du^2/2g}$ can be read off. Also, from fig.39 $\frac{hd - hu}{\bar{U}dd^2/2g}$ can be found corresponding to η_2, and this number in conjunction with the above value of $\frac{hu}{\bar{U}du^2/2g}$ can be used to determine $\frac{hu}{\bar{U}du^2/2g}$ for N°5 aperture. In turn, this last figure enables the ratio of b/B for N°5 aperture to be read from fig.38.

This procedure is repeated, as exemplified below, to obtain the ratios of b/B for the remaining two apertures. Of course, as the ratios obtained are all dimensionless, actual values of aperture breadth b will depend upon the choice of the breadth of duct B, and similarly the pressure upstream of an aperture hu will depend upon the aperture upstream velocity $\bar{U}du$.

9.2. Requisite aperture areas for equal aperture air volume flow rates.

A common requirement in ventilation is for the outlets along a terminal duct to discharge equal quantities of air so, although the above method applies to any proportions of flow, the case where it is desired that each outlet will discharge the same proportion of the

TABLE 12.

PREDICTION OF REQUISITE APERTURE AREAS FOR EQUAL APERTURE AIR VOLUME FLOWS.

Column (a) : Desired aperture air discharge expressed as a proportion of the air entering the duct.

Column (b) : Desired aperture air discharge expressed as a proportion of the duct air volume flow upstream of the aperture. (η)

Column (c) : Average air velocity in duct downstream of an aperture expressed as a proportion of the average air velocity in duct upstream of an aperture.

Column (d) : Value of $\frac{hd - hu}{\overline{U}dd^2/2g}$ corresponding to η. (From fig.39)

Column (e) : Calculated value of $\frac{\eta}{b/B}$ for N°2 aperture.

Column (f) : Value of $\frac{hu}{\overline{U}du^2/2g}$ corresponding to (e). (From fig.38)

Column (g) : Value of $\frac{hu}{\overline{U}du^2/2g}$ deduced from (c), (d) and foregoing (f).

Column (h) : Value of $\frac{\eta}{b/B}$ corresponding to (g). (From fig.38)

Column (i) : Value of b/B.

Column (j) : Value of b/B expressed as a percentage of b/B for N°2, the most upstream aperture.

Common data independent of aperture size and air volume flow entering duct.

	(a)	(b)	(c)	(d)
N°2 Aperture	0.250	0.250	0.750	0.52
N°5 Aperture	0.250	0.333	0.667	0.84
N°8 Aperture	0.250	0.500	0.500	1.52
N°11 Aperture	0.250	1.000	0	0

Selected size of N°2 aperture 6" by 2" (b = 2")
Breadth of duct B = 3.90" ∴ b/B = 0.513 for N°2 aperture.

	(e)	(f)	(g)	(h)	(i)	(j)
N°2 Aperture	0.490	1.26			0.513	100%
N°5 Aperture			2.76	0.76	0.44	86%
N°8 Aperture			7.04	1.31	0.38	74%
N°11 Aperture			29.7	3.00	0.33	64%

Selected size of N°2 aperture 6" by 3" (b = 3")
Breadth of duct B = 3.90" ∴ b/B = 0.769 for N°2 aperture.

	(e)	(f)	(g)	(h)	(i)	(j)
N°2 Aperture	0.325	0.62			0.769	100%
N°5 Aperture			1.63	0.57	0.58	75%
N°8 Aperture			4.51	1.03	0.48	62%
N°11 Aperture			19.6	2.38	0.42	55%

incoming air will be considered. Table 12 embodies the calculations required for predicting the regulation of the remaining aperture breadths when N°2 aperture is selected firstly to have a breadth of 2" and then secondly 3". A breadth of 1" has not been included because at the relatively narrow openings the disparity in aperture flows is quite small and hardly makes regulation of area worthwhile.

9.3 Predicted variation of static pressure along duct.

Columns (f) and (g) of Table 12 allow the static gauge pressure upstream of an aperture to be determined for known values of the average velocity in the duct upstream of an aperture. For example, for a duct entry velocity of 32.8 ft/sec., $\bar{U}_{du}^2/2g$ for N°2 aperture will be 16.7 and for equal aperture air flows $\bar{U}_{du}^2/2g$ for N°s 5, 8 & 11 apertures will therefore be $(\frac{3}{4})^2.16.7$, $(\frac{1}{2})^2.16.7$, and $(\frac{1}{4})^2.16.7$ respectively. Consequently, hu can be evaluated as indicated below.

Column (a) : Value of $\frac{hu}{\bar{U}_{du}^2/2g}$ from columns (f) or (g) of Table 12.

Column (b) : Value of $\bar{U}_{du}^2/2g$.

Column (c) : hu = (a) x (b) ft. of air.

Selected size of N°2 aperture 6" by 2"

	(a)	(b)	(c)
N°2 Aperture	1.26	16.7	21.1
N°5 Aperture	2.76	9.40	25.9
N°8 Aperture	7.04	4.17	29.4
N°11 Aperture	29.7	1.04	30.9

Selected size of N°2 aperture 6" by 3"

	(a)	(b)	(c)
N°2 Aperture	0.62	16.7	10.4
N°5 Aperture	1.63	9.40	15.3
N°8 Aperture	4.51	4.17	18.8
N°11 Aperture	19.6	1.04	20.4

SECTION 10. TRIAL-AND-ERROR SETTING OF APERTURE SIZES FOR EQUAL APERTURE AIR DISCHARGE RATES.

10.1 Experimentally determined areas.

Prior to the predictions of Section 9 being calculated, an experimental balancing of the air flows had been carried out by trial-and-error methods, first with N°2 aperture set at 6" by 2" and second with it set at 6" by 3". In each case the other three apertures were adjusted in area until flow measurements indicated that each aperture was discharging at approximately the same rate.

The resulting air flow patterns are shown by figs.40 to 43 and a summary of the relevant data is given in Table 13 in which the areas of apertures N°s5, 8 & 11 have been expressed as percentages of the area of N°2 aperture. For purposes of comparison the predicted and experimentally determined percentages from Tables 12 and 13 respectively are given below.

For N°2 aperture 6" by 2"

	Predicted percentage	Experimental percentage
N°2 Aperture	100%	100%
N°5 Aperture	86%	89%
N°8 Aperture	74%	84%
N°11 Aperture	64%	83%

For N°2 aperture 6" by 3"

	Predicted percentage	Experimental percentage
N°2 Aperture	100%	100%
N°5 Aperture	75%	73%
N°8 Aperture	62%	57%
N°11 Aperture	55%	57%

For the above two tests the air volume flow entering the duct was arranged to be approximately the same as for the main test programme, that is, 7.1 ft^3/sec. This was not really necessary, however, because the method given in Section 9 predicts aperture areas, for specified proportional aperture air discharges, which are independent of the rate of flow of air at duct entry.

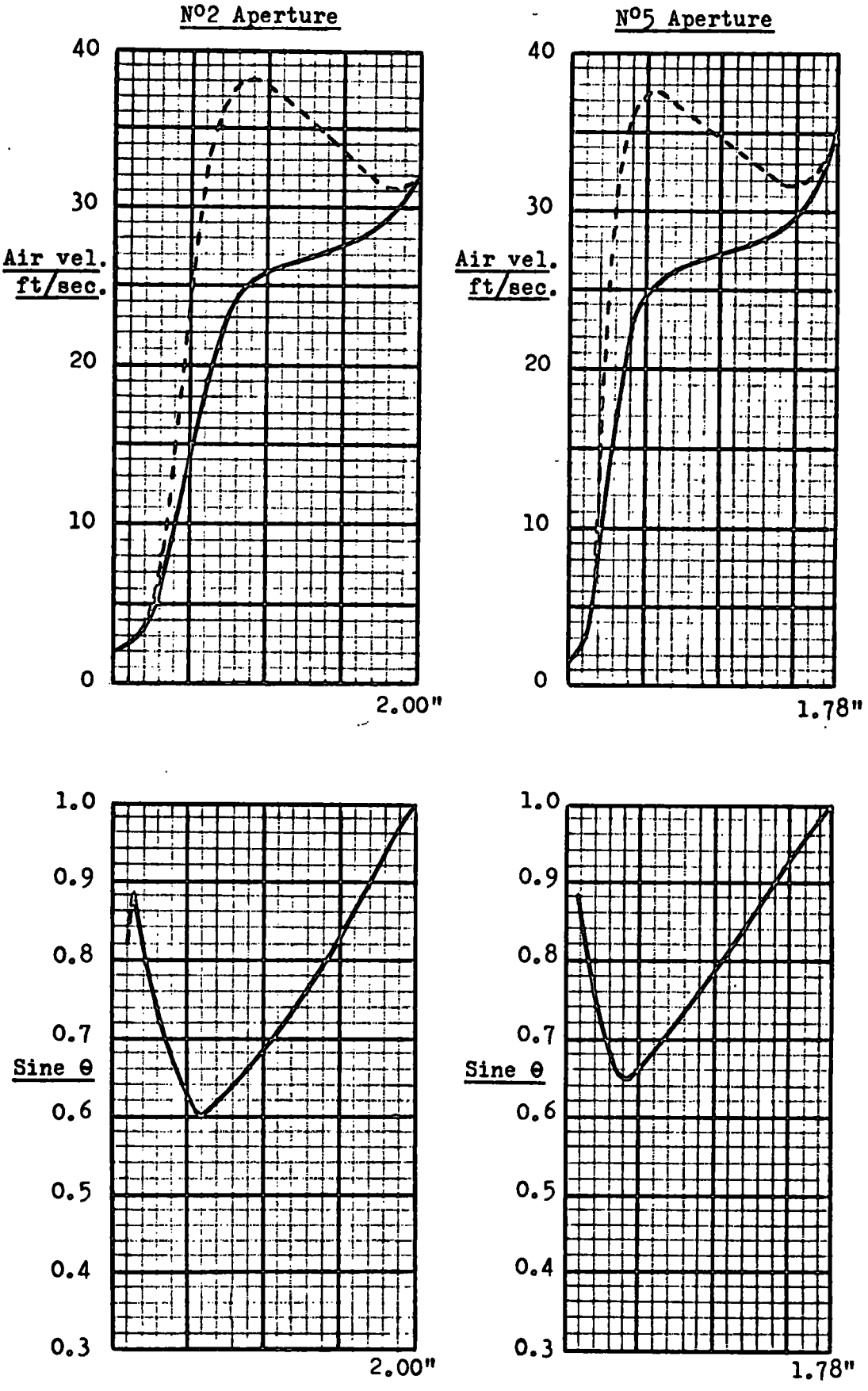

FIG.40 APERTURE AIR FLOW PATTERNS FOR EQUAL APERTURE FLOW RATES.

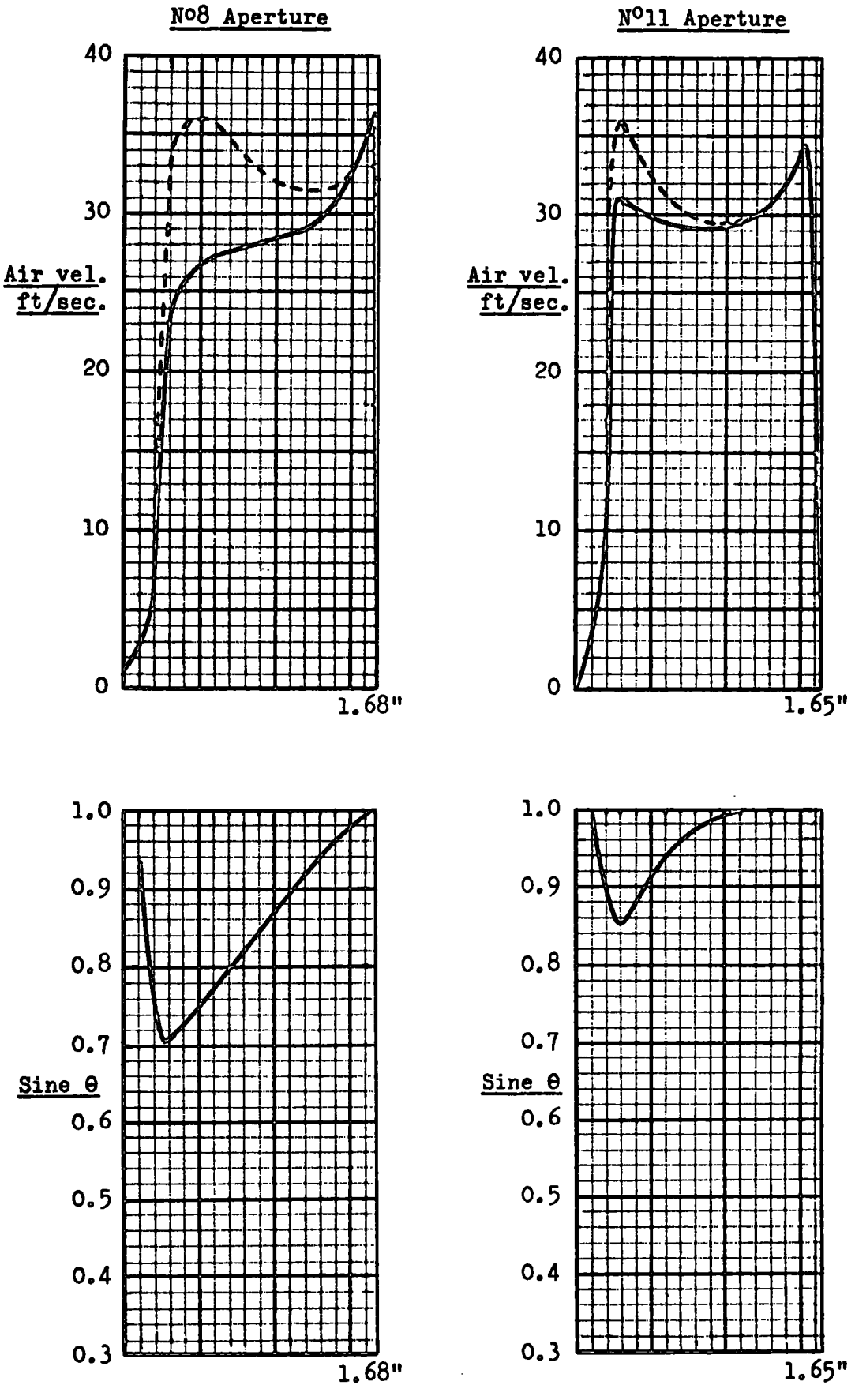

FIG.41 APERTURE AIR FLOW PATTERNS FOR EQUAL APERTURE FLOW RATES.

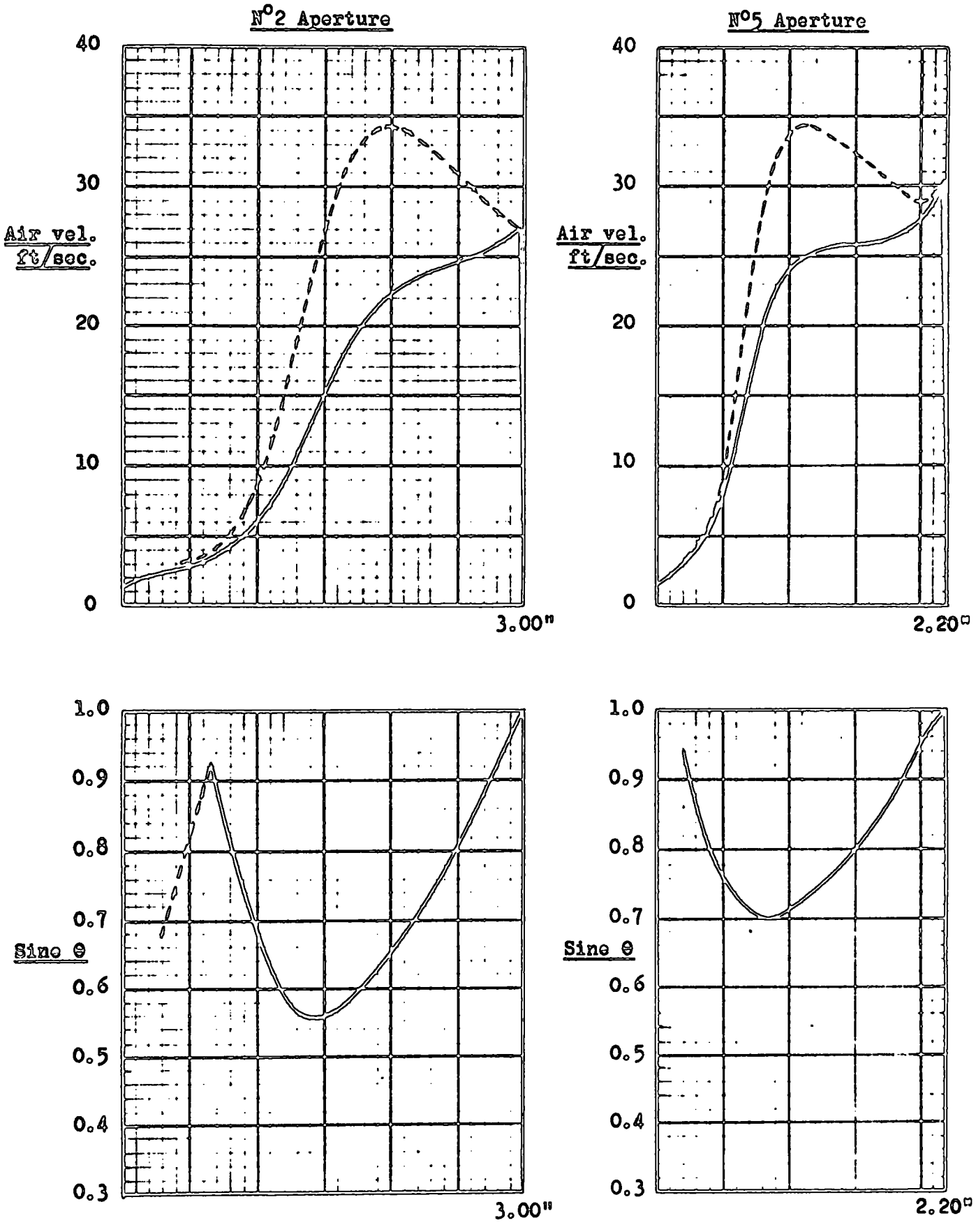

FIG.42 APERTURE AIR FLOW PATTERNS FOR EQUAL APERTURE FLOW RATES.

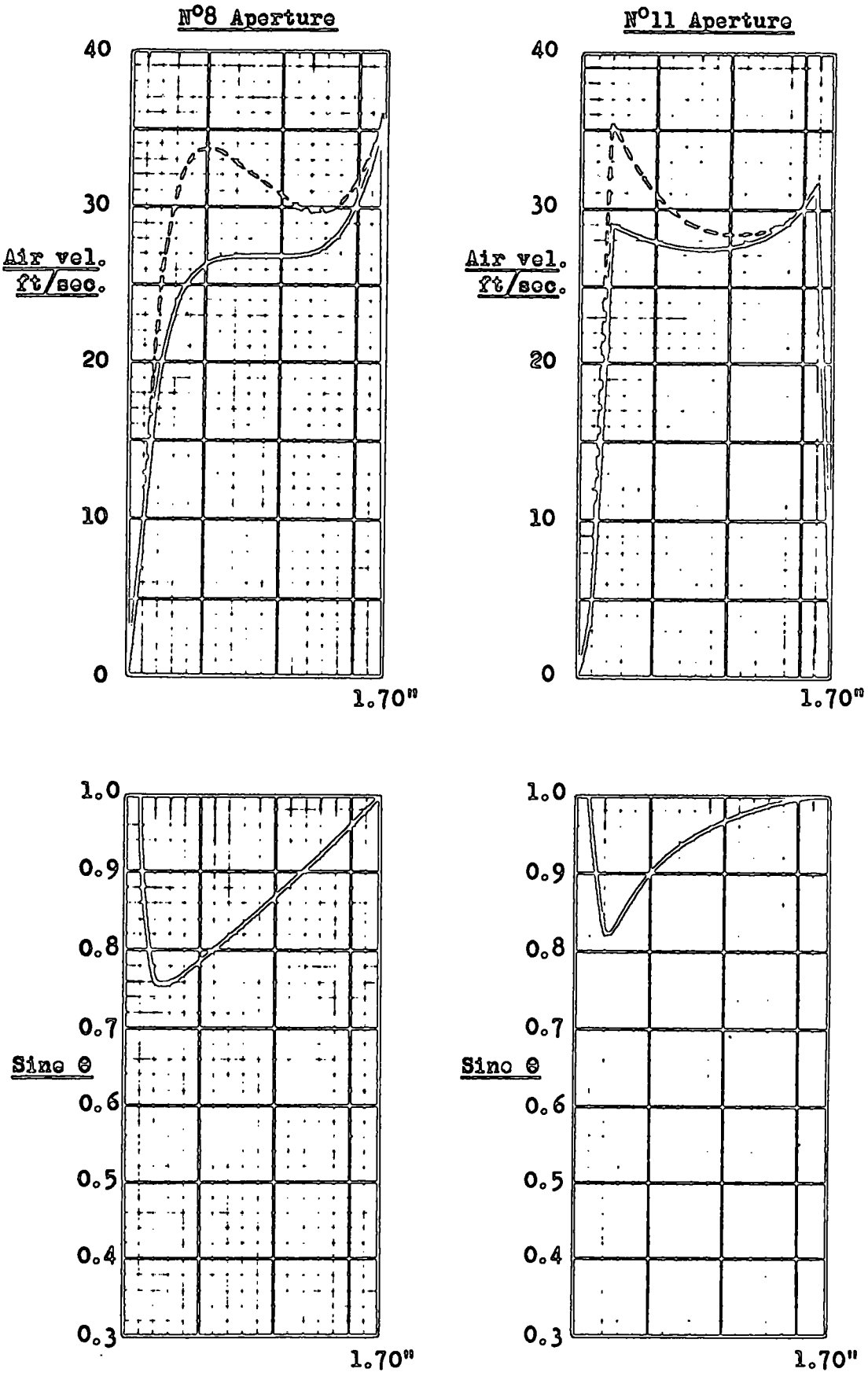

FIG.43 APERTURE AIR FLOW PATTERNS FOR EQUAL APERTURE FLOW RATES.

TABLE 13.

RELEVANT DATA FOR EQUAL APERTURE AIR DISCHARGE RATES.

Column (a) : Aperture area. in^2.

Column (b) : Aperture area expressed as a percentage of N°2 aperture area.

Column (c) : Area under aperture normal velocity curve. in^2.

Column (d) : Average aperture normal velocity $\bar{U}_n$. ft/sec.

Column (e) : Aperture air discharge q. ft^3/sec.

Column (f) : Aperture air discharge expressed as a proportion of the air entering the duct.

Column (g) : Average velocity in duct upstream of aperture. ft/sec.

Column (h) : Average velocity in duct downstream of aperture. ft/sec.

Column (i) : Static gauge pressure at aperture upstream tapping point. ft. of air at 80°F.

Column (j) : Static gauge pressure at aperture downstream tapping point. ft. of air at 80°F.

N°2 Aperture set at 6" by 2"										
Aperture	(a)	(b)	(c)	(d)	(e)	(f)	(g)	(h)	(i)	(j)
N°2	12.0	100%	4.24	21.4	1.78	0.250	32.9	24.6	14.0	18.6
N°5	10.7	89%	4.23	24.0	1.78	0.250	24.6	16.4	18.6	22.1
N°8	10.1	84%	4.21	25.3	1.77	0.249	16.4	8.2	22.1	24.0
N°11	9.9	83%	4.26	26.1	1.79	0.251	8.2	—	24.0	24.6

N°2 Aperture set at 6" by 3"										
Aperture	(a)	(b)	(c)	(d)	(e)	(f)	(g)	(h)	(i)	(j)
N°2	18.0	100%	4.23	14.2	1.78	0.250	32.8	24.6	11.3	15.6
N°5	13.2	73%	4.21	19.3	1.77	0.250	24.6	16.4	15.6	19.3
N°8	10.2	57%	4.22	25.1	1.78	0.250	16.4	8.2	19.3	20.3
N°11	10.2	57%	4.23	25.1	1.78	0.250	8.2	—	20.3	21.9

10.2 Comparison of measured and predicted duct gauge static pressures.

For purposes of comparison the measured values of pressure given in column (i) of Table 13 are shown below alongside those predicted in Section 9.3.

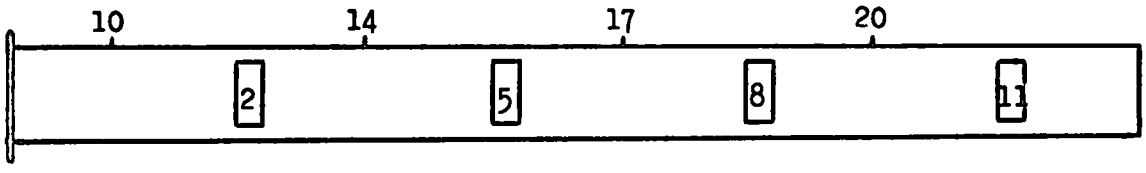

For N°2 aperture 6" by 2"

	Measured pressure ft air	Predicted pressure ft air
h_{10}	14.0	21.1
h_{14}	18.6	25.9
h_{17}	22.1	29.4
h_{20}	24.0	31.0

For N°2 aperture 6" by 3"

	Measured pressure ft air	Predicted pressure ft air
h_{10}	11.3	10.4
h_{14}	15.6	15.3
h_{17}	19.3	18.8
h_{20}	20.3	20.4

SECTION 11. EFFECT OF VARYING AIR VOLUME FLOW AT DUCT ENTRY ON APERTURE PROPORTIONAL AIR DISCHARGE.

11.1 Variation of air flow into duct.

Up to the present juncture all of the tests on the small-scale duct had been conducted for an air volume flow entering the duct of approximately 7.1 ft^3/sec. in order, as mentioned earlier in the thesis, to keep the number of possible variants to a minimum. However, the method provided in Section 9 for regulating the areas of the outlets along the duct to give desired air flows through the outlets requires that for a given setting of the aperture areas the aperture proportional air discharges should be independent of the amount of air entering the duct.

Although it was not feasible to inaugurate a series of tests comprehensive enough to establish the truth of this beyond question, it was both practicable and desirable to ascertain its validity, or otherwise, for one fixed arbitrary setting of the aperture sizes. Consequently, three tests were conducted with the four apertures set to their middle size of 6" by 2", the air flowing into the duct being varied over as wide a range as was practicable with the test rig.

The results of these tests, together with the appropriate data relating to 6" by 2" apertures abstracted from Table 7, are given in Table 14 and plotted as shown by fig.44. As may be seen, for this case at least, variation in the air volume flow entering the duct had little effect on the proportions of the flow leaving through the apertures. Although no generalisation can be made from such a limited result it points in an encouraging direction, because it would be a simplification of air distribution problems if it

TABLE 14.

RELEVANT DATA FOR VARIATION IN PROPORTIONAL APERTURE AIR DISCHARGE WITH AIR VOLUME FLOW ENTERING DUCT.

(Aperture Nos 2, 5, 8 & 11 open 6" by 2")

Column (a) : Aperture air discharge q. $ft^3/sec.$

Column (b) : Aperture air discharge expressed as a proportion of the air entering the duct.

	(a)	(b)	(a)	(b)	(a)	(b)	(a)	(b)
No2 Aperture	0.77	0.199	1.07	0.195	1.39	0.192	1.68	0.193
No5 Aperture	0.90	0.233	1.29	0.235	1.71	0.236	2.08	0.239
No8 Aperture	1.08	0.279	1.52	0.277	2.03	0.280	2.41	0.277
No11 Aperture	1.12	0.289	1.61	0.293	2.12	0.292	2.53	0.291
Total disch.	3.87	1.000	5.49	1.000	7.25	1.000	8.70	1.000

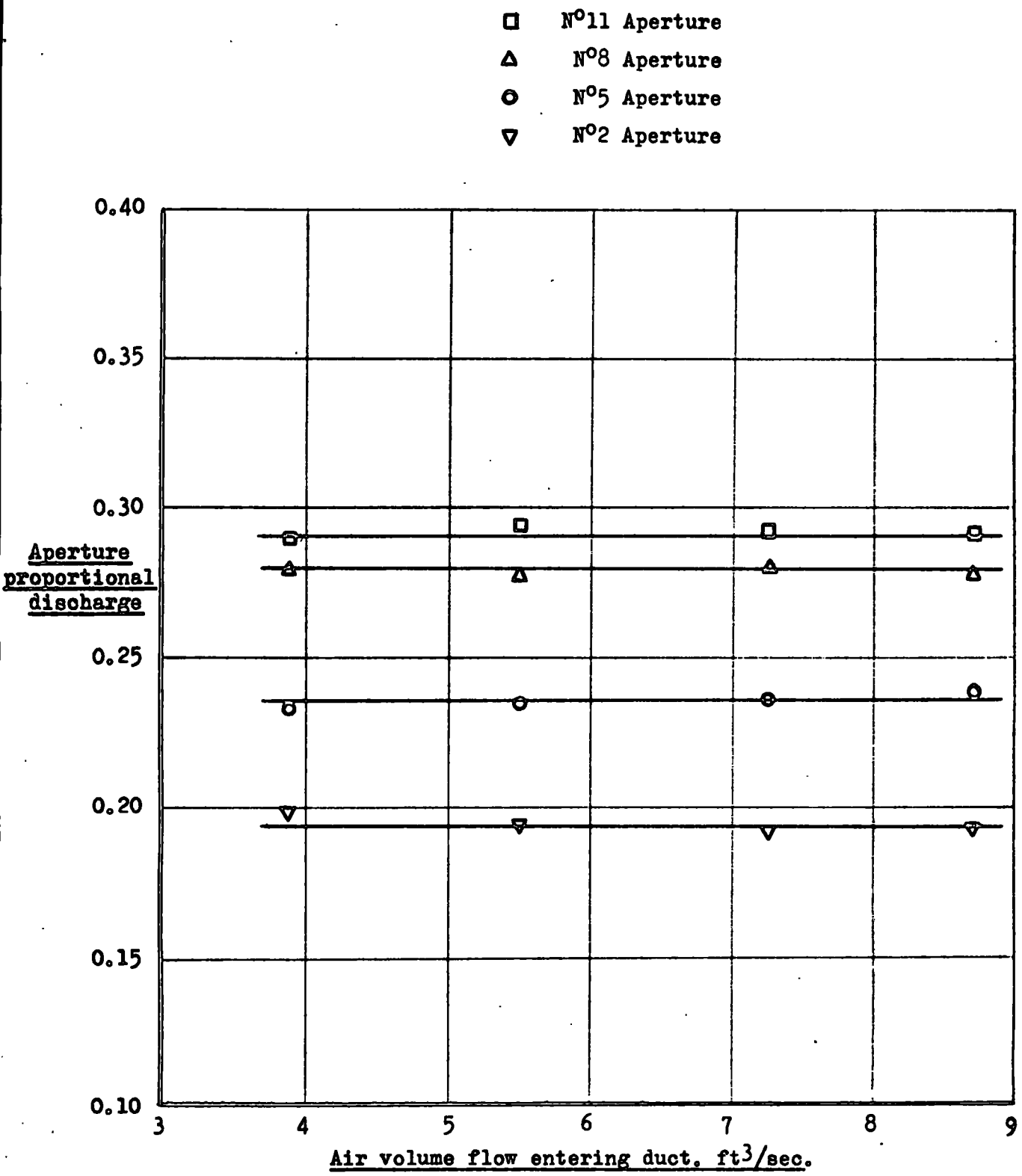

FIG.44 VARIATION IN APERTURE PROPORTIONAL AIR DISCHARGE WITH AIR VOLUME FLOW ENTERING DUCT.
(Aperture N°s 2, 5, 8 & 11 open 6" by 2".)

could be established with certainty that the proportional air discharges through outlets situated along a terminal ventilating duct were virtually independent of the magnitude of the air flowing into the duct.

SECTION 12. CONCLUSIONS AND RECOMMENDATIONS FOR FURTHER WORK.

12.1. Conclusions.

Ideally, it would be desirable to predict entirely theoretically how a given volume flow of air entering a terminal ventilating duct of known dimensions would be distributed through specified openings situated at selected locations along the duct. The results of this investigation, however, show that where the openings are situated relatively close together the air flow patterns both in the duct and in the plane of the openings are of such a complex nature that the attainment of this ideal is unlikely.

A reinforcement of this statement is supplied by a detailed examination of the aperture air flow patterns given in Section 6. These show that the magnitude of the velocity U_m of the issuing air varied in a complicated manner across the openings, in general reaching a maximum value at some distance from the upstream edge dependent on the size of the aperture. Although any given setting of the four apertures to the same size resulted in roughly the same velocity profile for each outlet, the shapes of these profiles varied appreciably with the size of the outlet.

Regarding the angles at which air was discharged through the apertures, the patterns show what might reasonably have been anticipated, namely, that the greater the difference between the pressure in the duct and the surrounding atmospheric air, the more did the air tend to be discharged perpendicular to the length of the duct. A further noticeable feature is the way in which the angle of discharge decreased to a minimum at some distance from the upstream edge of the aperture and thereafter rose to become perpendicular to the length of the duct at the downstream edge. Moreover, both the magnitude of this minimum angle and its position across an aperture were evidently dependent on

the aperture size.

For some purposes it is convenient to suppose that the static pressure of air issuing to atmosphere through an orifice is zero in, or near, the plane of the orifice. As figs.92 to 96 show, however, the actual variation of pressure across such an orifice can be quite complex. Taking this into account, together with the comments in the above two paragraphs, it is not surprising that the possibility of a rigorous analysis of the duct's performance seems somewhat remote.

Nevertheless, although an exact analysis of the duct's performance is hardly feasible it is possible, as this thesis shows, to evolve an empirical method, based on the correlations of the experimental data shown by figs.38 and 39, which is capable of predicting sufficiently accurately for most practical purposes the distribution characteristic of the duct. The comparisons between aperture areas predicted by the method and those determined experimentally for two different equal aperture flow conditions are given in Section 10. As may be seen, in one case, where N°2 aperture was open its maximum amount, 6" by 3", the agreement between predicted and experimentally determined values was very good, but in the other case, where N°2 aperture was open 6" by 2", the agreement was only fair. A similar comment applies to the comparisons between the predicted and measured values of static gauge pressure along the duct. Agreement was very good in the 6" by 3" case, but only fair in the 6" by 2" case.

Of course, considering the scatter of the experimental points about the straight line graphs of figs.38 and 39, it would be expected that some discrepancies would exist between predicted and experimentally determined areas and pressures and, bearing this in mind, the indications are that the method has substantial merit which, with possible refinement and development, could become of considerable

usefulness to designers of ventilating systems. In one respect in particular the method appears to be validated and that is in its implication that the aperture proportional discharge should be unaffected by the volume flow of air entering the duct. As fig.44 shows, this was experimentally confirmed for one selected size of aperture over a comparatively wide range of flows.

With regard to the scatter of the experimental points, it is self-evident that the less is the scatter, the better will be the correlation of the points, and the more accurate will be subsequent predictions of the duct's performance under various operating conditions. To this end it is suggested that better correlations and more accurate predictions could have been made if the existing small-scale duct had been fitted with piezometer rings, instead of single tapping points, to record static pressures along the duct and this practice is recommended for any future work on the duct.

Perhaps it should also be mentioned that the method of regulating aperture area by using cover plates which were thick compared with the thickness of the front side of the duct was probably not conducive to consistency of experimental results. This was because the rectangular openings formed by adjustment of the cover plates were distinctly 'stepped' to an extent which depended on the size of the openings required. That is, alteration of an aperture area involved not simply an alteration of the aspect ratio, depth/breadth, alone but an alteration of the aperture geometry in the transverse direction so that, in effect, an aperture set at 6" by 1" was a geometrically significantly different kind of orifice to one set at 6" by 2".

One noteworthy outcome of this investigation is the evident practicability of obtaining an appreciable amount of performance data from small-scale components of ventilating systems. Although the

component tested here was a simple terminal duct it is apparent that there would be no particular obstacle to testing larger and more complicated sections, space permitting, of course.

Consequently, the idea presents itself of using small-scale models of parts of ventilating systems which are in the design stage to assist in predicting the on-site behaviour of the full-size systems. Considering the relative cheapness of even a complex model, including ancillary equipment, with the amount of useful data it can supply, the idea of using models in association with the type of correlation given in this thesis should appeal to many designers as a most worthwhile exercise.

Of course, to achieve a rapid accumulation of data it would be necessary to discard the time consuming method employed in this experimental work of measuring aperture air velocities by recording individual voltages with the hot-wire anemometer at very closely spaced points across the aperture width. Although this was acceptable for the limited experimental work on which this thesis is based it would be obviously unsuitable for industrial research purposes.

A better method would be to arrange for the hot-wire probe to traverse an opening quickly and smoothly, firstly with the hot-wire vertical, then secondly with the hot-wire horizontal, a voltage recorder being used to obtain a permanent record of the variation in volts across the opening. From such a record and the appropriate calibration data of the probe used for testing, both the speed of the air flowing out of the opening and its particular pattern of flow could be ascertained in a short space of time. Because many such tests could be carried out in, say, several hours the difficulties caused by gradual contamination of the hot-wire probe would be reduced

to virtually negligible proportions and a large number of voltage records could be amassed relating to various operating conditions, these records being ultimately translated at leisure into the required air velocity and volume flow data.

It is perhaps worth emphasising here the point that in measuring the air volume flow through an aperture a multi-row traverse with the hot-wire probe is not necessary because, as shown in Section 4.2 a single, half-height, horizontal traverse of an aperture leads to a quite accurate determination of the flow.

12.2. Recommendations for further work.

With regard to the use of models mentioned in Section 12.1, a useful and probably rewarding line of investigation would be to ascertain what relationships exist between the performance of model components of ventilating systems and their full-size counterparts. For example, it would be instructive to construct a geometrically similar model of a component of an existing ventilating system from which considerable operational data had been obtained and compare the behaviour of the model with that of the full-size duct. In this way the extent to which the performance of models could be taken as a reliable guide to the behaviour of real systems when actually installed could be firmly established.

An implication of the method outlined in Section 9.1 is that aperture proportional air discharge should be independent of the volume flow of air entering the duct. The results of several tests, displayed graphically by fig.44, show that this was indeed so for one particular size of aperture. Quite obviously, of course, it is not possible to generalise from such a limited case and it would evidently be desirable to know the results of a comprehensive

investigation into this aspect of ventilation because clearly it would be an advantage to know under what circumstances the proportional aperture air flows were, or were not, influenced by the total flow of air into the duct.

REFERENCES.

1. Singstad, O. 'Ventilation of vehicular tunnels.' World Engineering Congress of Engineers, Tokyo, 1929, Paper 339.

2. Atkinson, F.S., Pursall, B.R. and Statham, I.C.F. 'The ventilation of vehicular road tunnels.' J.I.H.V.E., September 1962, pp.196 - 212.

3. Pursall, B.R. 'The theoretical and practical aspects of slot ventilation in connection with vehicular road tunnels.' J.I.H.V.E., July 1963, pp.113 - 124.

4. Ramsay, W.C. 'Testing of heating and air-conditioning plants.' J.I.H.V.E., 1956, 24, pp.97 - 134.

5. Harrison, E. and Gibbard, N.C. 'Balancing air flow in ventilating duct systems.' J.I.H.V.E., October 1965, pp.201 - 226.

6. Nelson, D.W. and Smedberg, G.E. 'The performance of side outlets on horizontal ducts.' Trans. A.S.H.V.E., 49, 1943, pp.58 - 74.

7. Horlock, J.H. 'An investigation of the flow in manifolds with open and closed ends.' Journal of the Royal Aeronautical Society, November 1956, pp.749 - 753.

8. Myles, D.J., Whitaker, J. and Jones, M.R. 'A simplified integration technique for measuring volume flow in rectangular ducts.' Ministry of Technology, National Engineering Laboratory Report N°251, October 1966.